Responses to Topical Editor

Comments to the author::

"Dear Authors,

You have addressed very well the concerns of reviewer in your "Author's Response", but keeping only a fraction of these discussions in the revised manuscript. Even if the discussion remains available in the GMDD website, you should consider including more of those elements in the final revised paper in order to benefit to all readers.

rgds"

AUTHOR'S RESPONSE: We thank the Topical Editor for evaluating positively the responses we provided in the review process. Following the recommendation made for including more of the responses to the final revised paper, we now present a new revised manuscript. Under each respective response provided for each comment below, we now provide in the category "**MINOR REVISIONS**" what further additions were made to the manuscript, concerning each respective comment. All new elements with regards to the new additions are given in blue, in the section "**MINOR REVISIONS**".

Major comments:

1st Comment:

I recommend more clearly laying out what the novelty or newness is of this work. Based on previous work it seems that precipitation in this region has been studied in similar ways before. Why is the method/results/approach in this work an improvement on those studies?

AUTHOR'S RESPONSE: Thank you very much for this comment. Indeed, precipitation over southern Africa has been studied before. More specifically, Nikulin et al. (2012) was the first to present an overview of the CORDEX-Africa ensemble and to analyze the spatiotemporal patterns of precipitation. They showed that during the rainy season (Jan-Mar as used in Nikulin et al. (2012)) there is a weak wet bias over southern Africa, and that the use of the ensemble mean was able to outperform individual models, highlighting the importance of ensemble-based approaches. The Nikulin et al. (2012) analysis was conducted on a pan-African scale. Similarly, Kalognomou et al., (2013) analyzed the same ensemble of CORDEX-Africa simulations, focusing over southern Africa and reported similar findings to Nikulin et al., (2012). In Shongwe et al. (2014) a particular emphasis was put on the onset and retreat of the rainy season, especially over the eastern part of southern Africa. Nonetheless, as stated in Shongwe et al. (2014) "No attempt is made in this paper to identify the model physics and dynamics responsible for the differences in RCM performance." All the aforementioned studies employed the evaluation (hindcast) simulations performed within CORDEX-Africa, driven by ERA-Interim; the analyzed ensemble was comprised of 10 RCMs. It is also worth mentioning that the regional climate model (RCM) versions used in the studies listed above, refer to previous versions of the respective RCMs, which have now been replaced by newer versions in more recent studies.

In Meque and Abiodun (2015) the same ensemble of 10 hindcast simulations was again used, but it was also compared with a set of CMIP5 GCM simulations, with the purpose to identify a causal association between ENSO and drought events over southern Africa. In Meque and Abiodun (2015) it was stated for the first time that RCMs were able to provide added value, compared to their driving GCMs. The issue of the added value of the CORDEX-Africa ensemble was clearly stated in Dosio et al. (2015), where 1 RCM participating in CORDEX-Africa (CCLM) was compared against 4 different driving GCMs. In Favre et al. (2016) a special focus was given on the annual cycle of precipitation over South Africa, using the same ensemble of 10 CORDEX-Africa hindcast simulations and in Abba Omar and Abiodun (2017), although the same hindcast ensemble was used, there was an effort to associate extreme precipitation events with dynamical processes such as the Tropical Temperate Troughs. A comprehensive assessment of the added value between historical CORDEX-Africa RCMs simulations and of their driving CMIP5 GCMs on a seasonal timescale over the whole of Africa, was performed in Dosio et al. (2019). The first time the CORDEX-Africa ensemble over southern Africa was compared with a plethora of observational and satellite products was presented in Abiodun et al., (2020), while the first time that CORDEX Africa at 0.44º and at 0.22º was analyzed compared to both CMIP5 and CMIP6 ensembles is presented in Dosio et al. (2021). More specifically, in Dosio et al. (2021) the analysis is performed on a seasonal timestep and on pan-African scale and its particular emphasis is placed on the projected changes of future precipitation, although a part of the analysis is dedicated to the period 1981-2010.

Our work aims to provide a comprehensive overview of the observed precipitation climatology particularly focusing over southern Africa, in all tools that are currently available in the climate community. For this reason, we employ all four ensembles used in Dosio et al. (2021) for the period 1986-2005 and we additionally employ a set of 12 observational (satellite, gridded and reanalysis) products. By doing so, we aim to highlight the precipitation uncertainty that exists even among different observational products, which is inherent in the methods used for their production. In addition, we attempt to make a connection between monthly precipitation climatology over southern Africa and a particularly important atmospheric feature, the Angola Low pressure system. To our knowledge, the Angola Low pressure system has not been studied yet within the context of CORDEX-Africa simulations. Although there has been an ample work of evaluating CORDEX-Africa simulations, we think that in order to better understand the reasons why RCM simulations do, or do not, display an improvement relative to their driving GCMs, there must be a shift towards process-based evaluations that examine particular (thermo)dynamic atmospheric processes over specific regions and specific time periods. For this reason, we also chose to perform our analysis on a monthly timescale during the rainy season (Oct-Mar). Often, seasonal means are conveniently used, however, seasonal averages might obscure spatio-temporal patterns that can only be identified on a finer temporal resolution. One of the main hindrances that often limits the ability to perform dynamic analysis in CORDEX-Africa (and CORDEX in general) simulations is the lack of available variables at different pressure levels. This was a shortcoming in our analysis also. In addition, we discuss the results with respect to monthly precipitation trends, as seen in all observational and modeling ensembles we use.

We agree that we need to present more clearly in the manuscript what the novelty and the newness of this work is. For this reason, we made the following changes in the Introduction:

AUTHOR'S CHANGES IN MANUSCRIPT: Section to last paragraph: "Therefore, in this paper we expand on previous research to investigate how monthly precipitation during the rainy season over southern Africa is simulated by different modelling systems, by analyzing the monthly precipitation climatologies, the interannual variability, specific precipitation indices and monthly precipitation trends during the period 1986-2005, in four different modeling systems (CORDEX 0.22º/0.44º, CMIP5/6) and observational ensembles (satellite, reanalysis and gridded datasets). Our main goal is to provide a comprehensive overview with regards to precipitation climatology over SAF as simulated by the state-of-the-art tools used by climate scientists. In addition, we investigate whether higher resolution models are able to provide an improved representation of precipitation over southern Africa and we investigated how a particularly important atmospheric feature, the Angola Low pressure system, is simulated in the RCM and GCM ensembles."

MINOR REVISIONS: In the Introduction we have added the following paragraph (now 3rd paragraph), which summarizes the main efforts conducted within CORDEX-Africa, with regards to the evaluation of precipitation:

"A comprehensive analysis of the performance of the CORDEX-Africa ensemble over Africa was first presented in Nikulin et al. (2012). They showed that during the rainy season (Jan-Mar as used in Nikulin et al. (2012)) there is a weak wet bias over southern Africa, and that the use of the ensemble mean was able to outperform individual models, highlighting the importance of ensemble-based approaches. The Nikulin et al. (2012) analysis was conducted on a pan-African scale. Similarly, Kalognomou et al. (2013) analyzed the same ensemble of CORDEX-Africa simulations, focusing over southern Africa and reported similar findings. In Meque and Abiodun (2015) the same ensemble of 10 evaluation simulations was again used, but it was also compared with a set of CMIP5 GCM simulations, with the purpose to identify a causal association between ENSO and drought events over southern Africa. In Meque and Abiodun (2015) it was stated that RCMs were able to provide added value, compared to their driving GCMs. A comprehensive assessment of the added value between historical CORDEX-Africa RCMs simulations and of their driving CMIP5 GCMs on a seasonal timescale over the whole of Africa, was performed in Dosio et al. (2019). The first time the CORDEX-Africa ensemble is compared to both CMIP5 and CMIP6 ensembles is presented in Dosio et al. (2021). More specifically, in Dosio et al. (2021) the analysis is performed on a seasonal timestep and on pan-African scale and its particular emphasis is placed on the projected changes of future precipitation, although a part of the analysis is dedicated to the period 1981-2010."

References:

Abba Omar, S., Abiodun, B.J., 2017. How well do CORDEX models simulate extreme rainfall events over the East Coast of South Africa? Theor. Appl. Climatol. 128, 453–464. https://doi.org/10.1007/s00704-015-1714-5

Abiodun, B.J., Mogebisa, T.O., Petja, B., Abatan, A.A., Roland, T.R., 2020. Potential impacts of specific global warming levels on extreme rainfall events over southern Africa in CORDEX and NEX-GDDP ensembles. Int. J. Climatol. 40, 3118–3141. https://doi.org/10.1002/joc.6386

Dosio, A., Jones, R.G., Jack, C., Lennard, C., Nikulin, G., Hewitson, B., 2019. What can we know about future precipitation in Africa? Robustness, significance and added value of projections from a large ensemble of regional climate models. Clim. Dyn. 53, 5833–5858. https://doi.org/10.1007/s00382-019-04900-3

Dosio, A., Jury, M.W., Almazroui, M., Ashfaq, M., Diallo, I., Engelbrecht, F.A., Klutse, N.A.B., Lennard, C., Pinto, I., Sylla, M.B., Tamoffo, A.T., 2021. Projected future daily characteristics of African precipitation based on global (CMIP5, CMIP6) and regional (CORDEX, CORDEX-CORE) climate models. Clim. Dyn. 57, 3135–3158. https://doi.org/10.1007/s00382-021-05859-w

Dosio, A., Panitz, H.-J., Schubert-Frisius, M., Lüthi, D., 2015. Dynamical downscaling of CMIP5 global circulation models over CORDEX-Africa with COSMO-CLM: evaluation over the present climate and analysis of the added value. Clim. Dyn. 44, 2637–2661. https://doi.org/10.1007/s00382-014-2262-x

Favre, A., Philippon, N., Pohl, B., Kalognomou, E.-A., Lennard, C., Hewitson, B., Nikulin, G., Dosio, A., Panitz, H.-J., Cerezo-Mota, R., 2016. Spatial distribution of precipitation annual cycles over South Africa in 10 CORDEX regional climate model present-day simulations. Clim. Dyn. 46, 1799–1818. https://doi.org/10.1007/s00382-015-2677-z

Kalognomou, E.-A., Lennard, C., Shongwe, M., Pinto, I., Favre, A., Kent, M., Hewitson, B., Dosio, A., Nikulin, G., Panitz, H.-J., Büchner, M., 2013. A Diagnostic Evaluation of Precipitation in CORDEX Models over Southern Africa. J. Clim. 26, 9477–9506. https://doi.org/10.1175/JCLI-D-12-00703.1

Kim, Y.-H., Min, S.-K., Zhang, X., Sillmann, J., Sandstad, M., 2020. Evaluation of the CMIP6 multi-model ensemble for climate extreme indices. Weather Clim. Extrem. 29, 100269. https://doi.org/10.1016/j.wace.2020.100269

Meque, A., Abiodun, B.J., 2015. Simulating the link between ENSO and summer drought in Southern Africa using regional climate models. Clim. Dyn. 44, 1881–1900. https://doi.org/10.1007/s00382-014-2143-3

Nikulin, G., Jones, C., Giorgi, F., Asrar, G., Büchner, M., Cerezo-Mota, R., Christensen, O.B., Déqué, M., Fernandez, J., Hänsler, A., Meijgaard, E. van, Samuelsson, P., Sylla, M.B., Sushama, L., 2012. Precipitation Climatology in an Ensemble of CORDEX-Africa Regional Climate Simulations. J. Clim. 25, 6057–6078. https://doi.org/10.1175/JCLI-D-11-00375.1

Shongwe, M.E., Lennard, C., Liebmann, B., Kalognomou, E.-A., Ntsangwane, L., Pinto, I., 2014. An evaluation of CORDEX regional climate models in simulating precipitation over Southern Africa. Atmospheric Sci. Lett. 16, 199–207. https://doi.org/10.1002/asl2.538

Wyser, K., van Noije, T., Yang, S., von Hardenberg, J., O'Donnell, D., Döscher, R., 2020. On the increased climate sensitivity in the EC-Earth model from CMIP5 to CMIP6. Geosci. Model Dev. 13, 3465–3474. https://doi.org/10.5194/gmd-13-3465-2020

2nd Comment:

In the second to last paragraph of the introduction the purpose and goals of the paper are given but there are several different statements of goals which I find somewhat unfocused. Is there a main goal that can be defined? It seems that the main focus of the paper is on how the RCM ensemble can be shown to be more useful for precipitation projections over this region compared to the GCMs but this is not clear. From the abstract it is also not very clear what are the main results the reader should see.

AUTHOR'S RESPONSE: Thank you very much for this comment and correction. Our analysis has two main goals: The first goal is to provide an intercomparison of how monthly precipitation during the rainy season over southern Africa is simulated by different modelling systems (CORDEX 0.22º/0. 44º, CMIP5/6) and to also provide an overview of the spread that is seen even among the so called "observational products", highlighting the need for improved modeling and monitoring efforts over the region. Our second goal is indeed, to highlight how RCMs are able to address certain deficiencies identified in GCMs. The second to last paragraph of the introduction has now changed to the following:

AUTHOR'S CHANGES IN MANUSCRIPT: **"**Therefore, in this paper we expand on previous research to investigate how monthly precipitation during the rainy season over southern Africa is simulated by different modelling systems, by analyzing the monthly precipitation climatologies, the interannual variability, specific precipitation indices and monthly precipitation trends during the period 1986-2005, in four different modeling systems (CORDEX 0.22º/0.44º, CMIP5/6) and observational ensembles (satellite, reanalysis and gridded datasets). Our main goal is to provide a comprehensive overview with regards to precipitation climatology over SAF as simulated by the state-of-the-art tools used by climate scientists. In addition, we investigate whether higher resolution models are able to provide an improved representation of precipitation over southern Africa and we investigated how a particularly important atmospheric feature, the Angola Low pressure system, is simulated in the RCM and GCM ensembles."

3rd Comment:

My understanding is that the CORDEX-Africa 0.22º data are available. If so, why was the older 50km dataset used when a newer one was available?

AUTHOR'S RESPONSE: Thank you for this comment. We have now included all the CORDEX-Africa 0.22º simulations available in the analysis. The CORDEX-Africa 0.22º simulations added, are listed in the table below. We have kept, however, all CORDEX-Africa 0.44º simulations, since they constitute a larger ensemble (26 ensemble members used).

Driving GCMs	RCMs	Realisations	Variables
CanESM2	CanRCM4	r1i1p1	Pr,
HadGEM2-ES	CCLM5-0-15	r1i1p1	Pr, hus850, ua850, va850, ta850
	REMO2015	r1i1p1	Pr, hus850, ua850, va850, ta850
	RegCM4-7	r1i1p1	Pr, hus850, ua850, va850, ta850
MPI-ESM-LR	CCLM5-0-15	r1i1p1	Pr, hus850, ua850, va850, ta850
	REMO2015	r1i1p1	Pr, hus850, ua850, va850, ta850
	RegCM4-7	r1i1p1	Pr, hus850, ua850, va850, ta850
NorESM1-M	CCLM5-0-15	r1i1p1	Pr, hus850, ua850, va850, ta850
	REMO2015	r1i1p1	Pr, hus850, ua850, va850, ta850
	RegCM4-7	r1i1p1	Pr, hus850, ua850, va850, ta850

Minor Comment:

1st Comment:

Line 17: SAF hasn't been defined yet, it should be defined here.

AUTHOR'S RESPONSE: We have defined SAF in line 10 (beginning of the abstract).

2nd Comment:

Lines 22-23: "…a similar behavior to CMIP5, however reducing slightly the ensemble spread." I would replace 'however' here with 'but'.

AUTHOR'S RESPONSE: Thank you! We made this change in the manuscript.

AUTHOR'S CHANGES IN MANUSCRIPT: The sentence now reads: "The CMIP6 ensemble displayed a similar behaviour to CMIP5 but reducing slightly the ensemble spread."

3rd Comment:

Line 61: Over what period is this trend seen? I assume it's a historical period but it would be good to explicitly say it here.

AUTHOR'S RESPONSE: Thank you! We will made this clarification in the manuscript.

AUTHOR'S CHANGES IN MANUSCRIPT: "During DJF, precipitation trends during the historical over SAF display…".

4th Comment:

Sentence starting at Line 71 "However,…": This sentence is a little bit confusing I would recommend removing 'still' and the comma between 'period' and 'persist'.

AUTHOR'S RESPONSE: Thank you! The sentence in the manuscript was changed to:

AUTHOR'S CHANGES IN MANUSCRIPT: "However, although the CMIP6 ensemble exhibits multiple improvements on various levels (Wyser et al., 2020), certain biases and challenges identified in CMIP5 during the historical period persist in CMIP6 (Kim et al., 2020)."

5th Comment:

Line 90: Provide more detail of what will be addressed in the results section (Section 3). For instance, describe the subsections of the results and what will be covered.

AUTHOR'S RESPONSE: Thank you very much for this comment! This sentence in the manuscript was changed to:

AUTHOR'S CHANGES IN MANUSCRIPT: "In Section 3 the results are presented. More specifically, the results are analyzed based on the monthly climatology, the annual cycle of precipitation, the Angola Low pressure system, the ETCCDI precipitation indices and the monthly precipitation trends. Lastly, in Section 4 we provide the discussion of the analysis along with some concluding remarks."

6th Comment:

Line 107: Should this be "less **than** or equal to"?

AUTHOR'S RESPONSE: Thank you very much.

AUTHOR'S CHANGES IN MANUSCRIPT: We changed the sentence to "The gauge-based products were chosen so that they have a spatial resolution less than or equal to 0.5º x 0.5º…"

7th Comment:

Line 183: How was the calculation of standard deviation done to get the within-ensemble agreement? Was the monthly mean of over the 1986-2005 period calculated for each model first and then the SD of the ensemble taken?

AUTHOR'S RESPONSE: Yes, we first calculated the monthly means over the period 1986-2005 for each model (or observational dataset) separately, and then we calculate the standard deviation.

8th Comment:

Figures 1, 2 and 7: The alignment and spacing of the panels is not consistent. I recommend making sure the Figures have consistent spacing and are aligned to improve their visual aesthetic.

AUTHOR'S RESPONSE: Thank you! We made this correction in all panel plots.

9th Comment:

Lines 355-356: Expand on what improvements can be made. This is an important statement for readers who may be interested in expanding on this work.

AUTHOR'S RESPONSE: Thank you very much for this comment. The paragraph in the manuscript has been changed to the following:

AUTHOR'S CHANGES IN MANUSCRIPT: "In conclusion, while CORDEX0.44 displays marked improvement over coarser resolution products, there are still further improvements to be made. More specifically, since the wet bias in RCM simulations persists (although considerably reduced relative to GCMs), it is necessary that precipitation over southern Africa is no longer assessed based on bulk descriptive statistics, but that there will be a shift towards process-based evaluation, where the dynamical and thermodynamical characteristics of specific atmospheric features are investigated more thoroughly in the CORDEX-Africa simulations. For this reason, it is imperative that all institutes submitting RCM simulations in data repositories such as the Earth System Grid Federation or the Copernicus Climate Data Store, provide model output data on multiple pressure levels, so that a fair comparison with the CMIP community would be possible. In addition, since the climate of southern Africa is highly coupled with the moisture transport coming from the adjacent oceans, it is necessary that the next generation of RCM simulations within CORDEX-Africa are performed coupled with ocean models. Lastly, since convection over southern Africa has a strong thermal component during specific months of the year (Oct-Nov), it is necessary that the land-atmosphere coupling processes within each RCM are examined in more detail, with coordinated efforts such as the LUCAS Flagship Pilot Study (https://ms.hereon.de/cordex_fps_lucas/index.php.en), as performed in the Euro-CORDEX domain. In the world of regional climate modelling community, the 0.44º resolution of CORDEX-Africa is no longer state of the art and ensemble efforts are now approaching convection permitting grid-spacing (i.e., < 4 km) in some parts of the world (Ban et al., 2021; Pichelli et al., 2021) (Ban et al., 2021;

Pichelli et al., 2021). We also note, that increasing effort should be made with regards to understanding the improvements made from CORDEX0.44 simulations to CORDEX0.22. Although higher resolution is a desired target in the climate modelling community due to the more realistic representation of processes that it offers, still it should not be used as a panacea. In the current work we identified certain weaknesses in the CORDEX0.22 ensemble, that should be addressed before the community populates further its simulation matrix. The next generation ensembles for Africa will hopefully provide insight and improvements to the challenges described here."

Responses to Anonymous Reviewer 2

General Comment:

This paper evaluates the representation of the southern African rainfall in the GCMs and RCMs compared to a set of observational data. The rainfall climatology, annual cycle, trends and a couple of ETCCDI indices are analyzed along with the representation of the Angola Low, which is one of the important driving circulations that affect the rainfall in the area. The paper is of high importance for model improvement. However, I suggest the following comments to be addressed before the paper is published in GMD.

AUTHOR'S RESPONSE: We would like to thank the Anonymous Reviewer #2 for the positive interpretation of the manuscript. Based on the suggestions and comments, we provide the following replies.

Major comments:

1st Comment:

Page 8, 235-240, an evaluation of the moisture transported through the north-easterly monsoon should be performed here to support the hypothesis that the improved representation of the topography led to a lower bias in the CORDEX models.

AUTHOR'S RESPONSE: Thank you very much for this comment. We now include the following figure in the main manuscript, displaying the moisture flux and moisture flux divergence at 850 hPa during each month of the rainy season, for the period 1986-2005. More specifically, the moisture flux divergence was calculated using the product of specific humidity and wind at 850 hPa, following the equation below (the vertical component ($\frac{\partial qw}{\partial z}$) is considered negligible).

$$\nabla \cdot q\vec{u} = \frac{\partial qu}{\partial x} + \frac{\partial qv}{\partial y}$$

With this plot we aim to contribute to the discussion developed in Figure 11 in Munday and Washington, (2017). More specifically, one of the reasons responsible for the wet bias of CMIP5 models over southern Africa (SAF), was that mountainous regions over the northeast part of SAF were underrepresented, due to the spatial resolution of the CMIP5 models Munday and Washington, (2018). The high elevation areas over Malawi and Tanzania were not represented accurately in CMIP5 GCMs, which allowed moisture transport entering SAF from the northeast to penetrate central SAF, rather than to recurve around the high mountains and result to large precipitation amounts over northern Madagascar. Since the underrepresentation of topography in GCMs is a matter of spatial resolution, we make the hypothesis that in high resolution RCMs this issue is resolved, since moisture entering SAF from the northeast is blocked by the adequately high elevation over the Tanzania and Malawi region.

As seen in the Figure 1 below, during all months the moisture flux field is very spatially inhomogeneous in ERA5 and in both CORDEX ensembles, while in CMIP5/6 the field is considerably smoother, indicating that in low resolution GCMs the surface characteristics are not detailed enough, so as to allow for adequate friction and cause the moisture fluxes to recurve around mountainous areas. Particularly during December and January when the north-easterly monsoon is intensified, the moisture flux at the northeast of SAF is intercepted in both CORDEX ensembles, however not in CMIP5/6. After February the atmospheric flow from the northeast is weakened and it is strengthened at the southeastern part, entering SAF through Mozambique. This moisture transport originates from the Mascarene High that has developed over the South Indian Ocean. The recurvature of moisture seen at the south-eastern part of Mozambique is caused by the Mozambique Channel Trough (Barimala et al., 2018).

AUTHOR'S CHANGES IN MANUSCRIPT: In the manuscript we comment concerning the moisture transport entering SAF from the northeastern part, by adding the following text as the last sentence of paragraph 3 in Section 3.2: "The improvement of orography has a further effect in blocking moisture transport entering SAF from the northeast, especially during Dec-Jan, as seen in Fig. 5."

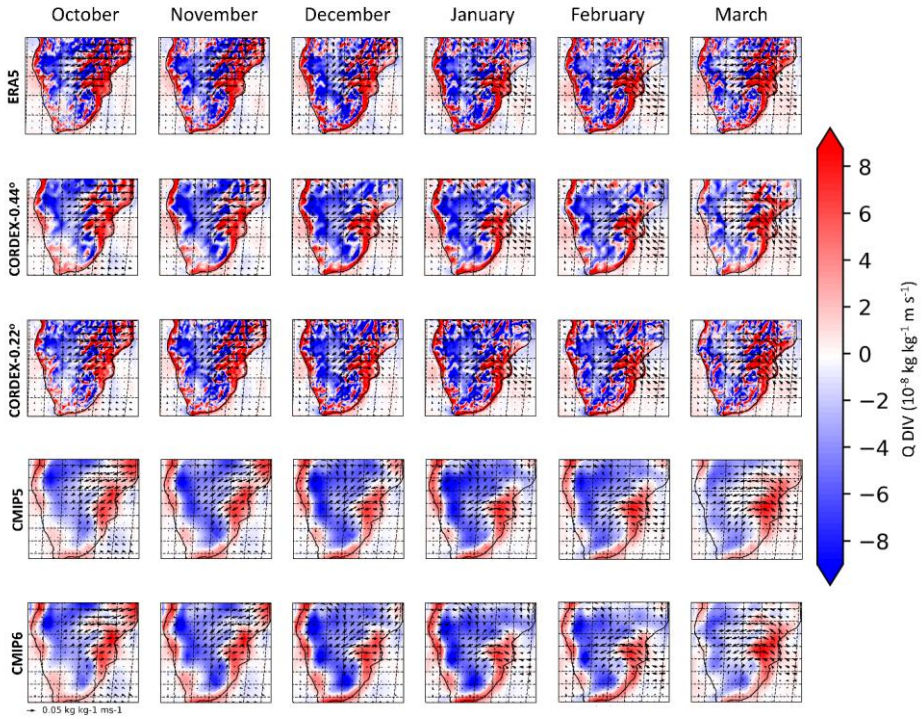

Figure 1: Moisture flux and divergence at 850 hPa.

2nd Comment:

Page 9, section 3.3. It should be made clear why there is a special focus on the Angola low given the different processes that significantly affect the rainfall in the area. For example, the cloudband or tropical temperate trough is one of the major processes that drive rainfall in SAF but is never mentioned here. I would even suggest including the cloudbands in the analyzes.

AUTHOR'S RESPONSE: Thank you very much for this comment. Indeed, not mentioning the Tropical Temperate Troughs (TTTs) in the manuscript is a lack, since TTTs are one of the main mechanisms producing precipitation over southern Africa. We now refer to the role they play for precipitation over southern Africa in the results section (section 3.3), where findings about the Angola Low have further implications for the formation of TTTs.

More specifically, the reason why we chose to put an emphasis on the Angola Low pressure system is that usually Angola Low events precede the formation of TTTs and hence, they can be considered as their precursor in the "climate process chain" controlling precipitation over southern Africa (Daron et al., 2019). As stated in Howard et al., 2018, it is common that Angola Low events precede TTT events, since the Angola Low pressure system functions as a key process necessary for the transport of water vapor from the tropics towards the extratropics (Hart et al., 2010).

In addition, based on a Scopus query investigating the number of documents with the keywords "Angola Low" and "Tropical Temperate Troughs" in the Title-Abstract-Keywords, we saw that TTTs have received almost the double attention in the literature (47 published papers), relative to the Angola Low (23 published papers). Hence, our work is, in part, an attempt to address this gap, considering the limitations set by the availability of variables in all the ensembles that are currently examined (CORDEX-Africa 0.22º/0.44º and CMIP5/6). For this reason, we did not include an analysis of the TTTs, since it is beyond of the scope of the current study, but it is imperative that a comparative analysis of how TTTs are simulated in CORDEX-Africa 0.22º/0.44º and CMIP5/6 is performed.

MINOR REVISIONS: In lines **749-755** we now include the following sentences:

"More specifically, the reason why we chose to put an emphasis on the AL pressure system, is that the AL redistributes low-tropospheric moisture entering SAF from the southern Atlantic and the southern Indian oceans and also, moisture transport originating from the Congo basin. In addition, AL events precede the formation of Tropical Temperate Troughs (TTTs) and hence, they can be considered as their precursor in the "climate process chain (Daron et al., 2019). As stated in Howard and Washington (2018), it is common that AL events precede TTT events, since the AL pressure system functions as a key process necessary for the transport of water vapor from the tropics towards the extratropics (Hart et al., 2010)."

3rd Comment:

Page 9, section 3.3. I wonder why theta850 is used to calculate the Angola low instead of the geopotential height (as in Munday et al., 2017) or the vorticity (as in Howard et al., 2018). The CMIP6 models do have these variables available and should be used for a fair comparison.

AUTHOR'S RESPONSE: Indeed, Munday and Washington, (2017) use the lowest 5% of mean DJF geopotential height at 850 hPa (zg850) over southern Africa. The reason why we were not able to use the same index in order to identify the Angola Low, was that within the context of CORDEX-Africa simulations, geopotential height at 850hPa is not available. Two of our ensembles (CORDEX-Africa 0.44º and CORDEX-Africa 0.22º) come from the CORDEX family and are lacking this variable. Hence, based on the variables that are already available within both CORDEX and CMIP5, we used potential temperature at 850 hPa (theta850) as an alternative "proxy" variable that provides thermodynamical information. In order to ensure that theta850 could be used instead of zg850, we examined the relationship between theta850 and zg850 over the study region in ERA5, for each month of the rainy season (Oct-Mar), using the climatological mean monthly values for the period 1986-2005. The comparison is depicted below as a series of maps and scatterplots. Each point in the scatterplots represents a pixel in the ERA5 dataset.

More specifically, in Figure 1 the mean monthly zg850 values for the period 1986-2005 are shown. During October, over the south-eastern part of Angola there is a region of low pressures. Moving towards the core of the rainy season, the low-pressure system deepens, while there seems to be a very weak extension of low pressures towards the south. In Figure 2 the mean monthly theta850 values for the period 1986-2005 are shown. As it is depicted, during October there is an array of high theta values located over south-eastern Angola, coinciding with the region of low zg850 values. As stated in Munday and Washington, (2017), this is indicative of the dry convection processes that are at play during the beginning of the rainy season over the region. Moving towards

DJF, the high theta850 values move southwards, indicating that in the core of the rainy season, convection over the greater Angola region is not thermally induced, but there is a rather dynamical large-scale driver. Through Figure 1 and Figure 2 we concluded that although theta850 is not a perfect proxy for zg850, it can be used to identify certain aspects of the Angola low pressure system, such as its strength and location during the rainy season.

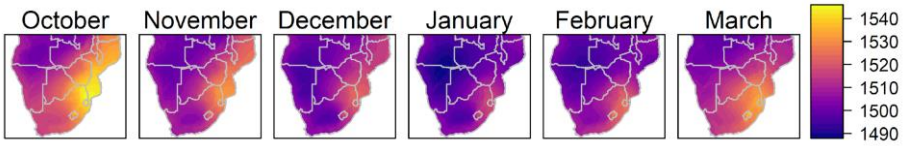

Figure 2: Mean monthly geopotential height at 850 hPa in ERA5 for the period 1986-2005.

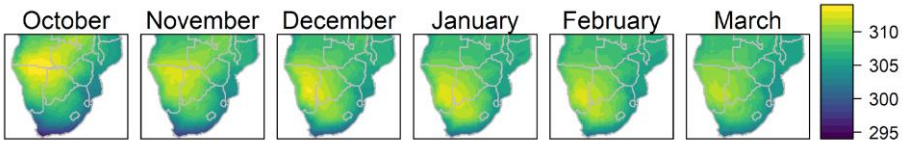

Figure 3: Mean monthly potential temperature at 850 hPa in ERA5 for the period 1986-2005.

In addition, in Figure 3 the scatterplots between zg850 (x-axis) and theta850 (y-axis) for each month of the rainy season for the period 1986-2005 are shown, over the whole southern Africa (land pixels only). The same plot, but with pixels only from the greater Angola region (14 ºE to 25 ºE and from 11 ºS to 19 ºS) is displayed in Figure 4. Although the relationship between the two variables is not perfectly linear, they display a considerable association, especially over the greater Angola region (Figure 4).

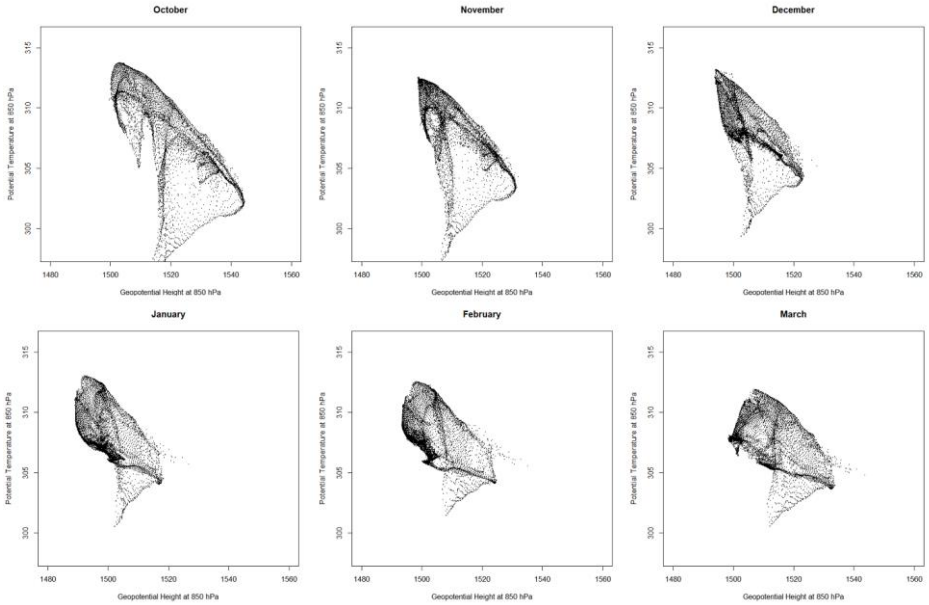

Figure 4: Geopotential height at 850 hPa (x-axis) plotted against Potential temperature at 850 hPa (y-axis). Values refer to climatological monthly means for the period 1986-2005. Each dot in the scatterplot represents a pixel of the ERA5 dataset over the whole southern Africa region 10 ºE to 42 ºE and from 10 ºS to 35 ºS.

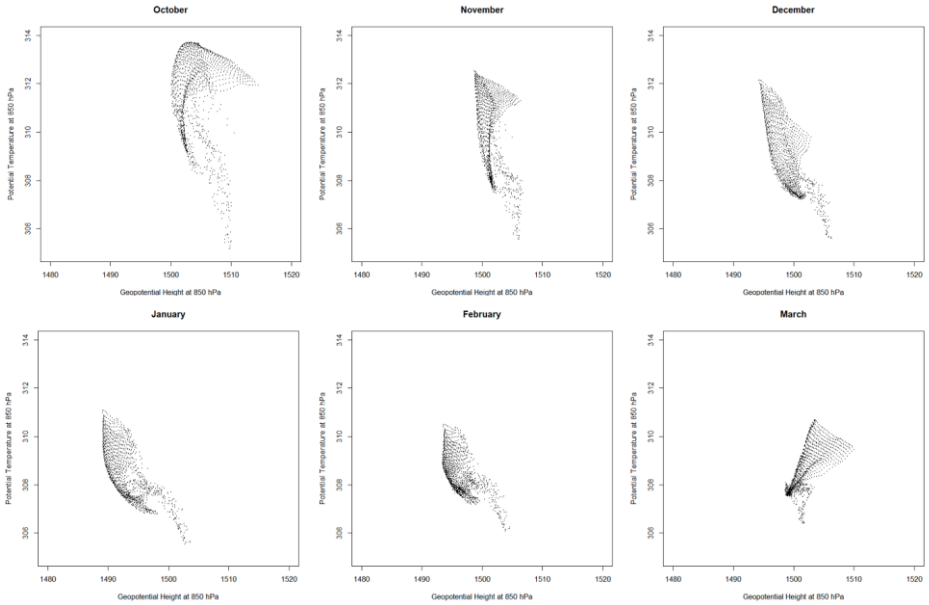

Figure 5: Geopotential height at 850 hPa (x-axis) plotted against Potential temperature at 850 hPa (y-axis). Values refer to climatological monthly means for the period 1986-2005. Each dot in the scatterplot represents a pixel of the ERA5 dataset over the whole southern Africa region 14 ºE to 25 ºE and from 11 ºS to 19 ºS.

Concerning relative vorticity (ζ) as used in Howard et al., 2018 we had to investigate the following issues: In Howard et al., 2018, they identify Angola Low events by using daily relative vorticity at 800 hPa. Although u and v wind components are available at 800 hPa in CMIP5/6, they are not available in CORDEX simulations. More specifically, in CORDEX-Africa, u and v wind components are only available at 850, 500 and 200 hPa. Hence, we had to investigate if we could use the 850 hPa pressure level (instead of 800) and if we did so, should we apply the same ζ threshold? In Howard et al., 2018, Angola Low events are identified within the region 14 ºE to 25 ºE and from 11 ºS to 19 ºS for mean daily ζ values $< -4 \times 10^{-5}$ s^{-1}. An additional issue that we took into account, is that u and v wind components at 850 hPa were not available on a daily timestep in CMIP6, but only on a monthly timestep. Hence, for consistency reasons we had to work with monthly files in all ensembles (both CMIP, CORDEX) and in ERA5. Lastly, some files from the CORDEX-Africa ensembles did not have complete timeseries (from 1986-2005), so they were not included in the calculation of the ensemble mean that eventually were used for the calculation of monthly relative vorticity. For CORDEX-Africa 0.22º these files were:

*850_AFR-22_MOHC-HadGEM2-ES_historical_r1i1p1_ICTP-RegCM4-7_v0.nc

*850_AFR-22_MPI-M-MPI-ESM-MR_historical_r1i1p1_ICTP-RegCM4-7_v0.nc

*850_AFR-22_NCC-NorESM1-M_historical_r1i1p1_ICTP-RegCM4-7_v0.nc

With regards to the fact that u and v wind components were available only on a monthly timestep in CMIP6, we compared the daily and monthly relative vorticity values at 800 hPa in ERA5 for all the months of the rainy season (Oct-Mar). The histograms are displayed below in Figure 6, with the daily ζ values as in Howard et al., 2018 on the left panel and the monthly values on the right. The difference in the y-axis results from the fact that when ζ is calculated using a daily timestep, the histogram is drawn using 5.421.825 values, while when the ζ is calculated using monthly u and v values, it is drawn using 178.200 values (for the period 1986-2005). The histograms display only cyclonic vorticities. Green lines display the threshold set by Howard et al., 2018 (ζ values $< -4 \times 10^{-5}$ s^{-1}), while red values display the threshold set by Desbiolles et al., 2020 (ζ values $< -1.5 \times 10^{-5}$ s^{-1}). As it is shown, using the distribution of the monthly values has a much shorter tail and the Howard et al., 2018 threshold appears to be very strict, as a criterion for the identification of Angola Low events.

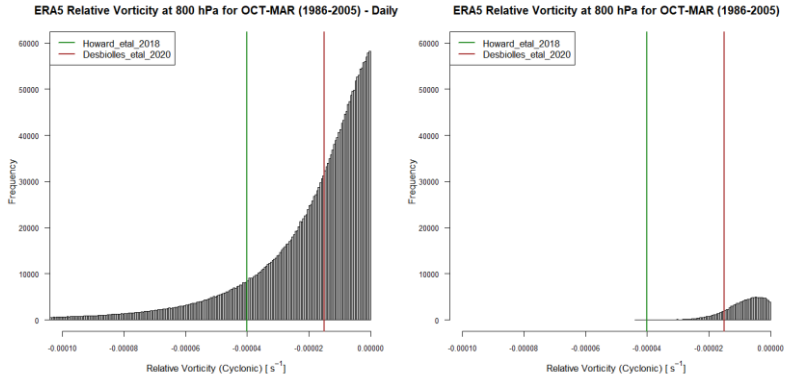

Figure 6: Histogram of relative vorticity for months Oct-Mar during 1986-2005 in ERA5 using daily u and v values (left) and using monthly u and v values (right). Pixels used are enclosed by the region from 14 ºE to 25 ºE and from 11 ºS to 19 ºS.

With regards to the question of whether the 850 pressure level can be used instead of 800 hPa as in Howard et al., 2018, we examine monthly relative vorticity in ERA5 in both pressure levels, within the region from 14 ºE to 25 ºE and from 11 ºS to 19 ºS. The results are displayed in Figure 6. Both distributions are very similar in shape, maxima and spread, although the distribution of ζ values at 800 hPa appear to have a shorter tail. On both panels, both the Howard et al., 2018 and Desbiolles et al., 2020 thresholds are indicated. We conclude that 850 pressure level can be used instead of 800 hPa.

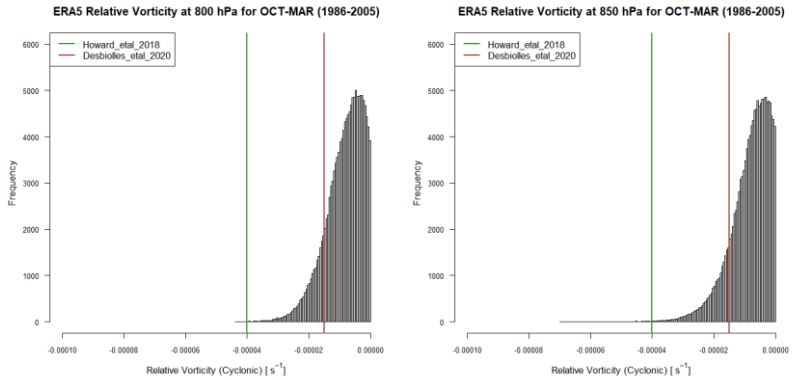

Figure 7: Histogram of relative vorticity for months Oct-Mar during 1986-2005 in ERA5 using u and v values at 800 hPa (left) and using u and v values at 850 hPa (right). Pixels used are enclosed by the region from 14 ºE to 25 ºE and from 11 ºS to 19 ºS. For both histograms mean monthly u and v values are used.

Lastly, with regards to the question of what the optimal threshold for the identification of Angola Low events in all datasets would be, we investigate the statistical distribution of mean monthly cyclonic vorticities in all ensembles used, for the 850 hPa pressure level. The results are displayed in Figure 7. In all histograms the Howard et al., 2018 and Desbiolles et al., 2020 thresholds are drawn. As it is indicated, the Howard et al., 2018 threshold is too strict and for 3 out of 4 ensembles it does not even correspond to existing ζ values. We conclude that the threshold used in Desbiolles et al., 2020 (ζ values $< -1.5 \times 10^{-5}$ s^{-1}) is reasonable, considering the shape of the distributions examined. However, when the Desbiolles et al., 2020 threshold was applied to the data, it was also found that it was too strict, especially for CMIP5/6. Hence, we now use monthly relative vorticity in order to identify Angola Low events, by employing the ζ values $< -1 \times 10^{-5}$ s^{-1} threshold.

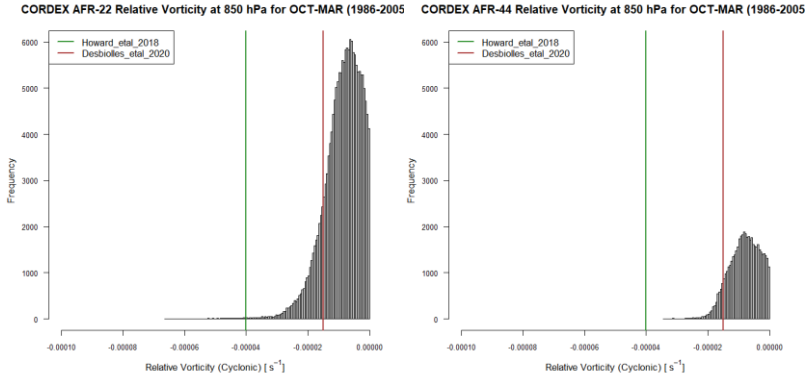

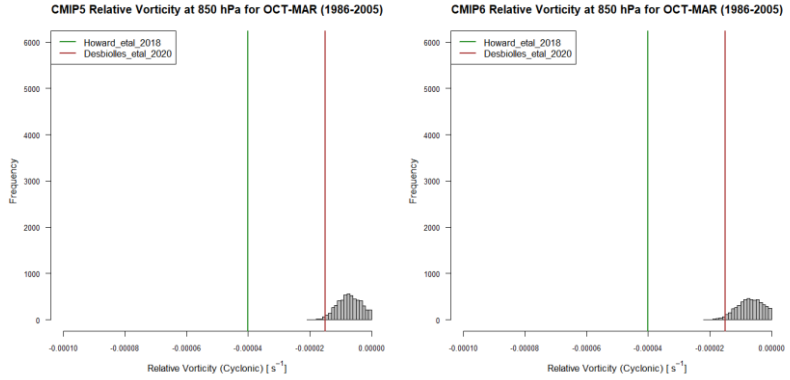

Figure 8: Histogram of relative vorticity for months Oct-Mar during 1986-2005 at 850 hPa for CORDEX-Africa at 0.22º (upper left), for CORDEX-Africa 0.44º (upper right), for CMIP5 (lower left), and for CMIP6 (lower right). Pixels used are enclosed by the region from 14 ºE to 25 ºE and from 11 ºS to 19 ºS. For all histograms mean monthly u and v values are used.

MINOR REVISIONS: In lines **756-797** we have added the following section, which is mainly taken from the answer provided above.

"In Munday and Washington (2017) AL events were identified using geopotential height at 850 hPa. However, since geopotential height is not available for CORDEX0.44/0.22 simulations, we could not employ this method. Hence, based on the variables that are already available within both CORDEX and CMIP5/6 ensembles, we use potential temperature at 850 hPa (theta850) as an alternative "proxy" variable that provides thermodynamical information. In order to ensure that theta850 can be used instead of zg850, we examine the relationship between theta850 and zg850 over the study region in ERA5, for each month of the rainy season (Oct-Mar), using the climatological mean monthly values for the period 1986-2005 (Fig. S1, S2). As shown in Fig. S1, during October over the south-eastern part of Angola, there is a region of low pressures. Moving towards the core of the rainy season, the low-pressure system deepens, while there seems to be a weak extension of low pressures towards the south. Also, as shown in Fig. S2, during October there is an area of high theta850 values located over south-eastern Angola, coinciding with the region of low zg850 values. As stated in Munday and Washington (2017), this is indicative of the dry convection processes that are at play during the beginning of the rainy season over the region. Moving towards DJF, the high theta850 values move southwards, indicating that in the core of the rainy season, convection over the greater Angola region is not thermally induced, but there is a rather dynamical large-scale driver. In Fig. S3 the scatterplots between zg850 (x-axis) and theta850 (y-axis) for each month of the rainy season are shown, over the whole southern Africa (land pixels only). The same plot, but with pixels only from the greater Angola region (14 ºE to 25 ºE and from 11 ºS to 19 ºS) is displayed in Fig. S4. Although the relationship between the two variables is not linear, they display a considerable association, especially over the greater Angola region.

In Howard and Washington (2018) AL events are identified using daily relative vorticity (ζ) at 800 hPa. Since u and v wind components are not available at 800 hPa (but at 850 hPa) for the CORDEX ensembles, we investigate whether the 850 hPa pressure level can be used instead. We also examine whether the ζ threshold has to be adjusted. In Howard and Washington (2018), AL events are identified within the region ranging from 14 ºE to 25 ºE and from 11 ºS to 19 ºS for mean daily ζ values $<-4 \times 10^{-5}$ s^{-1}. An additional issue that we take into account, is that u and v wind components are not available on a daily timestep for CMIP6, but only on a monthly timestep. Hence, for consistency reasons we work with monthly files in all ensembles (both CMIP, CORDEX) and in ERA5.

With regards to the question of whether the 850 hPa pressure level can be used instead of 800 hPa, we examine monthly relative vorticity in ERA5 in both pressure levels, within the region from 14 ºE to 25 ºE and from 11 ºS to 19 ºS (Fig. S5). Both distributions are very similar in shape, maxima and spread, although the distribution of ζ values at 800 hPa appear to have a shorter tail. On both panels, both the Howard and Washington (2018) and the Desbiolles et al. (2020) thresholds are indicated. We conclude that the 850 hPa pressure level can be used instead of 800 hPa. With regards to the fact that u and v wind components are available only on a monthly timestep in CMIP6, we compare the daily and monthly relative vorticity values at 800 hPa in ERA5 for all the months of the rainy season (Oct-Mar) (Fig. S6). The difference in the y-axis results from the fact that when ζ is calculated using a daily timestep, the histogram is drawn using 5.421.825 values, while when the ζ is calculated using monthly u and v values, it is drawn using 178.200 values (for the period 1986-2005). As shown, the distribution of the monthly values has a much shorter tail and the Howard and Washington (2018) threshold appears to be very strict, as a criterion for the identification of AL events.

Concerning the question of what the optimal threshold for the identification of AL events in all datasets is, we investigate the statistical distribution of mean monthly cyclonic vorticities in all ensembles used, for the 850 hPa pressure level (Fig. S7). We conclude that the threshold used in Desbiolles et al. (2020) (ζ values $<-1.5 \times 10^{-5}$ s^{-1}) is reasonable, considering the shape of the distributions examined. However, when the Desbiolles et al. (2020) threshold is applied to the data, it is also found to be too strict, especially for CMIP5/6. Hence, we identify AL events having ζ <-0.00001 s^{-1}. Lastly, we use geopotential height at 850 hPa for visual inspection only in ERA5 and CMIP5/6 ensembles."

4th Comment:

Page 9, section 3.3. Apart from the strength of the Angola Low, its position also plays an important role, which I suggest being included.

AUTHOR'S RESPONSE: Thank you. We now include mean monthly maps of relative vorticity (applying the $\zeta < -1 \times 10^{-5}$ s^{-1} threshold for the identification of Angola Low events) (shaded) and the potential temperature at 850 hPa overlayed on them in the form of contours.

AUTHOR'S CHANGES IN MANUSCRIPT: The following figure has been added displaying monthly climatologies of the Angola Low pressure system during the rainy season for the period 1986-2005. Filled contours indicate cyclonic relative vorticity (ζ) for $\zeta < -0.00001$ s^{-1} over the region extending from 14 ºE to 25 ºE and from 11 ºS to 19 ºS. Red lines indicate the isotherms of potential temperature at 850 hPa, having an increment of 2 K. Blue lines indicate isoheights of the geopotential height at 850 hPa, having an increment of 5 m. CORDEX0.44/0.22 are not plotted with geopotential isoheights, because this variable was not available for CORDEX simulations. From top to bottom: ERA5, ensemble mean of CORDEX0.22º, CORDEX0.44º, CMIP5 and CMIP6 simulations.

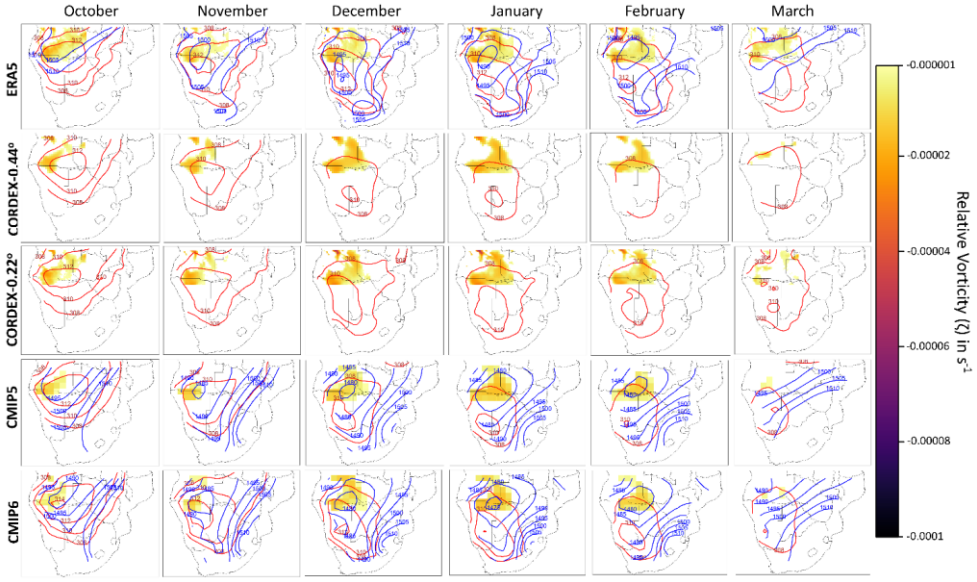

5th Comment:

Page 10, Section 3.5. It would be good to also see how many models agree on the sign of the trends in addition to the significance in Fig S5.

AUTHOR'S RESPONSE: Thank you for this suggestion. We now include the following figure in the supplementary material, displaying the number of models in each ensemble that display either increasing or decreasing trends.

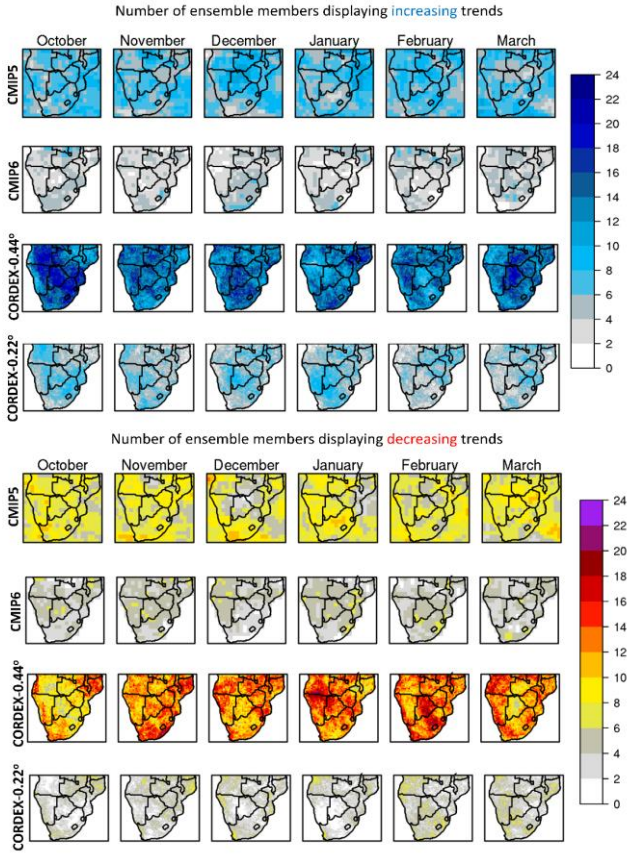

Figure 9: Number of ensemble members in each ensemble displaying increasing or decreasing trends.

Precipitation over southern Africa: Is there consensus among GCMs, RCMs and observational data?

Maria Chara Karypidou[1], Eleni Katragkou[1], Stefan Pieter Sobolowski[2]

[1] Department of Meteorology and Climatology, School of Geology, Faculty of Sciences, Aristotle University of Thessaloniki, Thessaloniki, Greece
[2] NORCE Norwegian Research Centre, Bjerknes Centre for Climate Research, Bergen, Norway

Correspondence to: karypidou@geo.auth.gr

Abstract. The region of southern Africa (SAF) is highly vulnerable to the impacts of climate change and is projected to experience severe precipitation shortages in the coming decades. Ensuring that our modelling tools are fit for the purpose of assessing these changes is critical. In this work we compare a range of satellite products along with gauge-based datasets. Additionally, we investigate the behaviour of regional climate simulations from the Coordinated Regional Climate Downscaling Experiment (CORDEX) – Africa domain, along with simulations from the Coupled Model Intercomparison Project Phase 5 (CMIP5) and Phase 6 (CMIP6). We identify considerable variability in the standard deviation of precipitation between satellite products that merge with rain gauges and satellite products that do not, during the rainy season (Oct-Mar), indicating high observational uncertainty for specific regions over SAF. Good agreement both in spatial pattern and the strength of the calculated trends is found between satellite and gauge-based products, however. Both CORDEX-Africa and CMIP5 ensembles underestimate the observed trends during the analysis period. The CMIP6 ensemble displayed persistent drying trends, in direct contrast to the observations. The regional ensembles exhibited improved performance compared to ~~its~~ their forcing (CMIP5), when the annual cycle and the extreme precipitation indices were examined, confirming the added value of the higher resolution regional climate simulations. The CMIP6 ensemble displayed a similar behaviour to CMIP5 but~~, however~~ reducing slightly the ensemble spread. However, we show that reproduction of some key SAF phenomena, like the Angolan Low (which exerts a strong influence on regional precipitation), still poses a challenge for the global and regional models. This is likely a result of the complex climatic process that take place. Improvements in observational networks (both in-situ and satellite), as well as continued advancements in high-resolution modelling will be critical, in order to develop a robust assessment of climate change for southern Africa.

1 Introduction

The region of Sub-Saharan Africa has been characterized as one of the most vulnerable regions to climate change (Kula et al., 2013; Serdeczny et al., 2017) and more specifically, the region of southern Africa (SAF) has been identified as a climate change hotspot (Diffenbaugh and Giorgi, 2012). Taking into consideration that the majority of the population living in SAF (70%) is dependent on rainfed agriculture (Mabhaudhi et al., 2018), any climate change induced alteration of the spatiotemporal patterns of precipitation will require a rapid adaptation of the agricultural sector. Concurrently, SAF is also characterized by low adaptive capacity to changes in climatic conditions (Davis and Vincent, 2017), hence, it emerges as a high risk region. In addition, approximately 26% of the SAF population is undernourished (AFDB, 2019). This figure is expected to increase significantly by 2050 (Tirado et al., 2015). Apart from the impacts on the agricultural sector though, climatic changes are expected to alter the spatiotemporal patterns of vector-borne disease occurrence (Rocklöv and Dubrow, 2020), cause severe damage to infrastructure and road networks (Chinowsky et al., 2015) and exacerbate poverty (Azzarri and Signorelli, 2020). Due to these impacts it is critical that the current spatiotemporal patterns of precipitation are accurately reproduced by our modelling systems and observations (whether in-situ, reanalysis or satellite) over SAF. Only then can we credibly assess future climate change impacts and inform strategies aiming to mitigate their effects on local communities.

Towards this end, satellite, gauge-based and reanalysis products are extensively used, in order to monitor current spatial and temporal precipitation patterns and to further characterize precipitation variability and change during recent decades. For future projections however, climate models able to simulate the (thermo)dynamical processes of the atmosphere are employed. Such an endeavor has been performed in the context of the Coupled Model Intercomparison Project Phase 5 (CMIP5) (Taylor et al., 2012) using General Circulation Models (GCMs) and in the context of the Coordinated Regional Climate Downscaling Experiment (CORDEX) – Africa domain (Giorgi and Gutowski, 2015) using Regional Climate Models (RCMs). The latest advancement in the climate modelling community involves GCMs and earth system models (ESMs), participating in the CMIP6 ensemble, providing input for the 6th Assessment Report of the Intergovernmental Panel on Climate Change (IPCC) (Eyring et al., 2016). However, the confidence with which one can claim future climate projections produced by GCMs, ESMs or RCMs are fit for purpose, is usually assessed based on their ability to simulate current climatic conditions. For instance, Munday and Washington (2018) showed that the CMIP5 ensemble displayed a systematic wet bias over the SAF region that was caused by the misrepresentation of orographic features located over the area of Tanzania. A wet bias caused by structural model errors was also identified in the dynamically downscaled and higher-resolution CORDEX-Africa ensemble (Kim et al., 2014). Therefore, a valid question arises as to what the most suitable dataset is, with which climate impact studies can be fed with when the SAF region is concerned. In addition, before the task of characterizing future precipitation trends is addressed, it is imperative to diagnose the degree to which observed precipitation trends over the recent decades are reproduced by GCMs and RCMs.

A comprehensive analysis of the performance of the CORDEX-Africa ensemble over Africa was first presented in (Nikulin et al., (2012a). They showed that during the rainy season (Jan-Mar as used in Nikulin et al. (2012)) there is a weak wet bias over southern Africa, and that the use of the ensemble mean was able to outperform individual models, highlighting the importance of ensemble-based approaches. The Nikulin et al. (2012) analysis was conducted on a pan-African scale. Similarly, (Kalognomou et al., (2013) analyzed the same ensemble of CORDEX-Africa simulations, focusing over southern Africa and reported similar findings. In (Meque and Abiodun, (2015) the same ensemble of 10 evaluation simulations was again used, but it was also compared with a set of CMIP5 GCM simulations, with the purpose to identify a causal association between ENSO and drought events over southern Africa. In Meque and Abiodun (2015) it was stated that RCMs were able to provide added value, compared to their driving GCMs. A comprehensive assessment of the added value between historical CORDEX-Africa RCMs simulations and of their driving CMIP5 GCMs on a seasonal timescale over the whole of Africa, was performed in (Dosio et al., (2019a). The first time the CORDEX-Africa ensemble is (Abba Omar and Abiodun, 2017) compared to both CMIP5 and CMIP6 ensembles is presented in Dosio et al. (2021). More specifically, in (Dosio et al., (2021) the analysis is performed on a seasonal timestep and on pan-African scale and its particular emphasis is placed on the projected changes of future precipitation, although a part of the analysis is dedicated to the period 1981-2010.

Satellite and gauge-based datasets display increasing trends during the historical period (Gu et al., 2016; Harrison et al., 2019) for annual and seasonal precipitation over SAF (32-42 mm year^{-1} per decade), an observation that is also identifiable in the Atmospheric Model Intercomparison Project (AMIP), but not in CMIP5 (Maidment et al., 2015). During DJF, precipitation trends over SAF display a remarkably robust signal in gauge-based, satellite and AMIP datasets (Maidment et al., 2015). In addition, Onyutha (2018) also reported on the increasing precipitation trends over SAF during DJF, especially after the 1960's. However, according to CMIP5, precipitation is projected to decrease over SAF in the 21st century (IPCC, 2013). This estimate also holds for simulations performed using RCMs forced with CMIP5 (Pinto et al., 2016; Dosio et al., 2019b). The increase of the observed precipitation trends over SAF has been attributed to the recent strengthening of the Pacific Walker Circulation (PWC) (Maidment et al., 2015), which is captured in observational datasets and in AMIP simulations, but not in CMIP5 (L'Heureux et al., 2013; Yim et al., 2016). CMIP6 displays an even more robust future decline in precipitation and increase of drought events over SAF, relative to its predecessor (Ukkola et al., 2020). However, although the CMIP6 ensemble exhibits multiple improvements on various levels (Wyser et al., 2020), still, certain biases and challenges identified in CMIP5 during the historical period, persist in CMIP6 (Kim et al., 2020). However, although the CMIP6 ensemble exhibits multiple improvements on various levels (Wyser et al., 2020), certain biases and challenges identified in CMIP5 during the historical period persist in CMIP6 (Kim et al., 2020).

RCMs are known to add value to climate simulations over regional scales, mainly because the spatial resolution increases, resolving atmospheric waves in a more detailed manner and also, because surface characteristics interacting with the atmosphere are represented more accurately (Denis et al., 2003; Giorgi et al., 2014). Considering the aforementioned challenges displayed in the CMIP5 simulations to accurately capture precipitation amounts under current climatic conditions and recent precipitation trends, we investigate the degree to which this observation holds also for RCMs, forced with GCMs

Formatted: Indent: First line: 0.19"

Formatted: Font: 10 pt

Formatted: Font: 10 pt

Formatted: Font: 10 pt

Formatted: Font: 10 pt

Formatted: Font: 10 pt

participating in the CMIP5 ensemble. Theory tells us that RCMs develop their own physics. However, often times the impact of the driving GCMs is evident on the RCM simulations (Denis et al., 2003; Laprise et al., 2008; Di Luca et al., 2013; Giorgi, 2019).

Therefore, in this paper we expand on previous research to investigate how monthly precipitation during the rainy season over southern Africa is simulated by different modelling systems, by analyzing the monthly precipitation climatologies, the interannual variability, specific precipitation indices and monthly precipitation trends during the period 1986-2005, in four different modeling systems (CORDEX 0.22º/0.44º, CMIP5/6) and observational ensembles (satellite, reanalysis and gridded datasets). Our main goal is to provide a comprehensive overview with regards to precipitation climatology over SAF as simulated by the state-of-the-art tools used by climate scientists. In addition, we investigate whether higher resolution models are able to provide an improved representation of precipitation over southern Africa and we investigated how a particularly important atmospheric feature, the Angola Low (AL), pressure system, is simulated in the RCM and GCM ensembles.~~Therefore, in this paper we investigate monthly precipitation climatologies and interannual variability and calculate precipitation trends in CMIP5 and CORDEX-Africa simulations, in order to assess whether the CORDEX-Africa ensemble provides any improvement in the simulation of precipitation over the SAF region. We also assess whether the CMIP6 ensemble resolves the issues identified in CMIP5. We additionally assess monthly precipitation climatologies and trends in a set of satellite, gauge-based and reanalysis datasets over the SAF region, in order to investigate the level of agreement between the various precipitation products that are often used for precipitation monitoring purposes or evaluation of climate models (Harrison et al., 2019; Alexander et al., 2020). The analysis is performed for the period 1986-2005 over the SAF region.~~

In Section 2 the data used are presented along with the methodology employed. ~~In Section 3 the results are presented and in Section 4 we provide the discussion of the analysis along with some concluding remarks.~~In Section 3 the results are presented. More specifically, the results are analyzed based on the monthly climatology, the annual cycle of precipitation, the AL pressure system, the ETCCDI precipitation indices and the monthly precipitation trends. Lastly, in Section 4 we provide the discussion of the analysis along with some concluding remarks.

2 Data and methodology

2.1 Data

We analyse daily and monthly precipitation from ~~4~~ 5 types of datasets, namely observational datasets (OBS), GCMs and ESMs that comprise the CMIP5 and CMIP6 ensembles and regional climate models (RCMs) that comprise the CORDEX-Africa ensemble at 0.44º of spatial resolution (CORDEX0.44) and at 0.22º of spatial resolution (CORDEX0.22). The analysis is concerned with the SAF region, which is defined as the area between 10 ºE to 42 ºE and 10 ºS to 35 ºS. The

Formatted: Font: 10 pt
Formatted: Font: 10 pt
Formatted: Font: 10 pt
Formatted: Font: 10 pt
Formatted: Font: 10 pt
Formatted: Font: 10 pt
Formatted: Font: 10 pt
Formatted: Font: 10 pt
Formatted: Superscript
Formatted: Superscript

analysed period is 1986-2005, as this is the period during which the estimates of all ~~4~~ 5 aforementioned datasets overlap. Although satellite and reanalysis products cannot be termed as purely "observational", in the context of the current work they are classified as such, in order to differentiate them from climate model datasets (CORDEX ~~-Africa~~0.44, CORDEX0.22, CMIP5, CMIP6). Hereafter "OBS" refers to satellite, gauge-based and reanalysis products.

2.1.1 Observational data

The OBS data used are based on the analysis of Le Coz and van de Giesen (2020) and are comprised of 5 gauge-based products (datasets that are derived by spatial interpolation of rain gauges and station data: CRU.v4.01, UDEL.v7, PREC/L.v0.5, GPCC.v7, CPC-Global.v1), 6 satellite products (given below) and 1 reanalysis product, ERA5. The datasets have a temporal coverage that extends through the analysed period (1986-2005). The gauge-based products were chosen so that they have a spatial resolution less than or equal to 0.5° x 0.5° and the satellite products have a spatial resolution less or equal to 0.25° x 0.25°. For satellite products however, there was an exception for 2 products (CMAP.v19.11and GPCP.v2.2) with a resolution equal to 2.5° x 2.5° that were also included in the analysis due to their wide use in the literature. The OBS ensemble is made of 12 products. More details concerning the OBS datasets are provided in Table S1. In certain parts of the following analysis the OBS products are either used collectively or they are split into sub-ensembles, based on the method(s) used for their production. More specifically, these sub-ensembles are the mean of all gauge-based precipitation products (Gauge-Based), the ensemble mean of satellite products that merge with rain gauges (Satellite-Merge) (ARC.v2, CMAP.v19.11, GPCP.v2.2) and the ensemble mean of satellite products that do not merge directly with rain gauges (Satellite-NoMerge) (CHIRPS.v2, TAMSAT.v3, PERSIANN-CDR), but they use alternative methods such as calibration, bias adjustment or artificial neural network techniques (Le Coz and van de Giesen, 2020).

2.1.2 Climate model simulations

We retrieved daily precipitation for a set of 26 RCM simulations performed as part of CORDEX-Africa historical simulations at 0.44° (~50 km) spatial resolution, comprising the CORDEX0.44 ensemble. We also retrieved a set of 10 RCM simulations performed also within CORDEX-Africa, as part of the CORDEX-CORE project (Coppola et al., 2021), available at 0.22° (~25 km) spatial resolution (CORDEX0.22). In addition, daily precipitation was retrieved for a set of 10 CMIP5 GCMs, with 3 additional simulations with variations in the GCM's resolution (IPSL-LR/IPSL-MR), the ocean model (GFDL-ESM2M/GFDL-ESM2G) and Realization/Initialization/Physics (ICHCE-EC-EARTH-r1i1p1/ ICHCE-EC-EARTH-r12i1p1). The CMIP5 models selected were the ones used as forcing in the CORDEX ~~-Africa~~0.44 historical simulations. In total, precipitation from a set of 13 CMIP5 simulations was used. Additionally, we exploited daily precipitation from a set of 8 CMIP6 GCM and ESM simulations. The CMIP6 simulations selected were performed with the updated versions of the same models that were part of the CMIP5 ensemble. This selection served to construct CMIP5 and CMIP6 ensembles that

Formatted: Superscript

were comparable. Precipitation data for all simulations were retrieved from the Earth System Grid Federation (ESGF). In addition, we retrieved temperature at 850 hPa for ~~the CORDEX-Africa~~both CORDEX0.44/0.22 from ESGF. For the CMIP5 and CMIP6 simulations temperature and geopotential height at 850 hPa was retrieved from the Climate Data Store (CDS). Geopotential height at 850 hPa was not available for CORDEX-Africa simulations. ~~Temperature at 850 hPa was not available for CMIP6, hence the CMIP6 ensemble is not included in the analysis employing temperature at 850 hPa.~~ Lastly, elevation data for CORDEX-Africa and CMIP5 were obtained from ESGF, while the Shuttle Radar Topography Mission (SRTM) (Farr et al., 2007) Digital Elevation Model was used as the observed elevation in the topography transects for a selected latitude over SAF. Details about the models used are provided in Tables S2-S5~~4~~.

2.2 Methodology

Precipitation climatologies are investigated on a monthly basis, due to the fact that precipitation over SAF arises as the result of atmospheric mechanisms that display high variability during the rainy season. The aggregation of precipitation to seasonal means might often obscure certain spatial characteristics that are better identified on a monthly basis. The within-ensemble agreement is investigated using the sample standard deviation (SD), which is calculated using monthly mean values over the period 1986-2005 for each model (or observational dataset) separately.~~.~~ We also employ 4 precipitation indices constructed in the context of the Expert Team on Climate Change Detection and Indices (ETCCDI) (Peterson and Manton, 2008), utilising daily precipitation amounts for the period 1986-2005. The 4 ETCCDI indices are used to describe total annual precipitation (PRCPTOT), annual maximum daily precipitation (Rx1Day), annual number of days with daily precipitation >10 mm (R10mm) and annual number of days with daily precipitation >20 mm (R20mm). These indices are calculated for each individual simulation (CMIP5, CMIP6, ~~and~~ CORDEX0.44 and CORDEX0.22), and OBS products, separately and yield a value for every year (Jan ~~Dec~~-Dec) during the period 1986-2005. The calculation of indices required data having a daily temporal resolution, hence, observational datasets that provided monthly aggregates are excluded. The spatial averages calculated over SAF for the annual cycle and the ETCCDI indices consider land pixels only. For the construction of ensemble means, either in observational or model ensembles, datasets were remapped to the coarser grid using conservative remapping for precipitation and bilinear interpolation for temperature at 850 hPa.

In order to investigate some basic thermodynamical aspects that may differentiate precipitation in the CMIP5/6 and the CORDEX-~~Africa~~0.44/0.22 ensembles, we look into the seasonal representation of the Angola L~~l~~ow (AL) pressure system over SAF. The AL pressure system is a semi-permanent synoptic scale system, that plays a strong role in modulating precipitation over SAF (Reason and Jagadheesha, 2005; Lyon and Mason, 2007; Crétat et al., 2019; Munday and Washington, 2017; Howard and Washington, 2018). More specifically, the reason why we chose to put an emphasis on the AL pressure system, is that the AL redistributes low-tropospheric moisture entering SAF from the southern Atlantic and the southern Indian oceans and also, moisture transport originating from the Congo basin. In addition, AL events precede the

Formatted: Font: 10 pt

Formatted: Indent: First line: 0.16"

formation of Tropical Temperate Troughs (TTTs) and hence, they can be considered as their precursor in the "climate process chain (Daron et al., 2019). As stated in (Howard and Washington, (2018), it is common that AL events precede TTT events, since the AL pressure system functions as a key process necessary for the transport of water vapor from the tropics towards the extratropics (Hart et al., 2010).

In (Munday and Washington, (2017) AL events were identified using geopotential height at 850 hPa(Howard and Washington, 2018). However, since geopotential height is not available for CORDEX0.44/0.22 simulations, we could not employ this method. Hence, based on the variables that are already available within both CORDEX and CMIP5/6 ensembles, we use potential temperature at 850 hPa (theta850) as an alternative "proxy" variable that provides thermodynamical information. In order to ensure that theta850 can be used instead of zg850, we examine the relationship between theta850 and zg850 over the study region in ERA5, for each month of the rainy season (Oct-Mar), using the climatological mean monthly values for the period 1986-2005 (Fig. S1, S2). As shown in Fig. S1, during October over the south-eastern part of Angola, there is a region of low pressures. Moving towards the core of the rainy season, the low-pressure system deepens, while there seems to be a weak extension of low pressures towards the south. Also, as shown in Fig. S2, during October there is an area of high theta850 values located over south-eastern Angola, coinciding with the region of low zg850 values. As stated in (Munday and Washington, (2017), this is indicative of the dry convection processes that are at play during the beginning of the rainy season over the region. Moving towards DJF, the high theta850 values move southwards, indicating that in the core of the rainy season, convection over the greater Angola region is not thermally induced, but there is a rather dynamical large-scale driver. In Fig. S3 the scatterplots between zg850 (x-axis) and theta850 (y-axis) for each month of the rainy season are shown, over the whole southern Africa (land pixels only). The same plot, but with pixels only from the greater Angola region (14 °E to 25 °E and from 11 °S to 19 °S) is displayed in Fig. S4. Although the relationship between the two variables is not linear, they display a considerable association, especially over the greater Angola region.

In (Howard and Washington, (2018) AL events are identified using daily relative vorticity (ζ) at 800 hPa. Since u and v wind components are not available at 800 hPa (but at 850 hPa) for the CORDEX ensembles, we investigate whether the 850 hPa pressure level can be used instead. We also examine whether the ζ threshold has to be adjusted. In (Howard and Washington, (2018), AL events are identified within the region ranging from 14 °E to 25 °E and from 11 °S to 19 °S for mean daily ζ values $< -4 \times 10^{-5}$ s^{-1}. An additional issue that we take into account, is that u and v wind components are not available on a daily timestep for CMIP6, but only on a monthly timestep. Hence, for consistency reasons we work with monthly files in all ensembles (both CMIP, CORDEX) and in ERA5.

With regards to the question of whether the 850 hPa pressure level can be used instead of 800 hPa, we examine monthly relative vorticity in ERA5 in both pressure levels, within the region from 14 °E to 25 °E and from 11 °S to 19 °S (Fig. S5). Both distributions are very similar in shape, maxima and spread, although the distribution of ζ values at 800 hPa appear to have a shorter tail. On both panels, both the(Howard and Washington, 2018; Desbiolles et al., 2020) (Howard and Washington, (2018) and the (Desbiolles et al., (2020) thresholds are indicated. We conclude that the 850 hPa pressure level can be used instead of 800 hPa. With regards to the fact that u and v wind components are available only on a monthly

Formatted: Normal, Line spacing: single

Formatted: Font: (Default) Times New Roman, Font color: Text 1

Formatted: English (United States)

timestep in CMIP6, we compare the daily and monthly relative vorticity values at 800 hPa in ERA5 for all the months of the rainy season (Oct-Mar) (Fig. S6). The difference in the y-axis results from the fact that when ζ is calculated using a daily timestep, the histogram is drawn using 5.421.825 values, while when the ζ is calculated using monthly u and v values, it is drawn using 178.200 values (for the period 1986-2005). ~~(Howard and Washington, 2018)(Desbiolles et al., 2020)~~As shown, the distribution of the monthly values has a much shorter tail and the ~~(~~Howard and Washington~~,~~ ~~(~~2018) threshold appears to be very strict, as a criterion for the identification of AL events.

Concerning the question of what the optimal threshold for the identification of AL events in all datasets is, we investigate the statistical distribution of mean monthly cyclonic vorticities in all ensembles used, for the 850 hPa pressure level (Fig. S7). We conclude that the threshold used in ~~(~~Desbiolles et al.~~,~~ ~~(~~2020) (ζ values $<-1.5 \times 10^{-5}$ s^{-1}) is reasonable, considering the shape of the distributions examined. However, when the Desbiolles et al. (2020) threshold is applied to the data, it is also found to be too strict, especially for CMIP5/6. Hence, we identify AL events having ζ <-0.00001 s^{-1}. Lastly, we use geopotential height at 850 hPa for visual inspection only in ERA5 and CMIP5/6 ensembles.

~~In order to investigate some basic thermodynamical aspects that may differentiate precipitation in the CMIP5 and the CORDEX-Africa ensembles, we look into the seasonal representation of the Angola low (AL) pressure system over SAF. The AL pressure system is a semi-permanent synoptic scale system, that plays a strong role in modulating precipitation over SAF (Reason and Jagadheesha, 2005; Lyon and Mason, 2007; Crétat et al., 2019; Munday and Washington, 2017; Howard and Washington, 2018). In the current work, we use potential temperature at 850 hPa (theta850), as an indication of the strength of the AL pressure system over the SAF region. Potential temperature at 850 hPa is calculated using Poisson's equation (https://glossary.ametsoc.org/wiki/Poisson_equation).~~

Lastly, the Theil-Sen's slope (Theil, 1992; Sen, 1968) for monthly precipitation during the period 1986-2005 is calculated for each dataset. This is a non-parametric approach to estimate trends, that is insensitive to outliers. Statistical significance is assessed using the Mann-Kendall test (Mann, 1945; Kendall, 1948).

3 Results

3.1 Climatology

Figure 1 displays monthly precipitation climatologies during Oct-Mar (rainy season over the study region) for ERA5 and for the ensemble means of ~~6~~ 7 additional types of datasets. At the beginning of the rainy season (Oct) all products display precipitation maxima at the north-western part of the study region. Another precipitation maxima is observed at eastern South Africa. For both regions, there is a slight tendency for gauge-based products to yield approximately 1 mm d^{-1} less precipitation than reanalysis and satellite products. The CMIP5, CMIP6, CORDEX0.44 and CORDEX0.22 ~~and CORDEX-Africa~~ ensembles are also in agreement with regards to the location and amounts, however, ~~CORDEX-Africa~~CORDEX0.44

Formatted: Indent: First line: 0"

Formatted: English (United States)

Formatted: English (United States)

Formatted: Superscript

Formatted: English (United States)

displays approximately 2 mm d^{-1} more precipitation over Angola. During November, the rainband extends southwards and the region over South Africa experiencing high precipitation enlarges.

Moving towards the core of the rainy season (DJF) the precipitation maxima extends southwards following the collapse of the Ceongo air boundary (CAB) (Howard and Washington, 2019) and high precipitation amounts are also observed over the eastern part of the study region. More specifically~~,~~ during January, high precipitation amounts (>10 mm d^{-1}) are observed over an extended region in northern Mozambique for non-merging satellite products (Satellite-NoMerge). This area is also identified as a region of high precipitation in gauge-based products and in merging satellite products, however, with a smaller magnitude. In ERA5, the spatial pattern of precipitation is more patchy and exhibits higher than observed precipitation amounts in the wider region of lake Malawi, reaching extremely high values (34 mm d^{-1}), as also indicated in the known precipitation issues of ERA5 over Africa (Hersbach et al., 2020). During DJF ~~the~~both CORDEX0.44 ~~CORDEX-Africa~~ and CORDEX0.22 ensembles display~~s~~ precipitation values >3 mm d^{-1} over almost all of the SAF region. This observation is also consistent in CMIP5 and CMIP6, however, maximum precipitation amounts in CMIP5 and CMIP6 are approximately >3 mm d^{-1} larger than in the CORDEX ~~-Africa~~ ensembles. It is noteworthy, that in CORDEX0.22 during DJF, there are parts over northern SAF experiencing precipitation amounts >10 mm d^{-1} a feature that is not seen in any of the observational products. After investigating the individual ensemble members used in the CORDEX0.22 ensemble (Fig. S8), we see that the excess amount of precipitation is removed from the CORDEX0.22 ensemble mean when RegCM4-7 simulations are not included (Fig. S9). In March, the rainband starts its northward shift, nevertheless, high precipitation amounts are still observed over the eastern parts of the study region and over the coastal region of Angola. The retreat of the rainband is evident in both CORDEX0.44 and CORDEX0.22 ~~CORDEX-Africa,~~ however, CMIP5 and CMIP6 still exhibit extended regions of high precipitation.

In Fig. 2, SD values for the ~~6~~7 ensembles are~~is~~ presented during months Oct-Mar for the period 1986-2005 expressed as mm d^{-1}. SD~~and~~ is used as a measure of the within-ensemble agreement. As it is shown for gauge-based products, during October and November high SD values are observed primarily over Angola. For months Dec-Mar Angola remains a high SD region, however, increased SD values are also observed over the eastern parts of ~~the study region~~SAF and especially over northern Mozambique. An important aspect influencing gauge-based products is the spatiotemporal coverage of the rain gauges used (Le Coz and van de Giesen, 2020), which is highly variable between regions and reporting periods. More specifically, after the 1970's the rain gauge coverage over Africa has decreased significantly (Janowiak, 1988) and the gauge network has been particularly sparse over the SAF region (Lorenz and Kunstmann, 2012; Giesen et al., 2014), which further implies that gauge-based products depend on extrapolating values from surrounding gauges. Therefore, station density and the interpolation method employed are key factors in determining the accuracy of the final product (Le Coz and van de Giesen, 2020). The high SD values over Angola, are mainly due to the scarcity of available rain gauges used in the interpolation method (Fig. ~~S1~~S10). After 1995, there is a noticeable reduction of the station/rain gauge data used over the SAF region (Fig. ~~S2~~S11) for 3 of the gauge-based products.

Formatted: English (United States)

Formatted: Subscript

Formatted: Not Superscript/ Subscript

Formatted: English (United States)

Formatted: English (United States)

A similar spatiotemporal pattern of SD is also observed in satellite-based products (Satellite-Merge) which employ algorithms that merge rain gauges with thermal-infrared (TIR) images. This is indicative of the strong impact that the location and number of rain gauges exert on satellite algorithms that employ merging techniques (Maidment et al., 2014, 2015). The spatiotemporal pattern of SD for satellite-based products that do not merge with gauges (Satellite-NoMerge) displays low SD values for October and November, however, during DJF localized areas of high SD appear over Angola, Zambia, Malawi and Mozambique. The satellite products used in this ensemble are based on TIR images and precipitation is indirectly assessed through cloud top temperature (Tarnavsky et al., 2014; Ashouri et al., 2015; Funk et al., 2015). Hence, the occurrence and severity of precipitation is calculated based on a temperature threshold. In cases that the threshold is set to very low cloud top temperature values, the algorithm has high skill at identifying deep convection, however, warm rain events are not adequately captured (Toté et al., 2015). As it is shown in Fig. 2, high SD values in non-merging satellite products are primarily observed over coastal regions and over regions where the elevation increases rapidly. These type of regions can be associated with orographic or frontal lifting of air masses (Houze, 2012), resulting in precipitation, without the threshold temperature of the cloud top being reached.

In the CORDEX-Africa0.44 ensemble SD values are >0.8 mm d^{-1} over almost all of the SAF region, however, very high SD values (3-9.8 mm d^{-1}) are observed in the coastal part of Angola and over the lake Malawi region during Nov-Mar. SD values in CORDEX0.22 are considerably larger throughout the greater part of SAF, especially during DJF. In the CMIP5 ensemble the spatiotemporal pattern of SD values exceeds 2 mm d^{-1} during Nov-Mar throughout the whole SAF region. CMIP6 displays a similar SD pattern. During March however, CMIP6 displays a substantial improvement in the agreement between its ensemble members. Overall, for the whole extent of SAF, the CORDEX-Africa ensembles displays greater agreement among ensemble members, however SD values become large over specific localized regions, mainly at western Angola and in the Malawi region. The CMIP5 and CMIP6 ensembles although not displaying the localized extreme SD values as CORDEX-Africa, displays generally high SD values throughout the whole extent of SAF.

3.2 Annual cycle

Figure 3 displays the annual cycle of precipitation in the CORDEX-AfricaCORDEX0.44, CORDEX0.22, CMIP5, CMIP6 and observational ensembles for land grid points. All datasets capture the unimodal distribution of precipitation over SAF, however considerable differences in precipitation amount and spread are observed.

Specifically, the CMIP5 ensemble exhibits significantly higher precipitation amounts than the CORDEX-Africaboth CORDEX and observational ensembles. This difference becomes particularly pronounced during the rainy season, with CMIP5 yielding approximately 2 mm d^{-1} more precipitation than the observational ensemble. It is also notable that for Nov-Feb, even the driest ensemble members of CMIP5 yield approximately 1 mm d^{-1} more precipitation than the wettest ensemble members of the observational data. This is in agreement with Munday and Washington (2018) who identified a systematic wet bias over SAF in CMIP5, that was associated with an intensified north-easterly transport of moisture that erroneously reaches SAF, due to the poorly represented orography in the region of Tanzania and Malawi (which would

hinder moisture originating from the Indian ocean from reaching SAF and instead force it to recurve towards the region of Madagascar). The behaviour of CMIP6 is similar to CMIP5, with a slightly smaller ensemble spread during Jan-Mar and a considerable reduction in spread during November.

The ~~CORDEX-Africa~~CORDEX0.44 ensemble reduces precipitation amounts during the core of the rainy season (DJF) compared to CMIP5, however, its behavior during the rest of the months is complicated. More specifically, during Aug-Oct ~~CORDEX-Africa~~CORDEX0.44 displays slightly higher precipitation amounts compared to CMIP5. During November, the difference between the CORDEX0.44~~CORDEX-Africa~~ and the CMIP5 ensembles becomes noticeable, with the CMIP5 ensemble mean becoming 0.4 mm d^{-1} larger than the CORDEX0.44~~-Africa~~ ensemble mean. During DJF the differences between the 2 ensembles maximize, with the CORDEX0.44~~-Africa~~ ensemble displaying good agreement with the OBS ensemble (<1 mm d^{-1} difference in the ensemble means of CORDEX0.44~~-Africa~~ and OBS). From March until July, the difference between the CORDEX0.44~~-Africa~~ and CMIP5 ensembles starts to reduce gradually. The ensemble mean of the CORDEX0.22 ensemble is similar to that of the CORDEX0.44 ensemble, however its spread during the rainy season is considerably larger. Taking into consideration that excess precipitation in the CORDEX0.22 ensemble is introduced by RegCM4-7, we observe that the ensemble spread of the CORDEX0.22 ensemble is reduced, when RegCM4-7 is not included in the CORDEX0.22 ensemble (Fig. S12).

Since the maximum impact of the north-easterly moisture transport into SAF responsible for the wet bias in CMIP5 occurs during DJF (Munday and Washington, 2018), the impact of the CORDEX~~-Africa~~0.44 and CORDEX0.22 increase in resolution and the effect of the improved representation of topography is also more intensely identified during DJF. As it is displayed in Fig. 4, surface orography is substantially improved in the CORDEX~~-Africa~~ ensembles, relative to CMIP5/6. The improvement of orography has a further effect in blocking moisture transport entering SAF from the northeast, especially during Dec-Jan, as seen in Fig. 5.

~~During the wet season (Oct-Mar) the spread within the members of each ensemble maximizes and is particularly large for CMIP5 (approximately 2 mm d^{-1}). In CORDEX-Africa the ensemble spread reaches 1 mm/d during the rainy season, while for the observational ensemble the spread is <0.5 mm d^{-1}. Overall, both CMIP5 and CORDEX-Africa ensembles capture the seasonal cycle of precipitation over SAF, however, CORDEX-Africa displays a substantial improvement with regards to precipitation amounts and spread.~~

3.3 Angola low

In Fig. 6~~5~~ the mean monthly climatology of the AL pressure system during the rainy season is displayed for the period 1986-2005. The AL is explored by means of relative vorticity, only within the region extending from 14 ºE to 25 ºE and from 11 ºS to 19 ºS. This region is characterized by ~~(~~Howard and Washington~~,~~ (2018) as the main region of interest for the AL. The relative vorticity for ζ <-0.00001 s^{-1} over the whole SAF is shown in Fig. S13. In addition, potential temperature at 850 hPa (theta850) is overlaid on relative vorticity, with the first contour set at 308 K, the last contour set at 318 K and the increment

Formatted: Font: 10 pt, Not Italic

between the isotherms being set to 2 K. For ERA5 and the ensemble means of CMIP5/6 the geopotential height at 850 hPa was also available. ~~annual cycle of theta850 for the CMIP5 and CORDEX-Africa ensembles and for ERA5 is displayed~~.

As shown in Fig. 6, ζ values for October are greater than >-0.000025 s^{-1} for ERA5 and CORDEX0.44/0.22 and are relatively weaker in CMIP5 and even weaker in CMIP6. The high cyclonic vorticity values overlap with the 312 K isotherm for all datasets. We also observe that the isoheights in the ERA5 and CMIP5/6 ensembles are closely collocated with the 312 K isotherms, indicating that the low pressure system observed over the region is caused by the excess heating of the air and hence, it is indicative of a typical heat low pressure system (Munday and Washington, 2017; Howard and Washington, 2018). Moving to November, the picture is similar however, the isotherms display a southward extension, while the 850 hPa isoheigths deepen ~5 m in ERA5 and CMIP5/6. In December, all datasets display an increase in cyclonic vorticity, however, the maximum heating area has migrated southwards over the Kalahari region. This fact indicates that cyclonic activity over the AL region is no longer due to thermal causes. During December and January the cyclonic activity is enhanced in all datasets and the isotherms have migrated even more southwards, forming the Kalahari heat low, which is distinct from the AL. We also observe that during January, the isoheights in ERA5 and CMIP5/6 become even deeper. We also note that the elongated trough during Dec-Jan can be indicative of the formation of TTTs, which account for a large proportion of rainfall over SAF (Hart et al., 2010). February displays similar spatial patterns to January for all datasets, however slightly weakened for all variables. In March, cyclonic activity over the region has seized. ~~In the current work, theta850 is used as an indication of the strength of the AL pressure system that is identified as one of the major mechanisms modulating precipitation over the SAF region. During the rainy season (Oct-Mar) the CORDEX-Africa ensemble displays lower values, with larger uncertainty, compared to the CMIP5 ensemble. Both RCM and GCM ensembles, display lower theta850 values throughout the year, relative to ERA5.~~ Taking into consideration the distribution of the cyclonic vorticity field, we observe that in higher resolution datasets (ERA5, CORDEX0.22) high vorticity values are more severe, on very localized regions. With respect to potential temperature, we observe for October and November all datasets having a similar distribution of theta850 values. We also note that CMIP6, in general, displays higher theta850 values and lower geopotential heights, relative to CMIP5. ~~association between precipitation and the strength of the AL, we can deduce that the AL has a weaker representation in the CORDEX-Africa ensemble, relative to CMIP5. This is also captured in Fig. S3, where potential temperature differences at 850 hPa from ERA5 are displayed for the CORDEX-Africa ensemble (CORDEX-Africa – ERA5) and for the CMIP5 ensemble (CMIP5 – ERA5). Values refer to the monthly climatological mean differences, for the period 1986-2005. The regions of maximum heating at 850 hPa are displayed in Fig. S4. Both ensembles display the southward migration of the area of maximum heating during the rainy season, following the seasonal cycle of the AL pressure system (Munday and Washington, 2017). The region of maximum heating in both intensity and extent is observed during Oct-Nov for both the CORDEX-Africa and the CMIP5 ensembles, when the AL is primarily a heat low, while during Dec-Feb it acquires tropical low characteristics (Howard and Washington, 2018).~~

Formatted: Indent: First line: 0.19"

Formatted: English (United States)

Formatted: Superscript

~~The fact that the CORDEX-Africa ensemble displays lower values of potential temperature at 850 hPa relative to CMIP5, may partly explain why the CORDEX-Africa ensemble displays lower monthly precipitation values than the CMIP5 ensemble, at least over this region.~~

3.4 Precipitation indices

Total annual precipitation (PRCPTOT) is displayed in Fig. ~~6~~7 (a). The mean of the CMIP~~5~~6 ensemble displays the largest amounts of PRCPTOT (approximately 1000 mm year^{-1}), with CMIP5 following closely. The CORDEX~~-Africa~~0.44 and CORDEX0.22 ensembles~~ ensemble~~ display a very similar behaviour, systematically ~~reduces~~ reducing ~~this~~ PRCPTOT amounts seen in CMIP5/6 by approximately 200 mm year^{-1}, yielding PRCPTOT values closer to that of the observational datasets. Both CMIP5/6 and CORDEX~~-Africa~~0.22/0.44 ensembles display similar within-ensemble variability. The ensemble mean of the observational datasets is considerably lower than CORDEX~~-Africa~~ ensembles and ~~it~~ displays an interannual variability between 500-800 mm year^{-1}. Both the ensemble means of CMIP5/6 and CORDEX~~-Africa~~0.44/0.22 fail to reproduce the interannual variability of the observational ensemble. ~~The ensemble mean in CMIP6 is comparable to CMIP5, however, CMIP6 displays more distinct interannual variability.~~ In Fig. ~~6~~7 (b) the annual maximum 1 day precipitation (Rx1Day) is displayed. For Rx1Day, the mean of the CMIP5 ensemble is in close agreement with the mean of the observational ensemble (approximately 40 mm d^{-1}). The ensemble mean of CORDEX~~-Africa~~0.44 yields larger precipitation amounts (approximately 55 mm d^{-1}) than CMIP5 and the observational ensemble. The CORDEX0.22 ensemble mean displays even higher values (approximately 75 mm d^{-1}). As it is shown in Fig. ~~6~~7 (b), the CORDEX~~-Africa~~0.44 ensemble mean is influenced by higher Rx1Day values, originating from ensemble members that cluster within the range 65-85 mm d^{-1}. The spread of the CMIP5 ensemble is comparable to that of the observational data, however, the CORDEX~~-Africa~~0.44/0.22 ensemble spread~~s~~ ~~is~~ are still larger, ranging from 25-85 and from 55-100 mm d^{-1}~~.~~, respectively. The CMIP6 ensemble falls between the CORDEX0.44~~-Africa~~ and CMIP5 ensembles, with a spread comparable to that of CMIP5. In Fig. ~~6~~7 (c) the annual number of days with daily precipitation greater than 10 mm (R10mm) is presented. It is noted that the ensemble mean of the CORDEX~~-Africa~~0.44 ensemble close~~r~~ to that of the observational datasets (~~20-~~~25 days year^{-1}~~-~~ with daily precipitation greater than 10 mm), while the ensemble mean of CORDEX0.22 almost coincides with the mean of the observational datasets. The mean of the CMIP5 ensemble yields approximately 34 days of extreme precipitation annually. It is also highlighted that the CMIP5 ensemble displays a large range of R10mm values (10-55 days year^{-1}). Again, the CMIP6 ensemble mean coincides with that of CMIP5~~, however, displaying a smaller ensemble spread~~. In Fig. ~~6~~7 (d) the annual number of days with daily precipitation greater than 20 mm (R20mm) is shown. There is close agreement between the CMIP5 and CORDEX~~-Africa~~0.44 ensembles, however both datasets overestimate R20mm relative to the observational data. Again, the CMIP5 ensemble displays the largest spread and a very weak interannual variability is seen on both CMIP5 and CORDEX~~-Africa~~0.44 ensemble means. The CMIP6 ensemble mean is slightly ~~greater~~ larger than its predecessor. R20mm in CORDEX0.22 mean is almost identical to the mean of the CMIP6 ensemble.

Formatted: Superscript

3.5 Trends

In Fig. ~~7~~ 8 the monthly precipitation trends for the rainy season of the period 1986-2005 are displayed for all 3 observational data (gauge-based, SatelliteMerge Satellite-NoMerge) and for the CORDEX~~-Africa~~0.44, CORDEX0.22, CMIP5 and CMIP6 ensembles. Precipitation trends display considerable agreement among all 3 observational datasets, both concerning the signal and the magnitude of the trend. However, the CORDEX0.44/0,22~~-Africa~~ and CMIP5/6 ensembles display trends that are considerably smaller in magnitude. In addition, CORDEX0.44~~CORDEX-Africa~~, CMIP5 and CMIP6 ensembles display fairly distinct spatial patterns that are not in agreement either among them, or with the spatial pattern of precipitation trends displayed by the observational datasets~~.~~. In general, we observe that the signal between CORDEX0.44 and CORDEX0.22 is consistent, with trends in CORDEX0.22 displaying a larger magnitude.

More specifically, during October, all observational products display decreasing trends for the most part of SAF that reach up to -0.1 mm d^{-1} per 20 years. During November the signal changes and SAF experiences increasing trends, with an exception for NW SAF, northern Mozambique and regions of eastern South Africa. During December increasing trends become even more spatially extended and pronounced, especially for satellite products. During January, certain areas of decreasing trends over northern SAF appear, while during February decreasing trends are observed over almost the whole extent of SAF. In March, increasing trends are observed in the region extending from southern Mozambique and stretching towards Zimbabwe and southern Zambia.

Monthly precipitation trends in the CORDEX~~-Africa~~0.44 ensemble are significantly weaker than in the observational datasets and display precipitation increase during Oct–Dec. After January certain regions of intensified decreasing trends appear over southern Angola-northern Namibia and Botswana (Jan) and over Botswana and South Africa (Feb). The pattern of trends is relatively similar in CORDEX0.22, however, the trend magnitude is more enhanced. In CMIP5 decreasing trends are observed during October, but for November increasing trends are observed over the northern part of SAF. During December, strong increasing trends (0.1 mm d^{-1} per 20 years) appear for central SAF, ~~however~~while, during January almost all of the SAF region (with an exception for Mozambique) experiences decreasing precipitation trends. In CMIP6 persistent drying trends are observed almost throughout the whole of SAF and are particularly strong during Jan-Feb (-0.1 mm d^{-1} per 20 years). During March however, the signal is reversed. Statistical significance assessed with the Mann-Kendall test is shown in Fig. S14~~5~~. The number of ensemble members displaying increasing or decreasing trends in each ensemble is shown in Fig. S15.

4 Discussion and conclusions

The analysis of the SD among the different observational products highlights the fact that precipitation assessment requires consultation of multiple (gauge-based, satellite ~~or~~ and reanalysis) products. If this is not possible, then it is highly recommended that the spatial distribution and frequency of reporting of the underlying station data is examined, for each respective precipitation product in use. This should be also regarded in cases when gauge-based or satellite products are

utilized for model evaluation purposes. Moreover, satellite products that merge with rain gauges should not be considered independent from gauge-based products that exploit similar gauge-networks. In addition, we note that SD in the CORDEX-Africa0.44 ensemble is considerably lower than in the CMIP5/6 ensembles, supplying evidence that the CORDEX-Africa0.44 set of simulations provide more constrained results and can thus be considered to be a suitable dataset for climate impact assessment studies over SAF. However, that is not entirely the case for the CORDEX0.22 ensemble, which although it displays SD values smaller to that of CMIP5/6, it still yields SD values higher than that of CORDEX0.44.

Concerning the annual cycle of precipitation, we note that although the seasonality is captured reasonably by both the CMIP and CORDEX-Africa ensembles, still, there are considerable differences between the twothem. More specifically, we conclude that the CORDEX-Africa0.44 ensemble exhibits smaller ensemble spread for all months of the rainy season compared to the driving GCMs (CMIP5). We also conclude that the strong wet bias over SAF in the CMIP5 ensemble (Munday and Washington, 2018) is considerably reduced in the CORDEX-Africa0.44 ensemble. This bias is still evident in CMIP6. A plethora of references in the literature (Reason and Jagadheesha, 2005; Lyon and Mason, 2007; Crétat et al., 2019; Munday and Washington, 2017; Howard and Washington, 2018) have highlighted the importance of the AL pressure system in modulating precipitation over SAF. We note that the strength of the AL as assessed in the current study was simulated to be weaker in the CORDEX-Africa0.44 than in the CMIP5 CORDEX0.22 ensemble. This may partly explain why precipitation in the CORDEX-Africa0.44 ensemble is reduced, relative to the CORDEX0.22 CMIP5 ensemble. However, there is need for a more in-depth dynamical analysis of the simulation of the AL in the CORDEX-Africa ensemble (both CORDEX0.44 and CORDEX0.22) and its impact on modulating precipitation seasonality and patterns over SAF.

The use of the 4 ETCCDI indices demonstrated that the CORDEX-Africa ensemble yields results that are in closer agreement to the observational data, compared to CMIP5/6 ensembles. It is, nevertheless, noticed that the improvement in the CORDEX-Africa ensemble is most evident when the ensemble mean is used. This highlights the fact that the ensemble mean performance is improved, relative to the performance of individual models **(Nikulin et al., 2012b)**. For this reason, it is advisable that climate impact studies employ multi-model ensemble means, as a method of obtaining the consensus climatic information emanating from various models (Duan et al., 2019). In addition, we underline the fact that in all indices the ensemble means of CMIP5/6 and CORDEX-Africa were not able to reproduce the interannual variability that was seen in the observational ensemble. This remark is in agreement with the fact that the task of reproducing precipitation variability across various time-scales by the CMIP5 ensemble is known to present challenges (Dieppois et al., 2019), that inevitably cascade into the CORDEX-Africa simulations that are forced with CMIP5 GCMs (Dosio et al., 2015). Lastly, despite the fact thateven though the CORDEX-Africa ensembles reduces precipitation amounts over SAF, its their use in drought-related impact studies should take into consideration that still, it they yields larger precipitation amounts than the observational data, which might eventually lead to underestimation of drought risk.

Precipitation trends during the rainy season displayed high spatial variability depending on the month. All observed (gauge-based and satellite) trends display substantial spatial agreement. The precipitation trends obtained by the CMIP5/6, and CORDEX-Africa0.44/0.22 ensembles, did not display consistency with the trends obtained from the observational

datasets. This is not entirely unexpected, due to the role of internal variability compared to external forcing in recent decades (Pierce et al., 2009), unlike temperature trends which have been shown to have a good agreement between the CORDEX-Africa (at 0.44° degrees of spatial resolution) and CMIP5 ensembles with observed temperature trends (Dosio and Panitz, 2016; Warnatzsch and Reay, 2019). Nonetheless, we note that the trend signal between CORDEX0.44 and CORDEX0.22 is consistent, with CORDEX0.22 in general enhancing the CORDEX0.44 precipitation trends.

In conclusion, while CORDEX0.44 displays marked improvement over coarser resolution products, there are still further improvements to be made. More specifically, since the wet bias in RCM simulations persists (although considerably reduced relative to GCMs), it is necessary that precipitation over southern Africa is no longer assessed based on bulk descriptive statistics, but that there will be a shift towards process-based evaluation, where the dynamical and thermodynamical characteristics of specific atmospheric features are investigated more thoroughly in the CORDEX-Africa simulations. For this reason, it is imperative that all institutes submitting RCM simulations in data repositories such as the Earth System Grid Federation or the Copernicus Climate Data Store, provide model output data on multiple pressure levels, so that a fair comparison with the CMIP community would be possible. In addition, since the climate of southern Africa is highly coupled with the moisture transport coming from the adjacent oceans, it is necessary that the next generation of RCM simulations within CORDEX-Africa are performed coupled with ocean models. Lastly, since convection over southern Africa has a strong thermal component during specific months of the year (Oct-Nov), it is necessary that the land-atmosphere coupling processes within each RCM are examined in more detail, with coordinated efforts such as the LUCAS Flagship Pilot Study (https://ms.hereon.de/cordex_fps_lucas/index.php.en), as performed in the Euro-CORDEX domain. In the world of regional climate modelling community, the 0.44° resolution of CORDEX-Africa is no longer state of the art and ensemble efforts are now approaching convection permitting grid-spacing (i.e., < 4 km) in some parts of the world (Ban et al., 2021; Pichelli et al., 2021). We also note, that increasing effort should be made with regards to understanding the improvements made from CORDEX0.44 simulations to CORDEX0.22. Although higher resolution is a desired target in the climate modelling community due to the more realistic representation of processes that it offers, still it should not be used as a panacea. In the current work we identified certain weaknesses in the CORDEX0.22 ensemble, that should be addressed before the community populates further its simulation matrix. The next generation ensembles for Africa will hopefully provide insight and improvements to the challenges described here. ~~In conclusion, while CORDEX-Africa displays marked improvement over coarser resolution products, there are still improvements to be made. In the world of regional climate modelling community, the 0.44° resolution of CORDEX-Africa is no longer state of the art and ensemble efforts are now approaching convection permitting grid-spacing (i.e., < 4 km) in some parts of the world (Ban et al., 2021; Pichelli et al., 2021). The next generation ensembles for Africa will be around 0.22° degree and will hopefully provide insight and improvements to the challenges described here.~~

Code and data availability

Formatted: Superscript

Formatted: Font: 10 pt

Formatted: Font: 10 pt

Formatted: Font: 10 pt

Formatted: Font: 10 pt, Not Bold

Formatted: Font: 10 pt

Formatted: Font: 10 pt

Formatted: Font: 10 pt

Formatted: Font: 10 pt

Analysis was performed using the R Project for Statistical Computing (https://www.r-project.org/), the Climate Data Operators (CDO) (https://code.mpimet.mpg.de/projects/cdo/) and Bash programming routines. Processing scripts are available via ZENODO under DOI: https://doi.org/10.5281/zenodo.4725441. CMIP5, CMIP6 and CORDEX-Africa daily precipitation data were retrieved from the Earth System Grid Federation (ESGF) portal (https://esgf-data.dkrz.de/projects/esgf-dkrz/). CMIP5 temperature data at 850 hPa were retrieved from the Climate Data Store (CDS) (https://cds.climate.copernicus.eu/#!/home). CORDEX-Africa (both at 0.44º and 0.22º spatial resolution) temperature data at 850 hPa were retrieved from ESGF. Surface elevation data for CMIP5 and CORDEX-Africa were retrieved from ESGF. The Shuttle Radar Topography Mission (SRTM) Digital Elevation Model was retrieved from: https://srtm.csi.cgiar.org/. ERA5 data were retrieved from CDS. Climate Research Unit (CRU) data are available at: https://crudata.uea.ac.uk/cru/data/hrg/. The University of Delaware (UDEL) data are available at: https://psl.noaa.gov/data/gridded/data.UDel_AirT_Precip.html. The CPC Global Unified Gauge-Based Analysis of Daily Precipitation (CPC-Unified) was retrieved from: https://psl.noaa.gov/data/gridded/data.cpc.globalprecip.html. NOAA's PRECipitation REConstruction over Land dataset (PREC/L) was retrieved from: https://psl.noaa.gov/data/gridded/data.precl.html. The dataset of the Global Precipitation Climatology Centre (GPCC) was retrieved from: https://psl.noaa.gov/data/gridded/data.gpcc.html. The Tropical Applications of Meteorology using SATellite (TAMSAT) data were retrieved from: http://www.tamsat.org.uk/. The Precipitation Estimation from Remotely Sensed Information using Artificial Neural Networks – Climate Data Record (PERSIANN-CDR) are available at: https://chrsdata.eng.uci.edu/. The Climate Hazards Group InfraRed Precipitation with Station data (CHIRPS) products are available at: https://www.chc.ucsb.edu/data/chirps. The CPC Merged Analysis of Precipitation (CMAP) dataset was retrieved from: https://psl.noaa.gov/data/gridded/data.cmap.html. The Global Climatology Precipitation Project (GPCP) dataset was retrieved from: https://psl.noaa.gov/data/gridded/data.gpcp.html. The African Rainfall Climatology (ARC) dataset is available at: https://iridl.ldeo.columbia.edu/SOURCES/.NOAA/.NCEP/.CPC/.FEWS/.Africa/.DAILY/.ARC2/.daily/index.html?Set-Language=en.

Supplement

The supplement related to this article is available online.

Author contribution

MCK, EK and SPS designed the research. MCK implemented the analysis and prepared the manuscript. EK and SPS editted the manuscript and provided corrections.

Formatted: Superscript

Formatted: Superscript

Competing interests

The authors declare that they have no competing interests.

Acknowledgements

MCK was funded by the Hellenic Foundation for Research & Innovations, under the 2nd Call for PhD Candidates (application No. 1323). This article is funded by the AfriCultuReS project "Enhancing Food Security in African Agricultural Systems with the Support of Remote Sensing", (European Union's Horizon 2020 Research and Innovation Framework Programme under grant agreement No. 774652). The authors would like to thank the Scientific Support Centre of the Aristotle University of Thessaloniki (Greece) for providing computational/storage infrastructure and technical support.

References

Abba Omar, S., Abiodun, B.J., 2017. How well do CORDEX models simulate extreme rainfall events over the East Coast of South Africa? Theor. Appl. Climatol. 128, 453–464. https://doi.org/10.1007/s00704-015-1714-5

AFDB, 2019. Southern Africa Economic Outlook 2019. African Development Bank.

Ashouri, H., Hsu, K.-L., Sorooshian, S., Braithwaite, D.K., Knapp, K.R., Cecil, L.D., Nelson, B.R., Prat, O.P., 2015. PERSIANN-CDR: Daily Precipitation Climate Data Record from Multisatellite Observations for Hydrological and Climate Studies. Bull. Am. Meteorol. Soc. 96, 69–83. https://doi.org/10.1175/BAMS-D-13-00068.1

Azzarri, C., Signorelli, S., 2020. Climate and poverty in Africa South of the Sahara. World Dev. 125, 104691. https://doi.org/10.1016/j.worlddev.2019.104691

Ban, N., Caillaud, C., Coppola, E., Pichelli, E., Sobolowski, S., Adinolfi, M., Ahrens, B., Alias, A., Anders, I., Bastin, S., Belusic, D., Berthou, S., Brisson, E., Cardoso, R.M., Chan, S., Christensen, O.B., Fernandez, J., Fita, L., Frisius, T., Gasparac, G., Giorgi, F., Goergen, K., Haugen, J.E., Hodnebrog, O., Kartsios, S., Katragkou, E., Kendon, E.J., Keuler, K., Lavin-Gullon, A., Lenderink, G., Leutwyler, D., Lorenz, T., Maraun, D., Mercogliano, P., Milovac, J., Panitz, H.-J., Raffa, M., Remedio, A.R., Schar, C., Soares, P.M.M., Srnec, L., Steensen, B.M., Stocchi, P., Tolle, M.H., Truhetz, H., Vergara-Temprado, J., de Vries, H., Warrach-Sagi, K., Wulfmeyer, V., Zander, M., 2021. The first multi-model ensemble of regional climate simulations at the kilometer-scale resolution, Part I: Evaluation of precipitation. Clim Dynamics.

Formatted: Font: (Default) Times New Roman

Field Code Changed

Chinowsky, P.S., Schweikert, A.E., Strzepek, N.L., Strzepek, K., 2015. Infrastructure and climate change: a study of impacts and adaptations in Malawi, Mozambique, and Zambia. Clim. Change 130, 49–62. https://doi.org/10.1007/s10584-014-1219-8

Coppola, E., Raffaele, F., Giorgi, F., Giuliani, G., Xuejie, G., Ciarlo, J.M., Sines, T.R., Torres-Alavez, J.A., Das, S., di Sante, F., Pichelli, E., Glazer, R., Müller, S.K., Abba Omar, S., Ashfaq, M., Bukovsky, M., Im, E.-S., Jacob, D., Teichmann, C., Remedio, A., Remke, T., Kriegsmann, A., Bülow, K., Weber, T., Buntemeyer, L., Sieck, K., Rechid, D., 2021. Climate hazard indices projections based on CORDEX-CORE, CMIP5 and CMIP6 ensemble. Clim. Dyn. 57, 1293–1383. https://doi.org/10.1007/s00382-021-05640-z

Crétat, J., Pohl, B., Dieppois, B., Berthou, S., Pergaud, J., 2019. The Angola Low: relationship with southern African rainfall and ENSO. Clim. Dyn. 52, 1783–1803. https://doi.org/10.1007/s00382-018-4222-3

Davis, C.L., Vincent, K., 2017. Climate risk and vulnerability: A handbook for Southern Africa. CSIR.

Denis, B., Laprise, R., Caya, D., 2003a. Sensitivity of a regional climate model to the resolution of the lateral boundary conditions. Clim. Dyn. 20, 107–126. https://doi.org/10.1007/s00382-002-0264-6

~~Denis, B., Laprise, R., Caya, D., 2003b. Sensitivity of a regional climate model to the resolution of the lateral boundary conditions. Clim. Dyn. 20, 107–126. https://doi.org/10.1007/s00382-002-0264-6~~

Desbiolles, F., Howard, E., Blamey, R.C., Barimalala, R., Hart, N.C.G., Reason, C.J.C., 2020. Role of ocean mesoscale structures in shaping the Angola-Low pressure system and the southern Africa rainfall. Clim. Dyn. 54, 3685–3704. https://doi.org/10.1007/s00382-020-05199-1

Di Luca, A., de Elía, R., Laprise, R., 2013. Potential for added value in temperature simulated by high-resolution nested RCMs in present climate and in the climate change signal. Clim. Dyn. 40, 443–464. https://doi.org/10.1007/s00382-012-1384-2

Dieppois, B., Pohl, B., Crétat, J., Eden, J., Sidibe, M., New, M., Rouault, M., Lawler, D., 2019. Southern African summer-rainfall variability, and its teleconnections, on interannual to interdecadal timescales in CMIP5 models. Clim. Dyn. 53, 3505–3527. https://doi.org/10.1007/s00382-019-04720-5

Diffenbaugh, N.S., Giorgi, F., 2012. Climate change hotspots in the CMIP5 global climate model ensemble. Clim. Change 114, 813–822. https://doi.org/10.1007/s10584-012-0570-x

Dosio, A., Jones, R.G., Jack, C., Lennard, C., Nikulin, G., Hewitson, B., 2019a. What can we know about future precipitation in Africa? Robustness, significance and added value of projections from a large ensemble of regional climate models. Clim. Dyn. 53, 5833–5858. https://doi.org/10.1007/s00382-019-04900-3

~~Dosio, A., Jones, R.G., Jack, C., Lennard, C., Nikulin, G., Hewitson, B., 2019b. What can we know about future precipitation in Africa? Robustness, significance and added value of projections from a large ensemble of regional climate models. Clim. Dyn. 53, 5833–5858. https://doi.org/10.1007/s00382-019-04900-3~~

Dosio, A., Jury, M.W., Almazroui, M., Ashfaq, M., Diallo, I., Engelbrecht, F.A., Klutse, N.A.B., Lennard, C., Pinto, I., Sylla, M.B., Tamoffo, A.T., 2021. Projected future daily characteristics of African precipitation based on global (CMIP5, CMIP6) and regional (CORDEX, CORDEX-CORE) climate models. Clim. Dyn. 57, 3135–3158. https://doi.org/10.1007/s00382-021-05859-w

~~Dosio, A., Panitz, H.-J., 2016. Climate change projections for CORDEX-Africa with COSMO-CLM regional climate model and differences with the driving global climate models. Clim. Dyn. 46, 1599–1625. https://doi.org/10.1007/s00382-015-2664-4~~

~~Dosio, A., Panitz, H.-J., Schubert-Frisius, M., Lüthi, D., 2015. Dynamical downscaling of CMIP5 global circulation models over CORDEX-Africa with COSMO-CLM: evaluation over the present climate and analysis of the added value. Clim. Dyn. 44, 2637–2661. https://doi.org/10.1007/s00382-014-2262-x~~

Duan, H., Zhang, G., Wang, S., Fan, Y., 2019. Robust climate change research: a review on multi-model analysis. Environ. Res. Lett. 14, 033001. https://doi.org/10.1088/1748-9326/aaf8f9

Eyring, V., Bony, S., Meehl, G.A., Senior, C.A., Stevens, B., Stouffer, R.J., Taylor, K.E., 2016. Overview of the Coupled Model Intercomparison Project Phase 6 (CMIP6) experimental design and organization. Geosci. Model Dev. 9, 1937–1958. https://doi.org/10.5194/gmd-9-1937-2016

Farr, T.G., Rosen, P.A., Caro, E., Crippen, R., Duren, R., Hensley, S., Kobrick, M., Paller, M., Rodriguez, E., Roth, L., Seal, D., Shaffer, S., Shimada, J., Umland, J., Werner, M., Oskin, M., Burbank, D., Alsdorf, D., 2007. The Shuttle Radar Topography Mission. Rev. Geophys. 45. https://doi.org/10.1029/2005RG000183

Funk, C., Peterson, P., Landsfeld, M., Pedreros, D., Verdin, J., Shukla, S., Husak, G., Rowland, J., Harrison, L., Hoell, A., Michaelsen, J., 2015. The climate hazards infrared precipitation with stations—a new environmental record for monitoring extremes. Sci. Data 2, 150066. https://doi.org/10.1038/sdata.2015.66

Giesen, N. van de, Hut, R., Selker, J., 2014. The Trans-African Hydro-Meteorological Observatory (TAHMO). WIREs Water 1, 341–348. https://doi.org/10.1002/wat2.1034

Giorgi, F., 2019. Thirty Years of Regional Climate Modeling: Where Are We and Where Are We Going next? J. Geophys. Res. Atmospheres 124, 5696–5723. https://doi.org/10.1029/2018JD030094

Giorgi, F., Coppola, E., Raffaele, F., Diro, G.T., Fuentes-Franco, R., Giuliani, G., Mamgain, A., Llopart, M.P., Mariotti, L., Torma, C., 2014. Changes in extremes and hydroclimatic regimes in the CREMA ensemble projections. Clim. Change 125, 39–51. https://doi.org/10.1007/s10584-014-1117-0

Giorgi, F., Gutowski, W.J., 2015. Regional Dynamical Downscaling and the CORDEX Initiative. Annu. Rev. Environ. Resour. 40, 467–490. https://doi.org/10.1146/annurev-environ-102014-021217

Gu, G., Adler, R.F., Huffman, G.J., 2016. Long-term changes/trends in surface temperature and precipitation during the satellite era (1979–2012). Clim. Dyn. 46, 1091–1105. https://doi.org/10.1007/s00382-015-2634-x

Harrison, L., Funk, C., Peterson, P., 2019. Identifying changing precipitation extremes in Sub-Saharan Africa with gauge and satellite products. Environ. Res. Lett. 14, 085007. https://doi.org/10.1088/1748-9326/ab2cae

Hart, N.C.G., Reason, C.J.C., Fauchereau, N., 2010. Tropical–Extratropical Interactions over Southern Africa: Three Cases of Heavy Summer Season Rainfall. Mon. Weather Rev. 138, 2608–2623. https://doi.org/10.1175/2010MWR3070.1

Hersbach, H., Bell, B., Berrisford, P., Hirahara, S., Horányi, A., Muñoz-Sabater, J., Nicolas, J., Peubey, C., Radu, R., Schepers, D., Simmons, A., Soci, C., Abdalla, S., Abellan, X., Balsamo, G., Bechtold, P., Biavati, G., Bidlot, J., Bonavita, M., Chiara, G.D., Dahlgren, P., Dee, D., Diamantakis, M., Dragani, R., Flemming, J., Forbes, R., Fuentes, M., Geer, A., Haimberger, L., Healy, S., Hogan, R.J., Hólm, E., Janisková, M., Keeley, S., Laloyaux, P., Lopez, P., Lupu, C., Radnoti, G., Rosnay, P. de, Rozum, I., Vamborg, F., Villaume, S., Thépaut, J.-N., 2020. The ERA5 global reanalysis. Q. J. R. Meteorol. Soc. 146, 1999–2049. https://doi.org/10.1002/qj.3803

Houze, R.A., 2012. Orographic effects on precipitating clouds. Rev. Geophys. 50. https://doi.org/10.1029/2011RG000365

Howard, E., Washington, R., 2019. Drylines in Southern Africa: Rediscovering the Congo Air Boundary. J. Clim. 32, 8223–8242. https://doi.org/10.1175/JCLI-D-19-0437.1

Howard, E., Washington, R., 2018. Characterizing the Synoptic Expression of the Angola Low. J. Clim. 31, 7147–7165. https://doi.org/10.1175/JCLI-D-18-0017.1

IPCC, 2013. Annex I: Atlas of Global and Regional Climate Projections, in: Stocker, T.F., Qin, D., Plattner, G.-K., Tignor, M., Allen, S.K., Boschung, J., Nauels, A., Xia, Y., Bex, V., Midgley, P.M. (Eds.), Climate Change 2013: The Physical Science Basis. Contribution of Working Group I to the Fifth Assessment Report of the Intergovernmental Panel on Climate Change. Cambridge University Press, Cambridge, United Kingdom and New York, NY, USA, pp. 1311–1394. https://doi.org/10.1017/CBO9781107415324.029

Janowiak, J.E., 1988. An Investigation of Interannual Rainfall Variability in Africa. J. Clim. 1, 240–255. https://doi.org/10.1175/1520-0442(1988)001<0240:AIOIRV>2.0.CO;2

Kalognomou, E.-A., Lennard, C., Shongwe, M., Pinto, I., Favre, A., Kent, M., Hewitson, B., Dosio, A., Nikulin, G., Panitz, H.-J., Büchner, M., 2013. A Diagnostic Evaluation of Precipitation in CORDEX Models over Southern Africa. J. Clim. 26, 9477–9506. https://doi.org/10.1175/JCLI-D-12-00703.1

Kendall, M.G., 1948. Rank correlation methods, Rank correlation methods. Griffin, Oxford, England.

Kim, J., Waliser, D.E., Mattmann, C.A., Goodale, C.E., Hart, A.F., Zimdars, P.A., Crichton, D.J., Jones, C., Nikulin, G., Hewitson, B., Jack, C., Lennard, C., Favre, A., 2014. Evaluation of the CORDEX-Africa multi-RCM hindcast: systematic model errors. Clim. Dyn. 42, 1189–1202. https://doi.org/10.1007/s00382-013-1751-7

Kim, Y.-H., Min, S.-K., Zhang, X., Sillmann, J., Sandstad, M., 2020. Evaluation of the CMIP6 multi-model ensemble for climate extreme indices. Weather Clim. Extrem. 29, 100269. https://doi.org/10.1016/j.wace.2020.100269

Kula, N., Haines, A., Fryatt, R., 2013. Reducing Vulnerability to Climate Change in Sub-Saharan Africa: The Need for Better Evidence. PLoS Med. 10. https://doi.org/10.1371/journal.pmed.1001374

Laprise, R., de Elía, R., Caya, D., Biner, S., Lucas-Picher, P., Diaconescu, E., Leduc, M., Alexandru, A., Separovic, L., Canadian Network for Regional Climate Modelling and Diagnostics, 2008. Challenging some tenets of Regional Climate Modelling. Meteorol. Atmospheric Phys. 100, 3–22. https://doi.org/10.1007/s00703-008-0292-9

Le Coz, C., van de Giesen, N., 2020. Comparison of Rainfall Products over Sub-Saharan Africa. J. Hydrometeorol. 21, 553–596. https://doi.org/10.1175/JHM-D-18-0256.1

L'Heureux, M.L., Lee, S., Lyon, B., 2013. Recent multidecadal strengthening of the Walker circulation across the tropical Pacific. Nat. Clim. Change 3, 571–576. https://doi.org/10.1038/nclimate1840

Lorenz, C., Kunstmann, H., 2012. The Hydrological Cycle in Three State-of-the-Art Reanalyses: Intercomparison and Performance Analysis. J. Hydrometeorol. 13, 1397–1420. https://doi.org/10.1175/JHM-D-11-088.1

Lyon, B., Mason, S.J., 2007. The 1997–98 Summer Rainfall Season in Southern Africa. Part I: Observations. J. Clim. 20, 5134–5148. https://doi.org/10.1175/JCLI4225.1

Mabhaudhi, T., Mpandeli, S., Nhamo, L., Chimonyo, V.G.P., Nhemachena, C., Senzanje, A., Naidoo, D., Modi, A.T., 2018. Prospects for Improving Irrigated Agriculture in Southern Africa: Linking Water, Energy and Food. Water 10, 1881. https://doi.org/10.3390/w10121881

Maidment, R.I., Allan, R.P., Black, E., 2015. Recent observed and simulated changes in precipitation over Africa. Geophys. Res. Lett. 42, 8155–8164. https://doi.org/10.1002/2015GL065765

Maidment, R.I., Grimes, D., Allan, R.P., Tarnavsky, E., Stringer, M., Hewison, T., Roebeling, R., Black, E., 2014. The 30 year TAMSAT African Rainfall Climatology And Time series (TARCAT) data set. J. Geophys. Res. Atmospheres 119, 10,619-10,644. https://doi.org/10.1002/2014JD021927

Mann, H.B., 1945. Nonparametric Tests Against Trend. Econometrica 13, 245–259. https://doi.org/10.2307/1907187

Meque, A., Abiodun, B.J., 2015. Simulating the link between ENSO and summer drought in Southern Africa using regional climate models. Clim. Dyn. 44, 1881–1900. https://doi.org/10.1007/s00382-014-2143-3

Munday, C., Washington, R., 2018. Systematic Climate Model Rainfall Biases over Southern Africa: Links to Moisture Circulation and Topography. J. Clim. 31, 7533–7548. https://doi.org/10.1175/JCLI-D-18-0008.1

Munday, C., Washington, R., 2017. Circulation controls on southern African precipitation in coupled models: The role of the Angola Low. J. Geophys. Res. Atmospheres 122, 861–877. https://doi.org/10.1002/2016JD025736

Nikulin, G., Jones, C., Giorgi, F., Asrar, G., Büchner, M., Cerezo-Mota, R., Christensen, O.B., Déqué, M., Fernandez, J., Hänsler, A., Meijgaard, E. van, Samuelsson, P., Sylla, M.B., Sushama, L., 2012a. Precipitation Climatology in an Ensemble of CORDEX-Africa Regional Climate Simulations. J. Clim. 25, 6057–6078. https://doi.org/10.1175/JCLI-D-11-00375.1

~~Nikulin, G., Jones, C., Giorgi, F., Asrar, G., Büchner, M., Cerezo-Mota, R., Christensen, O.B., Déqué, M., Fernandez, J., Hänsler, A., van Meijgaard, E., Samuelsson, P., Sylla, M.B., Sushama, L., 2012b. Precipitation Climatology in an Ensemble of CORDEX-Africa Regional Climate Simulations. J. Clim. 25, 6057–6078. https://doi.org/10.1175/JCLI-D-11-00375.1~~

Onyutha, C., 2018. Trends and variability in African long-term precipitation. Stoch. Environ. Res. Risk Assess. 32, 2721–2739. https://doi.org/10.1007/s00477-018-1587-0

Peterson, T.C., Manton, M.J., 2008. Monitoring Changes in Climate Extremes: A Tale of International Collaboration. Bull. Am. Meteorol. Soc. 89, 1266–1271.

Pichelli, E., Coppola, E., Sobolowski, S., Ban, N., Giorgi, F., Stocchi, P., Alias, A., Belušić, D., Berthou, S., Caillaud, C., Cardoso, R.M., Chan, S., Christensen, O.B., Dobler, A., de Vries, H., Goergen, K., Kendon, E.J., Keuler, K., Lenderink, G., Lorenz, T., Mishra, A.N., Panitz, H.-J., Schär, C., Soares, P.M.M., Truhetz, H., Vergara-Temprado, J., 2021. The first multi-model ensemble of regional climate simulations at kilometer-scale resolution part 2: historical and future simulations of precipitation. Clim. Dyn. https://doi.org/10.1007/s00382-021-05657-4

Pierce, D.W., Barnett, T.P., Santer, B.D., Gleckler, P.J., 2009. Selecting global climate models for regional climate change studies. Proc. Natl. Acad. Sci. 106, 8441–8446. https://doi.org/10.1073/pnas.0900094106

Pinto, I., Lennard, C., Tadross, M., Hewitson, B., Dosio, A., Nikulin, G., Panitz, H.-J., Shongwe, M.E., 2016. Evaluation and projections of extreme precipitation over southern Africa from two CORDEX models. Clim. Change 135, 655–668. https://doi.org/10.1007/s10584-015-1573-1

Reason, C.J.C., Jagadheesha, D., 2005. A model investigation of recent ENSO impacts over southern Africa. Meteorol. Atmospheric Phys. 89, 181–205. https://doi.org/10.1007/s00703-005-0128-9

Rocklöv, J., Dubrow, R., 2020. Climate change: an enduring challenge for vector-borne disease prevention and control. Nat. Immunol. 21, 479–483. https://doi.org/10.1038/s41590-020-0648-y

Sen, P.K., 1968. Estimates of the Regression Coefficient Based on Kendall's Tau. J. Am. Stat. Assoc. 63, 1379–1389. https://doi.org/10.1080/01621459.1968.10480934

Serdeczny, O., Adams, S., Baarsch, F., Coumou, D., Robinson, A., Hare, W., Schaeffer, M., Perrette, M., Reinhardt, J., 2017. Climate change impacts in Sub-Saharan Africa: from physical changes to their social repercussions. Reg. Environ. Change 17, 1585–1600. https://doi.org/10.1007/s10113-015-0910-2

Tarnavsky, E., Grimes, D., Maidment, R., Black, E., Allan, R.P., Stringer, M., Chadwick, R., Kayitakire, F., 2014. Extension of the TAMSAT Satellite-Based Rainfall Monitoring over Africa and from 1983 to Present. J. Appl. Meteorol. Climatol. 53, 2805–2822. https://doi.org/10.1175/JAMC-D-14-0016.1

Taylor, K.E., Stouffer, R.J., Meehl, G.A., 2012. An Overview of CMIP5 and the Experiment Design. Bull. Am. Meteorol. Soc. 93, 485–498. https://doi.org/10.1175/BAMS-D-11-00094.1

Theil, H., 1992. A Rank-Invariant Method of Linear and Polynomial Regression Analysis, in: Raj, B., Koerts, J. (Eds.), Henri Theil's Contributions to Economics and Econometrics: Econometric Theory and Methodology, Advanced Studies in Theoretical and Applied Econometrics. Springer Netherlands, Dordrecht, pp. 345–381. https://doi.org/10.1007/978-94-011-2546-8_20

Tirado, M.C., Hunnes, D., Cohen, M.J., Lartey, A., 2015. Climate Change and Nutrition in Africa. J. Hunger Environ. Nutr. 10, 22–46. https://doi.org/10.1080/19320248.2014.908447

Toté, C., Patricio, D., Boogaard, H., Van der Wijngaart, R., Tarnavsky, E., Funk, C., 2015. Evaluation of Satellite Rainfall Estimates for Drought and Flood Monitoring in Mozambique. Remote Sens. 7, 1758–1776. https://doi.org/10.3390/rs70201758

Ukkola, A.M., Kauwe, M.G.D., Roderick, M.L., Abramowitz, G., Pitman, A.J., 2020. Robust Future Changes in Meteorological Drought in CMIP6 Projections Despite Uncertainty in Precipitation. Geophys. Res. Lett. 47, e2020GL087820. https://doi.org/10.1029/2020GL087820

Warnatzsch, E.A., Reay, D.S., 2019. Temperature and precipitation change in Malawi: Evaluation of CORDEX-Africa climate simulations for climate change impact assessments and adaptation planning. Sci. Total Environ. 654, 378–392. https://doi.org/10.1016/j.scitotenv.2018.11.098

Wyser, K., van Noije, T., Yang, S., von Hardenberg, J., O'Donnell, D., Döscher, R., 2020. On the increased climate sensitivity in the EC-Earth model from CMIP5 to CMIP6. Geosci. Model Dev. 13, 3465–3474. https://doi.org/10.5194/gmd-13-3465-2020

Yim, B.Y., Yeh, S.-W., Sohn, B.-J., 2016. ENSO-Related Precipitation and Its Statistical Relationship with the Walker Circulation Trend in CMIP5 AMIP Models. Atmosphere 7, 19. https://doi.org/10.3390/atmos7020019

Formatted: Font: (Default) Times New Roman

Formatted: Font: (Default) Times New Roman

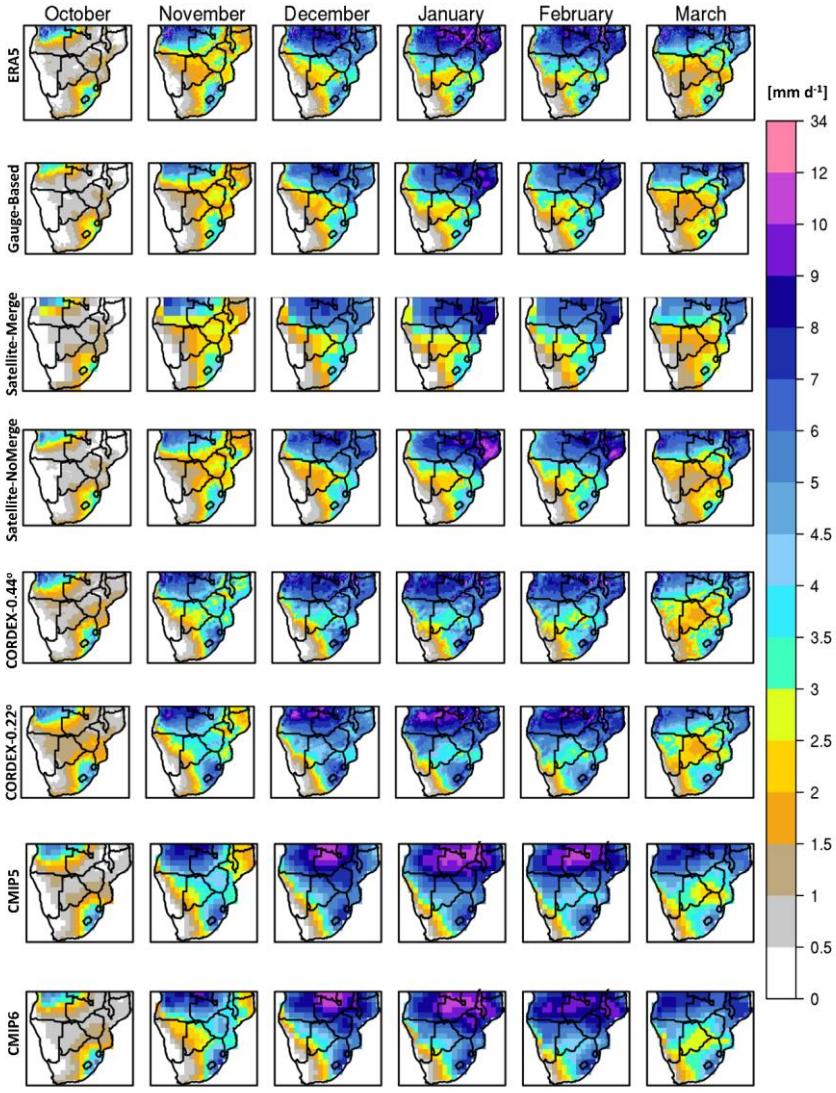
October
November
December
January
February
March
ERA5
Gauge-Based
Satellite-Merge
Satellite-NoMerge
CORDEX-0.44°
CORDEX-0.22°
CMIP5
CMIP6
[mm d-1]
34
12
10
9
8
7
6
5
4.5
4
3.5
3
2.5
2
1.5
1
0.5
0

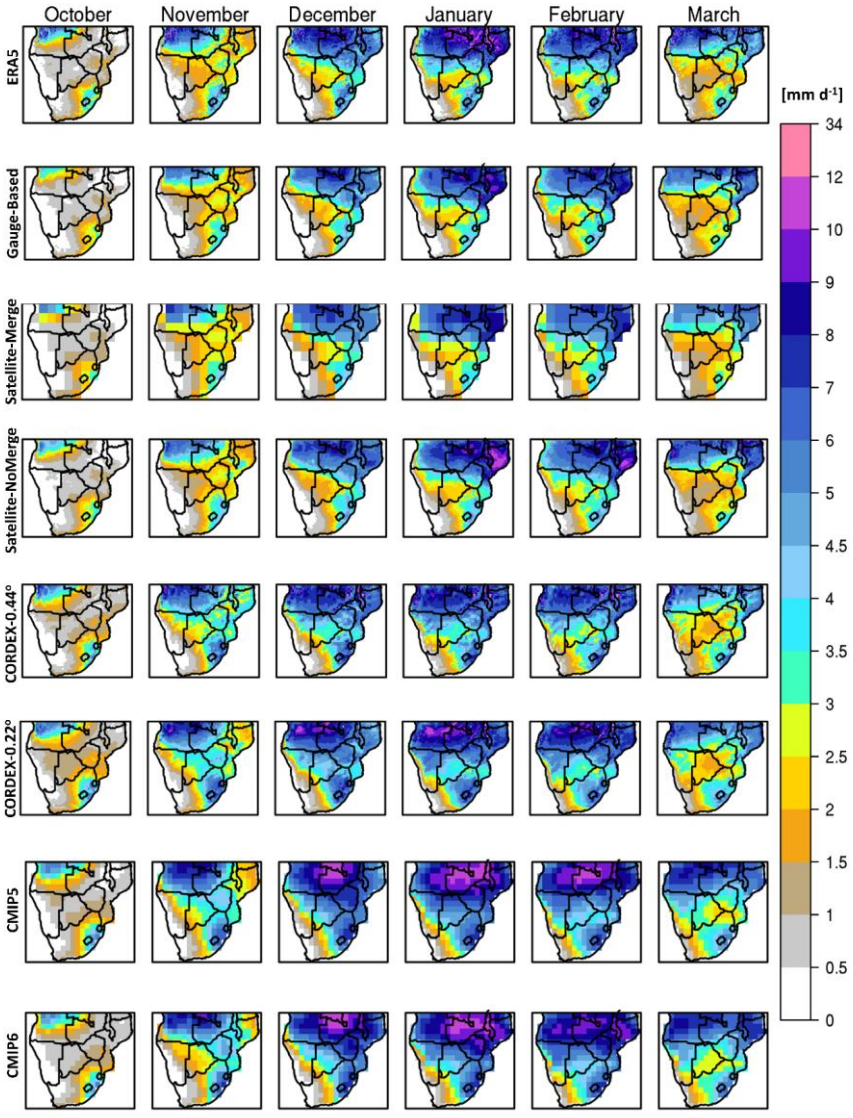
October
November
December
January
February
March
ERA5
Gauge-Based
Satellite-Merge
Satellite-NoMerge
CORDEX-0.44°
CORDEX-0.22°
CMIP5
CMIP6
[mm d-1]
34
12
10
9
8
7
6
5
4.5
4
3.5
3
2.5
2
1.5
1
0.5
0

Figure 1. Monthly precipitation climatologies during the period 1986-2005 in mm d^{-1}. More specifically, from top to bottom: ERA5 reanalysis dataset. Gauge-based: Ensemble mean of datasets that were produced by employing spatial interpolation methods using rain gauges/station data. Satellite-Merge: Ensemble mean of all satellite products that merge with rain gauges/station data. Satellite-NoMerge: Ensemble mean of satellite products that do not merge with rain gauges/station data. CORDEX-~~Africa~~0.44º: Ensemble mean of regional climate model simulations performed in the context of the Coordinated Regional Climate Downscaling Experiment (CORDEX) – Africa domain with a spatial resolution equal to 0.44º x 0.44º. CORDEX-0.22º: CORDEX-Africa simulations with a spatial resolution equal to 0.22º x 0.22º. CMIP5: Ensemble mean of general circulation models participating in the Coupled Model Intercomparison Project Phase 5 (CMIP5) that were used as forcing in the CORDEX-Africa simulations. ~~–~~CMIP6: Ensemble mean of general circulation models participating in the Coupled Model Intercomparison Project Phase 6.

Formatted: Superscript

Formatted: Superscript

Formatted: Superscript

Formatted: Superscript

Formatted: Not Superscript/ Subscript

Formatted: Not Superscript/ Subscript

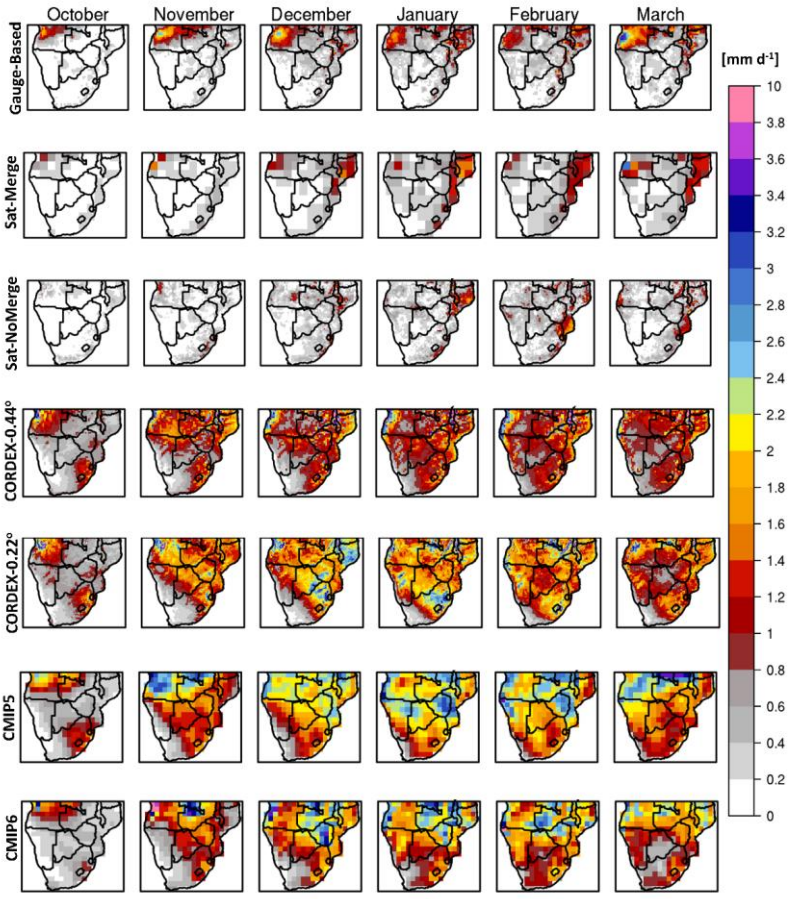
October
November
December
January
February
March
Gauge-Based
Sat-Merge
Sat-NoMerge
CORDEX-0.44°
CORDEX-0.22°
CMIP5
CMIP6
[mm d-1]
10
3.8
3.6
3.4
3.2
3
2.8
2.6
2.4
2.2
2
1.8
1.6
1.4
1.2
1
0.8
0.6
0.4
0.2
0

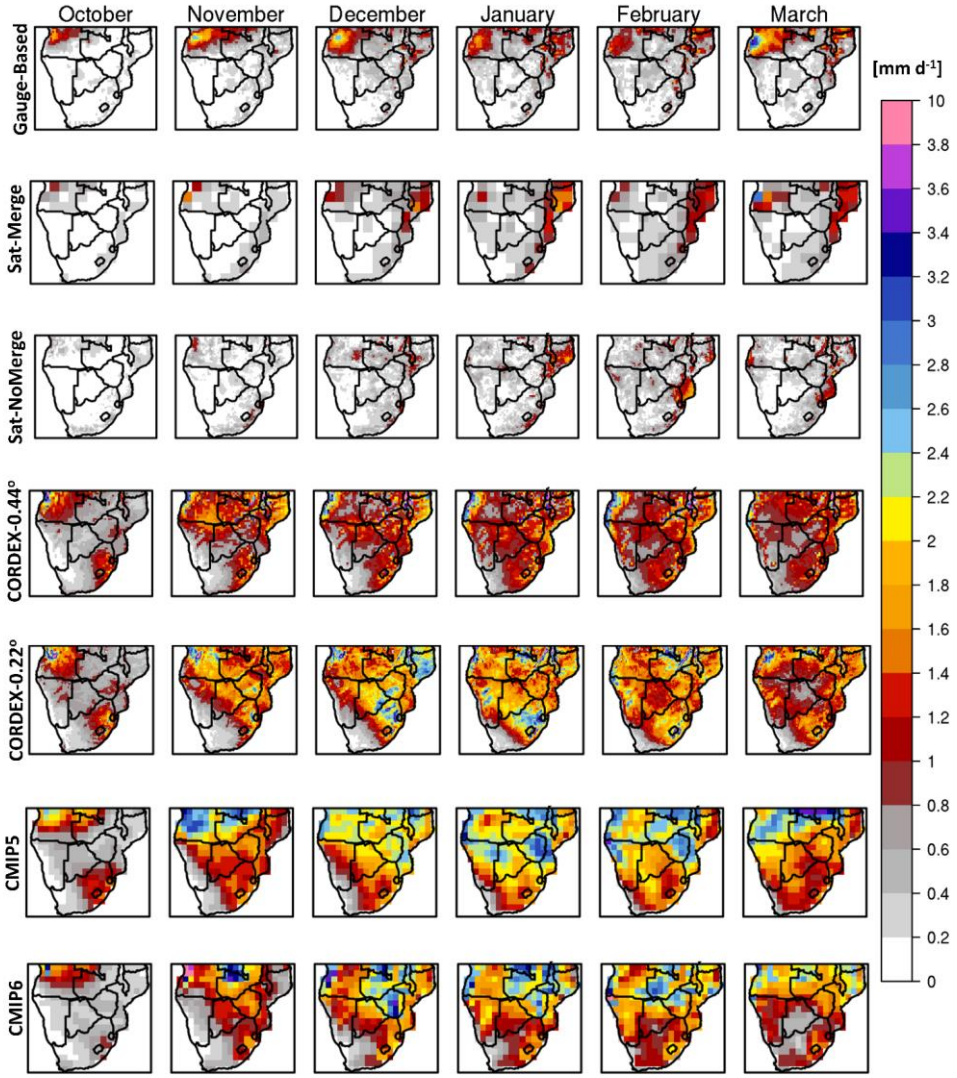

Formatted: Normal

Figure 2. Standard deviation of monthly precipitation [mm d^{-1}] during the period 1986-2005. Rows indicate the ensemble means analyzed. ~~More specifically, from~~From top to bottom: Gauge-based: Ensemble mean of datasets that were produced by employing spatial interpolation methods using rain gauges/station data. Sat~~ellite~~-Merge: Ensemble mean of all satellite products that merge with rain gauges/station data. Sat~~ellite~~-NoMerge: Ensemble mean of satellite products that do not merge with rain gauges/station data. CORDEX-~~0.44º Africa~~: Ensemble mean of regional climate model simulations performed in the context of the Coordinated Regional Climate Downscaling Experiment – Africa domain with a spatial resolution equal to 0.44º x 0.44º. CORDEX-0.22º: CORDEX-Africa simulations with a spatial resolution equal to 0.22º x 0.22º. ~~–~~CMIP5: Ensemble mean of general circulation models participating in the Coupled Model Intercomparison Project Phase 5 (CMIP5) that were used as forcing in the CORDEX-Africa simulations. CMIP6: Ensemble mean of general circulation models participating in the Coupled Model Intercomparison Project Phase 6.

Formatted: English (United States)

Formatted: English (United States)

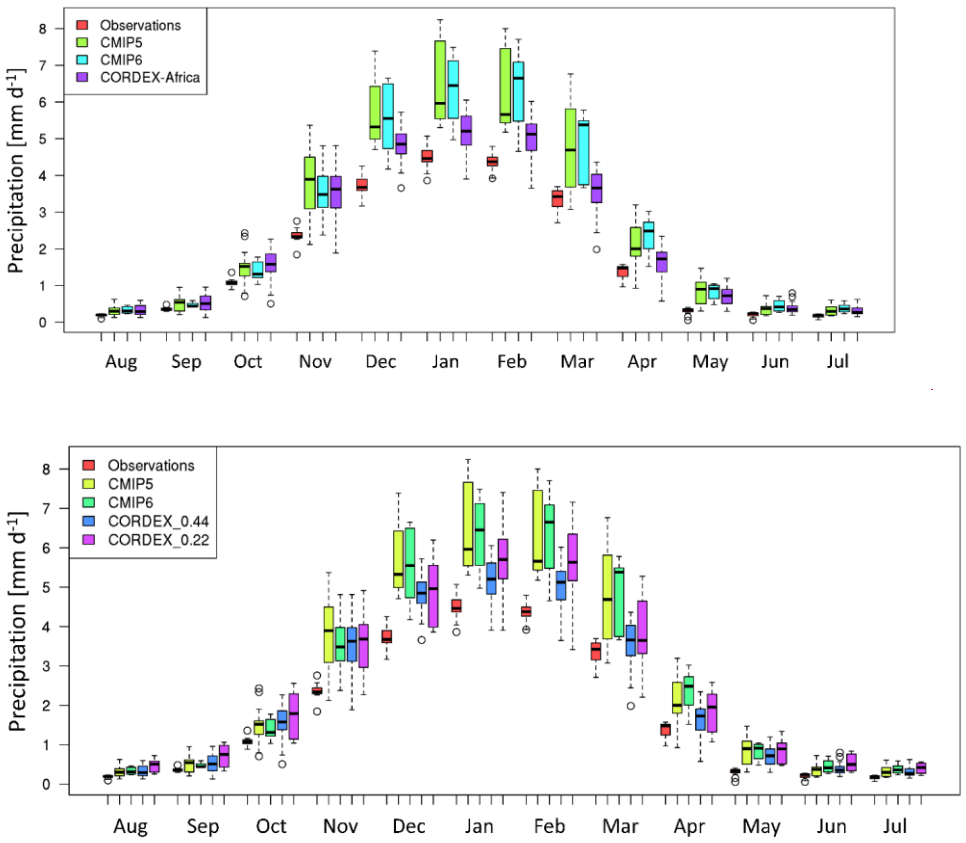

Figure 3. Annual cycle of monthly precipitation during 1986-2005 for the ensemble of observational data (gauge-based, satellite and reanalysis), CMIP5 (Coupled Model Intercomparison Project Phase 5), CMIP6 (Coupled Model Intercomparison Project Phase 6), ~~and~~ CORDEX0.44 ~~Africa~~ (Coordinated Regional Climate Downscaling Experiment – Africa domain with a spatial resolution equal to 0.44º x 0.44º) and CORDEX-0.22º (CORDEX-Africa simulations with a spatial resolution equal to 0.22º x 0.22º). The thick horizontal black lines indicate the ensemble median for each month, the box encloses the interquartile range, and the tails denote the full ensemble range. Circles represent the outliers for each ensemble. Grid points only are considered.

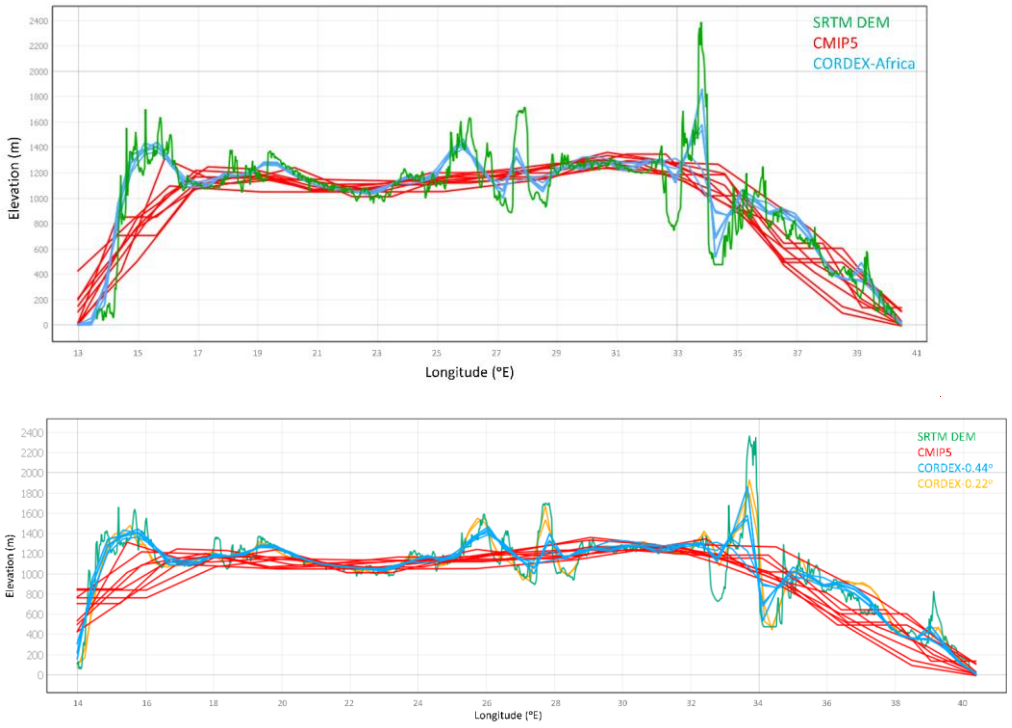

Figure 4. Cross section of surface elevation at ~~10.5~~11 ºS across southern Africa for the Shuttle Radar Topography Mission (SRTM) Digital Elevation Model (in green), the surface altitude as represented in the CMIP5 (Coupled Model Intercomparison Project Phase 5) global climate models (in red), ~~and~~ the surface ~~elevation~~ altitude as represented in the ~~CORDEX~~ CORDEX0.44 (Coordinated Regional Climate Downscaling Experiment – Africa domain with a spatial resolution equal to 0.44º x 0.44º) (in blue) and the surface altitude as represented in the CORDEX-0.22º (CORDEX-Africa simulations with a spatial resolution equal to 0.22º x 0.22º) (in yellow). ~~Africa (Coordinated Regional Climate Downscaling Experiment – Africa domain) regional climate models (in blue).~~

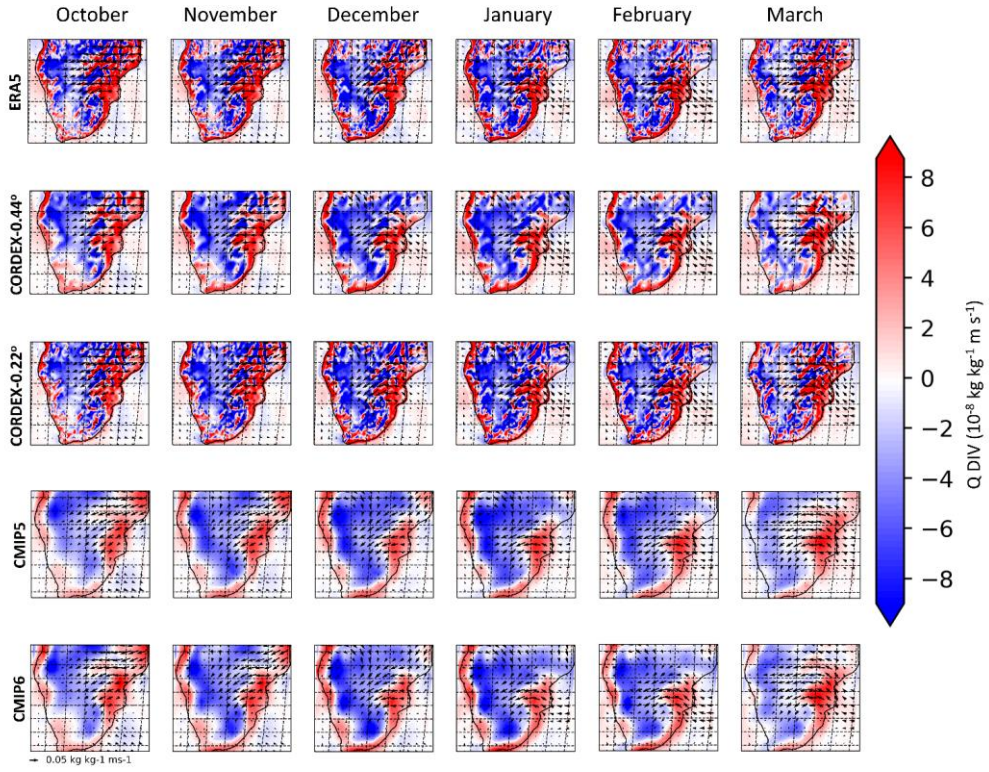

Figure 5. Mean monthly moisture flux and divergence at 850 hPa during the period 1986-2005. Rows indicate the ensemble means analyzed. From top to bottom: ERA5, ensemble mean of CORDEX0.44º, CORDEX0.22º, CMIP5 and CMIP6 simulations.

Formatted: Font: Not Bold

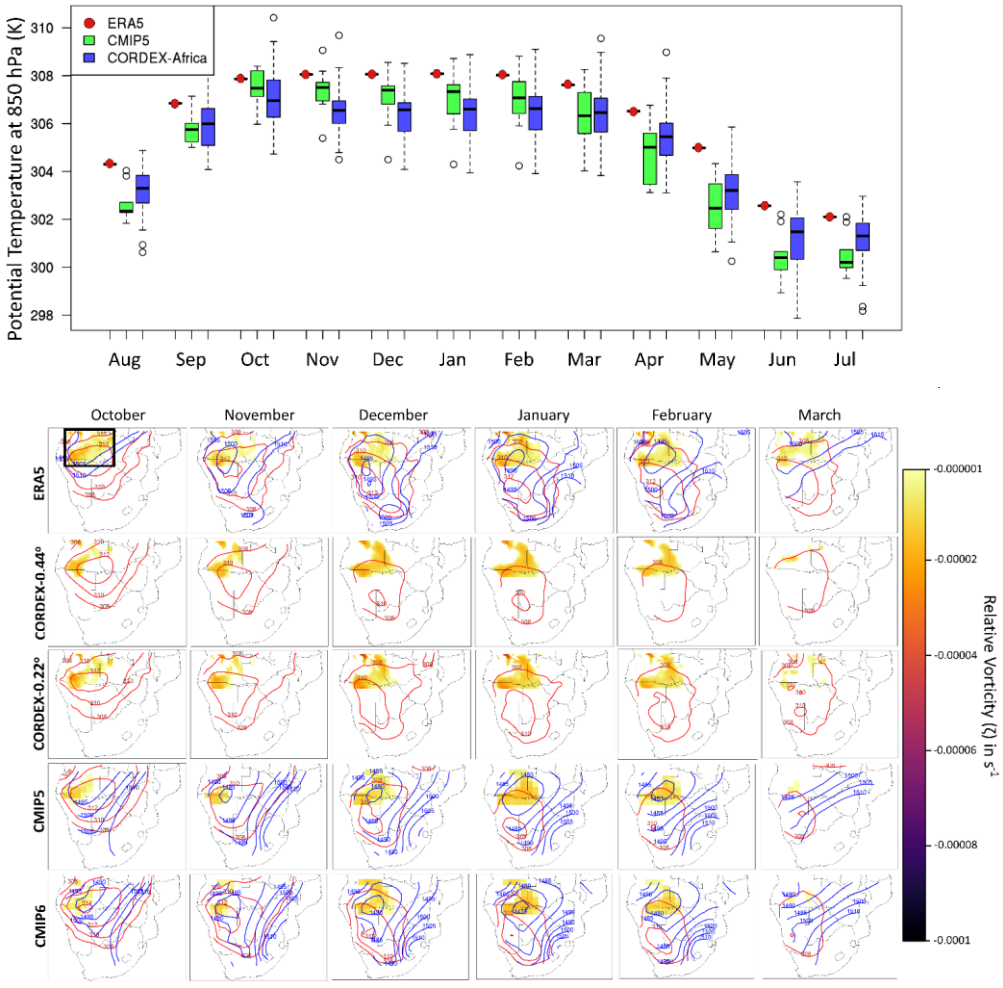

Figure 65. Monthly climatologies of the Angola Low pressure system during the rainy season for the period 1986-2005. Filled contours indicate cyclonic relative vorticity (ζ) for $\zeta < -0.00001\ s^{-1}$ over the region extending from 14 °E to 25 °E and from 11 °S to 19 °S. Red lines indicate the isotherms of potential temperature at 850 hPa, having an increment of 2 K. Blue lines indicate isoheights of the geopotential height at 850 hPa, having an increment of 5 m. CORDEX0.44/0.22 are not

Formatted: Font: Not Bold
Formatted: Font: Not Bold, English (United States)
Formatted: Font: Not Bold
Formatted: Font: Not Bold, English (United States)
Formatted: Font: Not Bold
Formatted: Font: 10 pt, Not Bold, English (United States)
Formatted: Font: 10 pt, Not Bold
Formatted: Font: Not Bold
Formatted: Font: 10 pt, Not Bold

plotted with geopotential isoheights, because this variable was not available for CORDEX simulations. From top to bottom: ERA5, ensemble mean of CORDEX0.44º, CORDEX0.22º, CMIP5 and CMIP6 simulations. ~~Annual cycle of potential temperature at 850 hPa (theta850) during 1986-2005 for the CMIP5 (Coupled Model Intercomparison Project Phase 5) and CORDEX-Africa CORDEX-Africa (Coordinated Regional Climate Downscaling Experiment – Africa domain) ensembles. The thick horizontal black lines indicate the ensemble median for each month, the box encloses the interquartile range, and the tails denote the full ensemble range. Circles represent the outliers for each ensemble. Red dot represents theta850 from ERA5. Temperature in CMIP6 was not available at 850 hPa, hence theta850 was not calculated for CMIP6. Grid points only are considered.~~ Black box indicates the region from 14 ºE to 25 ºE and from 11 ºS to 19 ºS.

Formatted: Font: 10 pt, Not Bold, Superscript

Formatted: Font: 10 pt, Not Bold

Formatted: Font: 10 pt, Not Bold, Superscript

Formatted: Font: 10 pt, Not Bold

Formatted: Font: Not Bold

Formatted: English (United States)

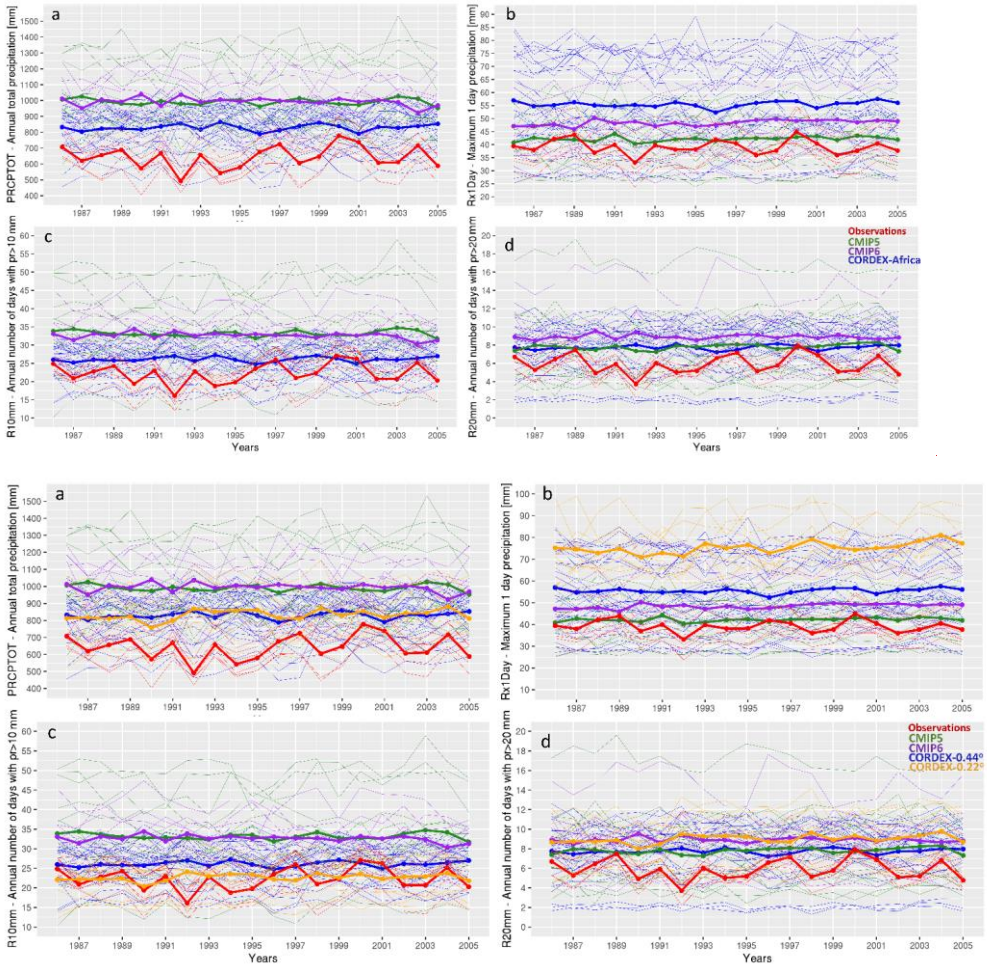

Figure 7 ~~6~~**.** Timeseries of the ETCCDI indices over southern Africa (10 ºE to 42 ºE and 10 ºS to 35 ºS) for the observational ensemble in red (gauge-based, satellite and reanalysis), CMIP5 (Coupled Model Intercomparison Project Phase 5) ensemble in green, CMIP6 (Coupled Model Intercomparison Project Phase 6) ensemble in purple, ~~and~~ CORDEX-0.44º: Ensemble mean of regional climate model simulations performed in the context of the Coordinated Regional Climate Downscaling Experiment – Africa domain with a spatial resolution equal to 0.44º x 0.44º in blue and CORDEX-0.22ºC in orange~~ORDEX-Africa (Coordinated Regional Climate Downscaling Experiment – Africa domain) ensemble in blue~~. Thin lines display single ensemble members, thick lines display ensemble means. Y-axis on each panel depicts: (a) PRCPTOT (total annual

precipitation), (b) Rx1Day (annual maximum daily precipitation), (c) R10mm (annual number of days with daily precipitation >10 mm), (d) R20mm (annual number of days with daily precipitation >20 mm).

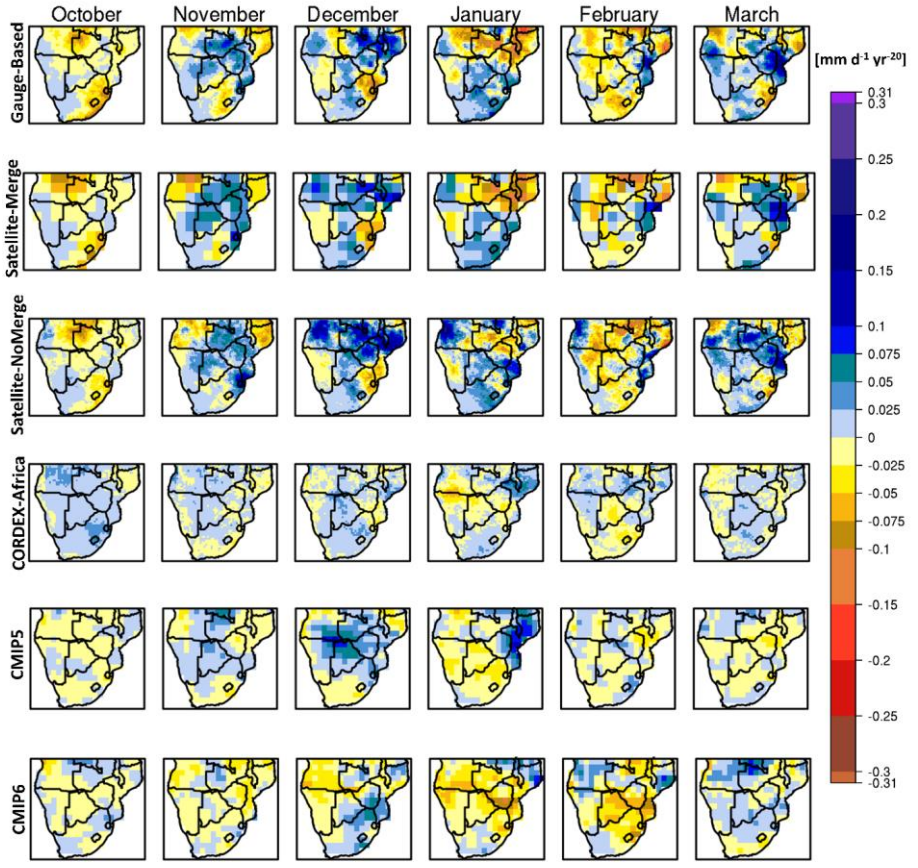
October
November
December
January
February
March
Gauge-Based
Satellite-Merge
Satellite-NoMerge
CORDEX-Africa
CMIP5
CMIP6
[mm d-1 yr-20]
0.31
0.3
0.25
0.2
0.15
0.1
0.075
0.05
0.025
0
-0.025
-0.05
-0.075
-0.1
-0.15
-0.2
-0.25
-0.3
-0.31

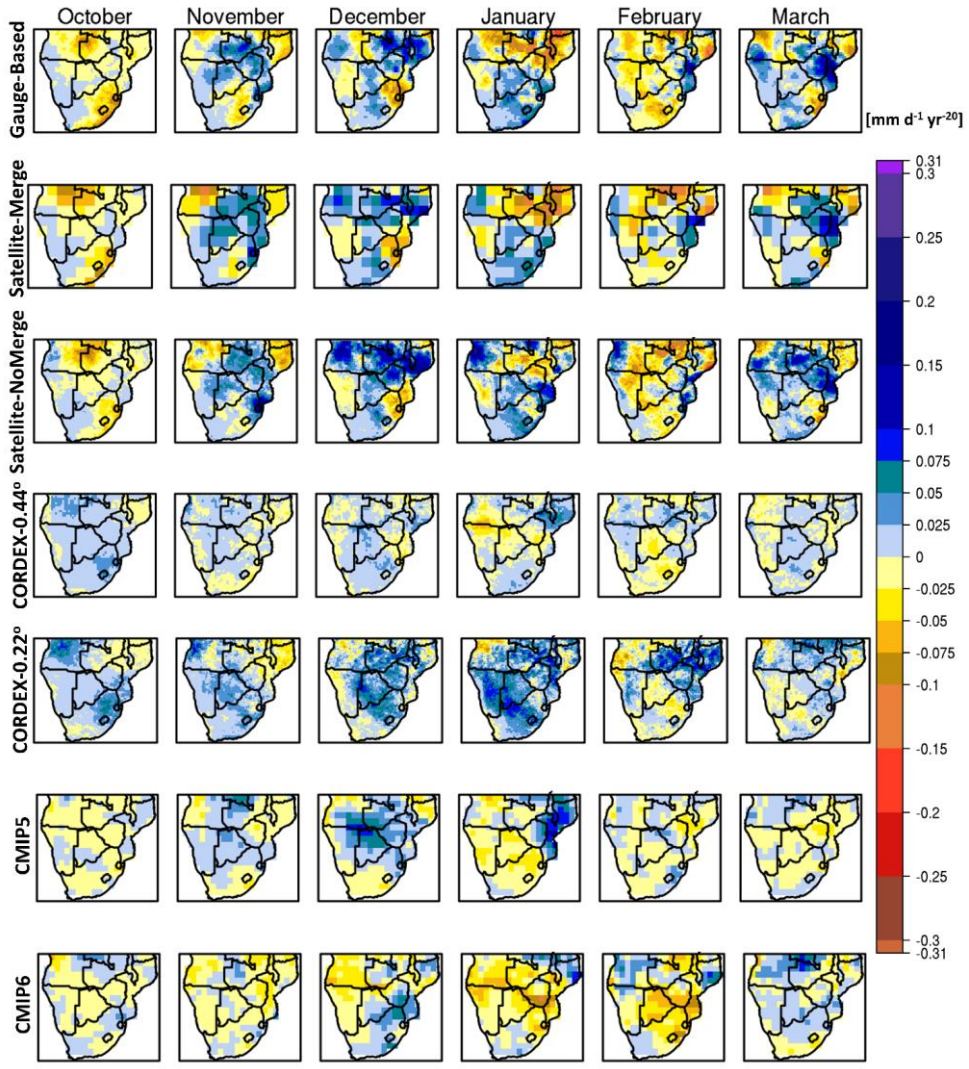
October
November
December
January
February
March
Gauge-Based
Satellite-Merge
Satellite-NoMerge
CORDEX-0.44°
CORDEX-0.22°
CMIP5
CMIP6
[mm d-1 yr-20]
0.31
0.3
0.25
0.2
0.15
0.1
0.075
0.05
0.025
0
-0.025
-0.05
-0.075
-0.1
-0.15
-0.2
-0.25
-0.3
-0.31

Figure ~~7~~8. Trends for monthly precipitation for the period 1986-2005 [mm d^{-1} per 20 years] calculated using Sen's Slope. Rows indicate the ensemble mean of trends produced by each ensemble member. ~~More specifically, f~~From top to bottom: Gauge-Based: Ensemble mean of datasets that were produced by employing spatial interpolation methods using rain gauges/station data. Satellite-Merge: Ensemble mean of all satellite products that merge with rain gauges/station data. Satellite-NoMerge: Ensemble mean of satellite products that do not merge with rain gauges/station data. CORDEX-0.44º: Ensemble mean of regional climate model simulations performed in the context of the Coordinated Regional Climate Downscaling Experiment – Africa domain with a spatial resolution equal to 0.44º x 0.44º. CORDEX-0.22º: CORDEX-Africa simulations with a spatial resolution equal to 0.22º x 0.22º. ~~CORDEX-Africa: Ensemble mean of regional climate model simulations performed in the context of Coordinated Regional Climate Downscaling Experiment – Africa domain.~~ CMIP5: Ensemble mean of general circulation models participating in the Coupled Model Intercomparison Project Phase 5 (CMIP5) that were used as forcing in the CORDEX-0.44º ~~CORDEX-Africa~~ simulations. CMIP6: Ensemble mean of general circulation models participating in the Coupled Model Intercomparison Project Phase 6.

Formatted: English (United States)

Precipitation over southern Africa: Is there consensus among GCMs, RCMs and observational data?

Table S1: Observational datasets used.

Dataset	Resolution	Frequency	Type	Period	Reference
ARC.v2	0.1º	Daily total	Satellite	1983-present	(Novella and Thiaw, 2013)
PERSIANN-CDR	0.25º	Daily total	Satellite	1983-present	(Ashouri et al., 2015)
CMAP	2.5º	Monthly mean	Satellite	1979-present	(Xie and Arkin, 1997)
TAMSAT.v3	0.0375 º	Daily total	Satellite	1983-present	(Tarnavsky et al., 2014; Maidment et al., 2017)
GPCP.v2	2.5º	Monthly mean	Satellite	1979-2015	(Adler et al., 2012)
CRU TS4.01	0.5º	Monthly total	Gauge-Based	1901-2016	(Harris et al., 2014)
GPCC.v7	0.5º	Monthly total	Gauge-Based	1901-2013	(Schneider et al., 2015)
PREC/L	0.5º	Monthly mean	Gauge-Based	1948-2012	(Chen et al., 2002)
UDEL.v4.01	0.5º	Monthly total	Gauge-Based	1900-2014	(Willmott and Matsuura, 1995)
CPC-Unified	0.5º	Daily total	Gauge-Based	1979-present	(Chen et al., 2008)
CHIRPS.v2	0.05º	Daily total	Satellite	1981-present	(Funk et al., 2015)
ERA5	~0.28125 º	Hourly	Reanalysis	1979-present	(C3S, 2017; Hersbach et al., 2020)

Table S2: General circulation models participating in the Coupled Model Intercomparison Project Phase 5 (CMIP5) that were used as forcing fields in the Coordinated Regional Climate Downscaling Experiment (CORDEX) – Africa historical simulations. Data for precipitation were retrieved from the Earth System Grid Federation (https://esgf-data.dkrz.de/projects/esgf-dkrz/). Data for temperature at 850 hPa were retrieved from the Climate Data Store (https://cds.climate.copernicus.eu/#!/home).

GCM	Institute	Ensemble	Latitude Res.	Longitude Res.	References
CanESM2	Canadian Centre for Climate Modelling and Analysis (CCCma)	r1i1p1	2.7906 º	2.8125 º	(CCCma, 2017)

Formatted: Font: Not Bold

Formatted: Font: Not Bold

Formatted: Font: Not Bold

Formatted: Font: Not Bold

Formatted: Font: Not Bold

CNRM-CM5	Centre Europeen de Recherche et de Formation Avancee en Calcul Scientifique (CERFACS)	r1i1p1	1.40008 º	1.40625 º	(Voldoire et al., 2013)
CSIRO-Mk3-6-0	Commonwealth Scientific and Industrial Research Organization (CSIRO)	r1i1p1	1.8653 º	1.875 º	(Jeffrey et al., 2013)
EC-EARTH	Sveriges Meteorologiska och Hydrologiska Institut (SMHI), Danmarks Meteorologiske Insitut (DMI)	r1i1p1 r12i1p1	1.1215 º	1.125 º	(Hazeleger et al., 2010)
GFDL-ESM-2M GFDL-ESM-2G	National Oceanic and Atmospheric Administration (NOAA)	r1i1p1	2.0225 º	2.5 º	(Dunne et al., 2012)
HadGEM2-ES	Met Office Hadley Centre	r1i1p1	1.25 º	1.875 º	(Collins et al., 2011)
IPSL-CM5A-MR	Institut Pierre Simon Laplace (IPSL)	r1i1p1	1.2676 º	2.5 º	(Dufresne et al., 2013)
IPSL-CM5A-LR			1.894737 º	3.75 º	
MIROC5	Atmospheric and Ocean Research Institute (AORI)	r1i1p1	1.4008 º	1.40625 º	(Watanabe et al., 2010)
MPI-ESM-LR	Max Planck Institute for Meteorology (MPI)	r1i1p1	1.8653 º	1.875 º	(Giorgetta et al., 2013)

NorESM1-M	EarthClim	r1i1p1	1.894737 °	2.5 °	(Bentsen et al., 2013)

Formatted: Font: Not Bold

Table S3: General circulation models participating in the Coupled Model Intercomparison Project Phase 6 (CMIP6). Data were retrieved from the Earth System Grid Federation (https://esgf-data.dkrz.de/projects/esgf-dkrz/). The CMIP6 models used were selected in accordance to their predeseccor CMIP5, so that the 2 ensembles (CMIP5 and CMIP6) would be comparable.

Formatted: Font: Not Bold

Formatted: Font: Not Bold

GCM	Institute	Ensemble	Latitude Res.	Longitude Res.	References
CanESM5	Canadian Centre for Climate Modelling and Analysis (CCCma)	r1i1p1f1	2.8 °	2.8 °	(Swart et al., 2019)
CNRM-CM6-1	Centre Europeen de Recherche et de Formation Avancee en Calcul Scientifique (CERFACS)	r1i1p1f2	1.4°	1.4 °	(Voldoire et al., 2019)
EC-EARTH3	Sveriges Meteorologiska och Hydrologiska Institut (SMHI), Danmarks Meteorologiske Insitut (DMI)	r1i1p1f1	0.7 °	0.7 °	(Massonnet et al., 2020)
GFDL-ESM4	National Oceanic and Atmospheric Administration (NOAA)	r1i1p1f1	1 °	1.3 °	(Held et al., 2019)
IPSL-CM6A-LR	Institut Pierre Simon Laplace (IPSL)	r1i1p1f1	1.3 °	2.5 °	-

MIROC6	Atmospheric and Ocean Research Institute (AORI)	r1i1p1f1	1.4 º	1.4 º	(Tatebe et al., 2019)
MPI-ESM-2-LR	Max Planck Institute for Meteorology (MPI)	r1i1p1f1	1.9 º	1.9 º	(Mauritsen et al., 2019)
NorESM2-LM	EarthClim	r1i1p1f1	1.894737 º	2.5 º	(Seland et al., 2020)

1475

Table S4: Regional climate model simulations participating in the Coordinated Regional Climate Downscaling Experiment (CORDEX) – Africa ensemble used in the current analysis, with a spatial resolution equal to 0.44º (CORDEX0.44). Data were retrieved from the Earth System Grid Federation (https://esgf-data.dkrz.de/projects/esgf-dkrz/).

Formatted: Font: Not Bold

Formatted: Font: Not Bold

Formatted: Font: Not Bold

RCM	Institute	Forcing	Realization	References
CCLM4-8-17.v1	Climate Limited-area Modelling Community (CLMcom)	CNRM-CM5 EC-EARTH HadGEM2-ES MPI-ESM-LR	r1i1p1 r12i1p1 r1i1p1 r1i1p1	(COSMO, 2020)
RACMO22T.v1	Royal Netherlands Meteorological Institute (KNMI)	EC-EARTH EC-EARTH HadGEM2-ES	r1i1p1 r12i1p1 r1i1p1	(van Meijgaard et al., 2008)
RCA4.v1	Swedish Meteorological and Hydrological Institute (SHMI)	CanESM2 CNRM-CM5 CSIRO-Mk3-6-0 EC-EARTH EC-EARTH IPSL-CM5A-MR HadGEM2-ES MPI-ESM-LR NorESM1-M GFDL-ESM2M MIROC5	r1i1p1 r1i1p1 r1i1p1 r12i1p1 r1i1p1 r1i1p1 r1i1p1 r1i1p1 r1i1p1 r1i1p1 r1i1p1	(Samuelsson et al., 2015)

REMO2009.v1	Max Planck Institut (MPI) and Climate Service Center Germany (CSC)	EC-EARTH MPI-ESM-LR IPSL-CM5A-MR MIROC5 HadGEM2-ES GFDL-ESM2G	r12i1p1 r1i1p1 r12i1p1 r1i1p1 r1i1p1 r1i1p1	(Jacob et al., 2012)
CRCM5.v1	Canadian Centre for Climate Modelling and Analysis (CCCma)	CanESM2 MPI-ESM-LR	r1i1p1 r1i1p1	(Scinocca et al., 2015)

Table S5: Regional climate model simulations participating in the Coordinated Regional Climate Downscaling Experiment (CORDEX) – Africa ensemble used in the current analysis, with a spatial resolution equal to 0.22° (CORDEX0.22). Data were retrieved from the Earth System Grid Federation (https://esgf-data.dkrz.de/projects/esgf-dkrz/).

Formatted: Font: Not Bold

Formatted: Font: Not Bold

Formatted: Font: Not Bold

RCM	Institute	Forcing	Realization	Variables available
CanESM2	Canadian Centre for Climate Modelling and Analysis	CanRCM4	r1i1p1	Pr
HadGEM2-ES	Royal Netherlands Meteorological Institute (KNMI)	CCLM5-0-15 REMO2015 RegCM4-7	r1i1p1 r1i1p1 r1i1p1	Pr, hus850, ua850, va850, ta850
MPI-ESM-LR	Swedish Meteorological and Hydrological Institute (SHMI)	CCLM5-0-15 REMO2015 RegCM4-7	r1i1p1 r1i1p1 r1i1p1	Pr, hus850, ua850, va850, ta850
NorESM1-M		CCLM5-0-15 REMO2015 RegCM4-7	r1i1p1 r1i1p1 r1i1p1	Pr, hus850, ua850, va850, ta850

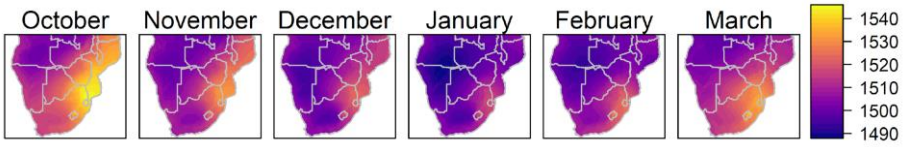

Figure S1: Mean monthly geopotential height at 850 hPa in ERA5 for the period 1986-2005.

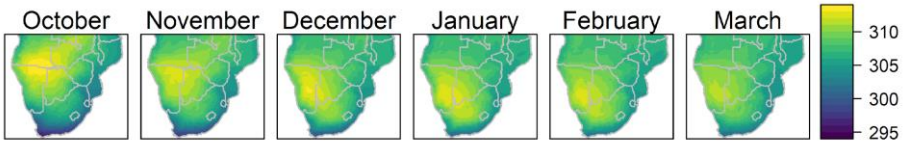

Figure S2: Mean monthly potential temperature at 850 hPa in ERA5 for the period 1986-2005.

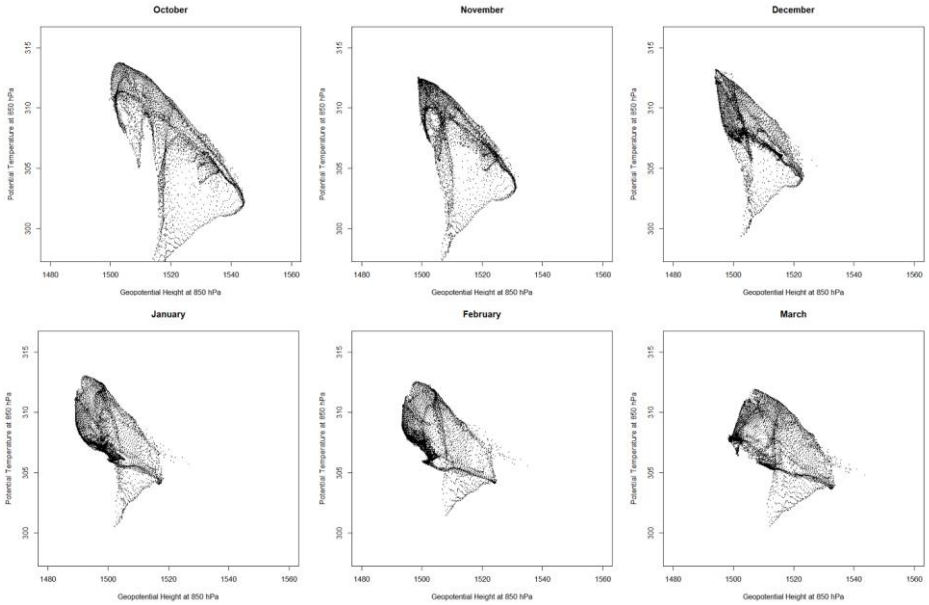

Figure S3: Geopotential height at 850 hPa (x-axis) plotted against potential temperature at 850 hPa (y-axis). Values refer to climatological monthly means for the period 1986-2005. Each dot in the scatterplot represents a pixel of the ERA5 dataset over the whole southern Africa region 10 ºE to 42 ºE and from 10 ºS to 35 ºS.

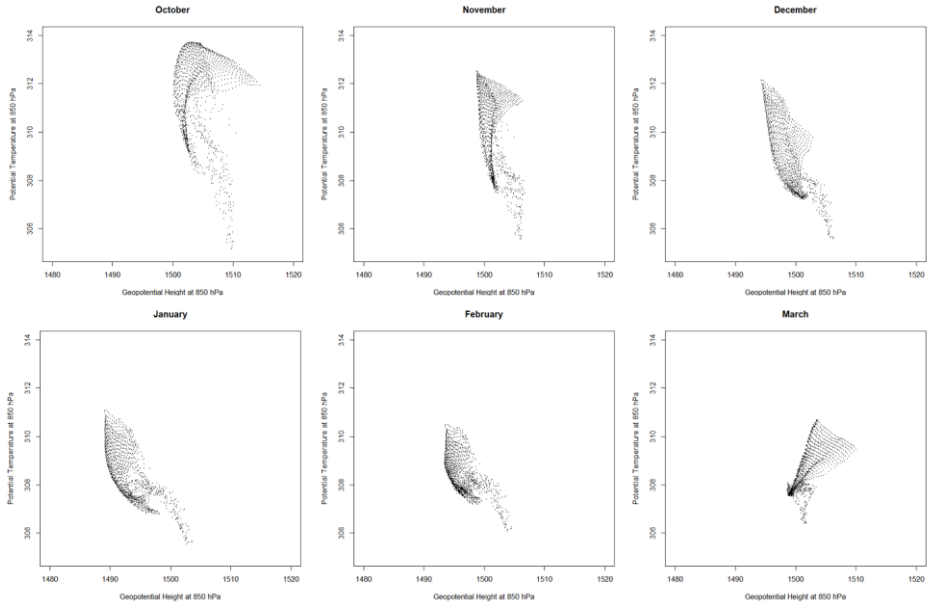

Figure S4: Geopotential height at 850 hPa (x-axis) plotted against potential temperature at 850 hPa (y-axis). Values refer to climatological monthly means for the period 1986-2005. Each dot in the scatterplot represents a pixel of the ERA5 dataset over the whole southern Africa region 14 ºE to 25 ºE and from 11 ºS to 19 ºS.

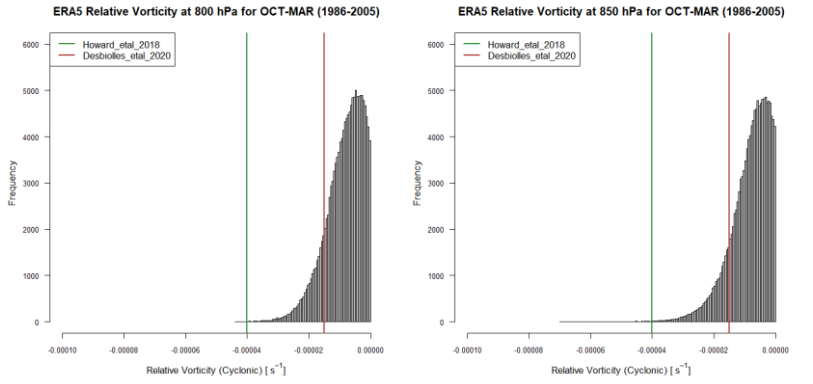

Figure S5: Histogram of relative vorticity for months Oct-Mar during 1986-2005 in ERA5 using u and v values at 800 hPa (left) and at 850 hPa (right). Pixels used are enclosed by the region from 14 ºE to 25 ºE and from 11 ºS to 19 ºS. For both histograms mean monthly u and v values are used.

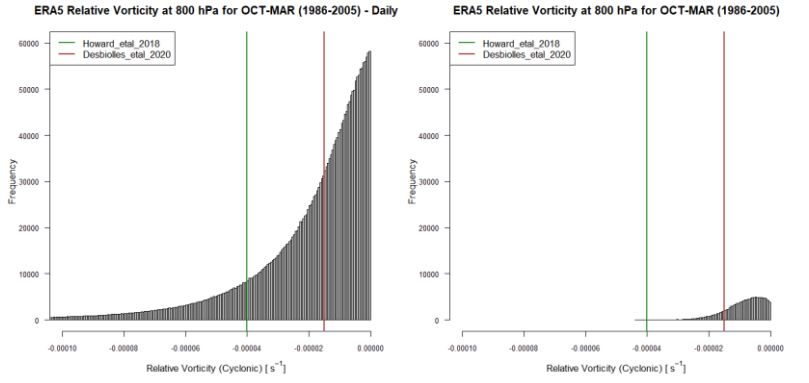

Figure S6: Histogram of relative vorticity for months Oct-Mar during 1986-2005 in ERA5 using daily u and v values (left) and using monthly u and v values (right). Pixels used are enclosed by the region from 14 ºE to 25 ºE and from 11 ºS to 19 ºS.

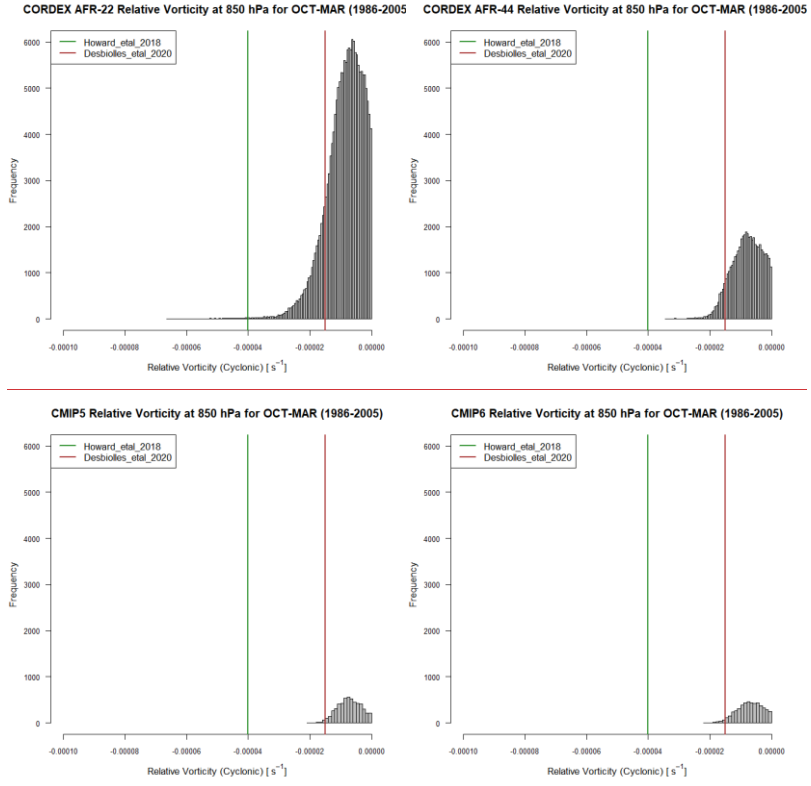

Figure S7: Histogram of relative vorticity for months Oct-Mar during 1986-2005 at 850 hPa for CORDEX-Africa at 0.22º (upper left), for CORDEX-Africa 0.44º (upper right), for CMIP5 (lower left), and for CMIP6 (lower right). Pixels used are

enclosed by the region from 14 ºE to 25 ºE and from 11 ºS to 19 ºS. For all histograms mean monthly u and v values are used.

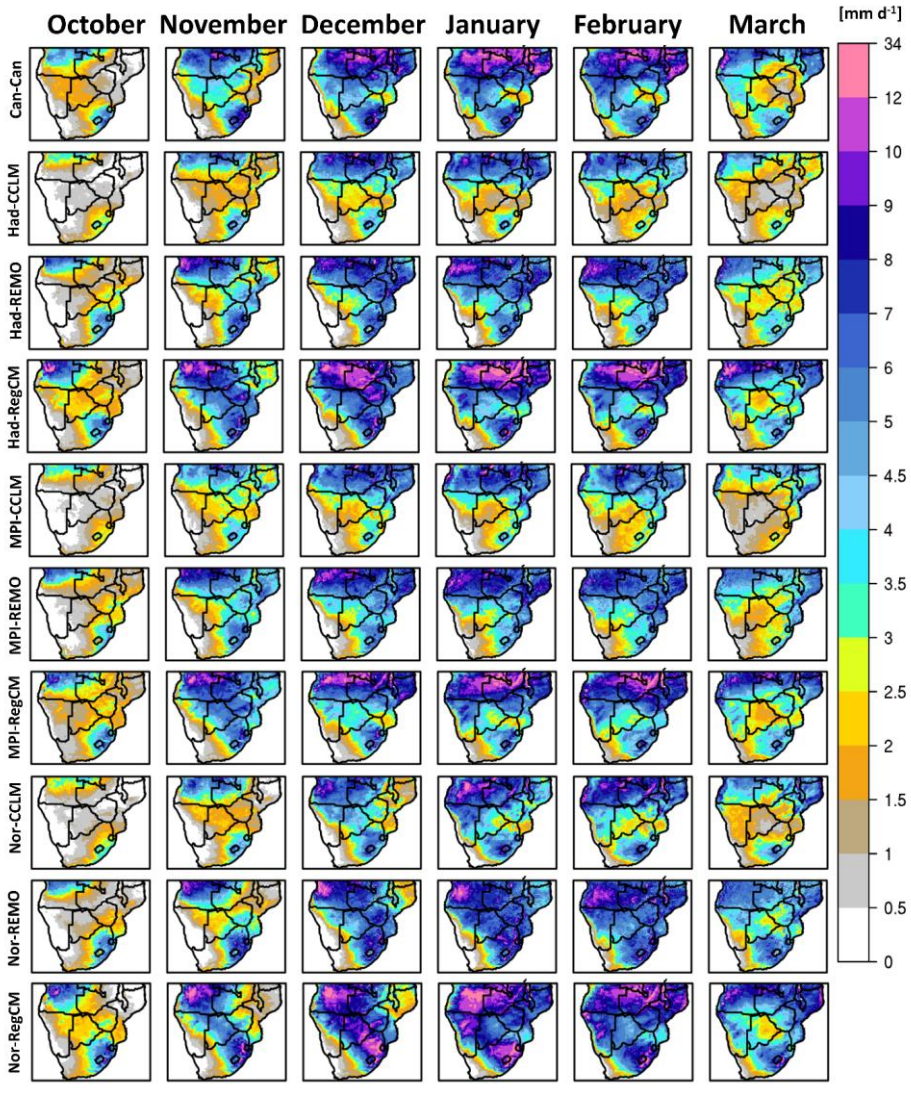
October
November
December
January
February
March
[mm d-1]
34
12
10
9
8
7
6
5
4.5
4
3.5
3
2.5
2
1.5
1
0.5
0
Can-Can
Had-CCLM
Had-REMO
Had-RegCM
MPI-CCLM
MPI-REMO
MPI-RegCM
Nor-CCLM
Nor-REMO
Nor-RegCM

Figure S8: Monthly precipitation climatologies during the period 1986-2005 in mm d^{-1} from the ensemble members of the CORDEX-Africa 0.22º simulations (CORDEX0.22).

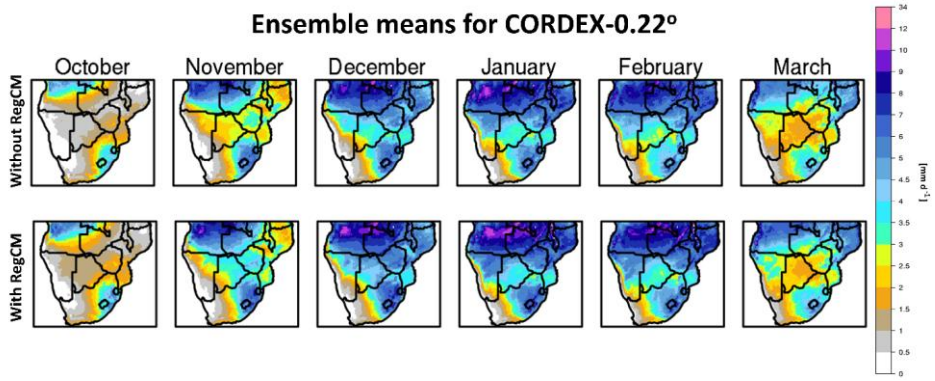

Figure S9: Ensemble mean of the CORDEX-Africa 0.22º ensemble (CORDEX0.22) by excluding the RegCM4-7 simulations (upper row) and by including all available simulations (bottom row).

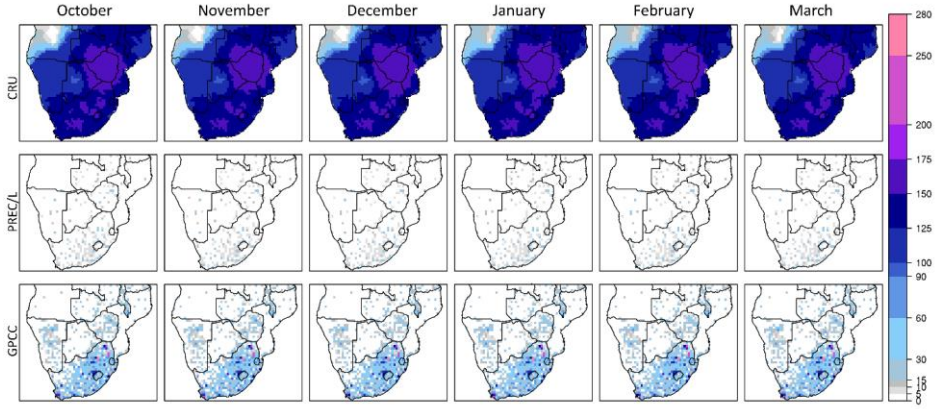

Figure S10. Total number of reporting stations/rain-gauges for each month during the period 1986-2005, used in the interpolation process of each gauge-based product (CRU, PREC/L, GPCC).

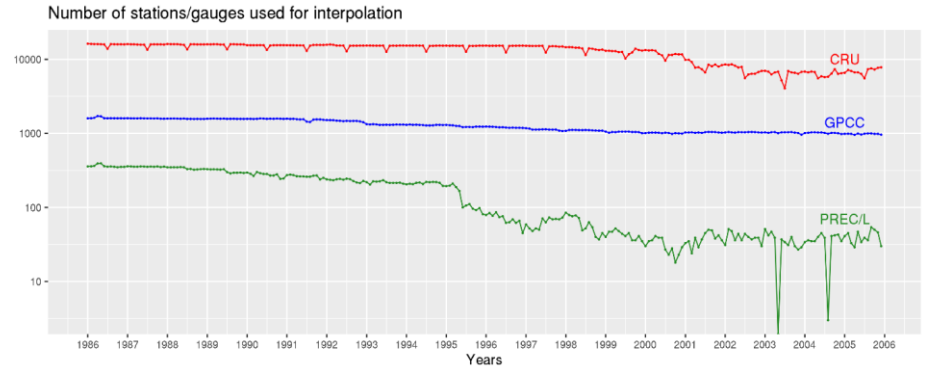

Figure S11. Timeseries of the number of stations/rain-gauges used in 3 gauge-based products, over the southern Africa region (10 ºE to 42 ºE and 10 ºS to 35 ºS).

Formatted: Font: Not Bold

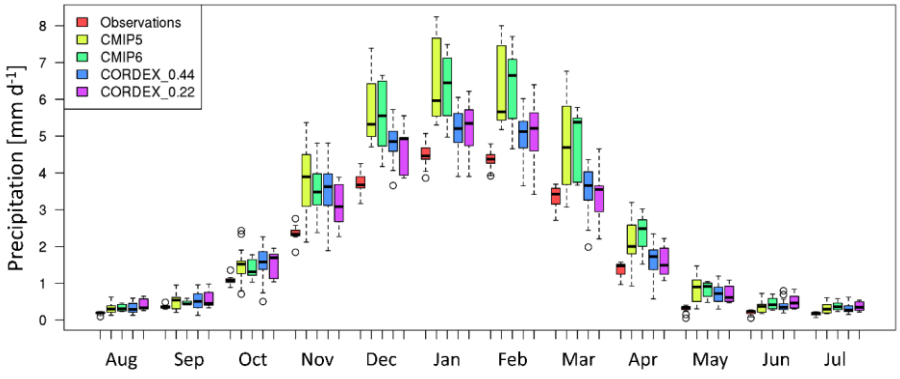

Figure S12: Annual cycle of monthly precipitation during 1986-2005 for the ensemble of observational data (gauge-based, satellite and reanalysis), CMIP5 (Coupled Model Intercomparison Project Phase 5), CMIP6 (Coupled Model Intercomparison Project Phase 6), CORDEX0.44 (Coordinated Regional Climate Downscaling Experiment – Africa domain with a spatial resolution equal to 0.44º x 0.44º) and CORDEX-0.22º (CORDEX-Africa simulations with a spatial resolution equal to 0.22º x 0.22º, excluding the RegCM4-7 simulations from the ensemble). The thick horizontal black lines indicate the ensemble median for each month, the box encloses the interquartile range, and the tails denote the full ensemble range. Circles represent the outliers for each ensemble. Grid points only are considered.

Formatted: Font: Not Bold, Not Italic

Formatted: Font: Not Bold

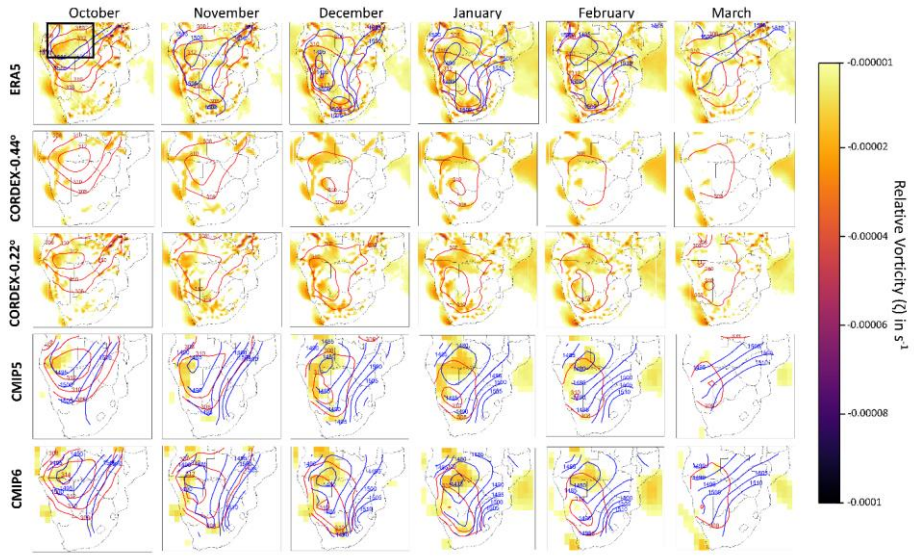

Figure S13: Monthly climatologies of the Angola Low pressure system during the rainy season for the period 1986-2005. Filled contours indicate cyclonic relative vorticity (ζ) for $\zeta < -0.00001\ s^{-1}$ over the whole southern Africa region. Red lines indicate the isotherms of potential temperature at 850 hPa, having an increment of 2 K. Blue lines indicate isoheights of the geopotential height at 850 hPa, having an increment of 5 m. CORDEX0.44/0.22 are not plotted with geopotential isoheights, because this variable was not available for CORDEX simulations. From top to bottom: ERA5, ensemble mean of CORDEX0.22º, CORDEX0.44º, CMIP5 and CMIP6 simulations. Black box indicates the region from 14 ºE to 25 ºE and from 11 ºS to 19 ºS.

Formatted: Font: Not Bold, Not Italic
Formatted: Font: Not Bold
Formatted: Font: Not Bold, Not Italic
Formatted: Font: Not Bold
Formatted: Font: Not Bold, Not Italic
Formatted: Font: Not Bold
Formatted: Font: Not Bold, Not Italic
Formatted: Font: Not Italic

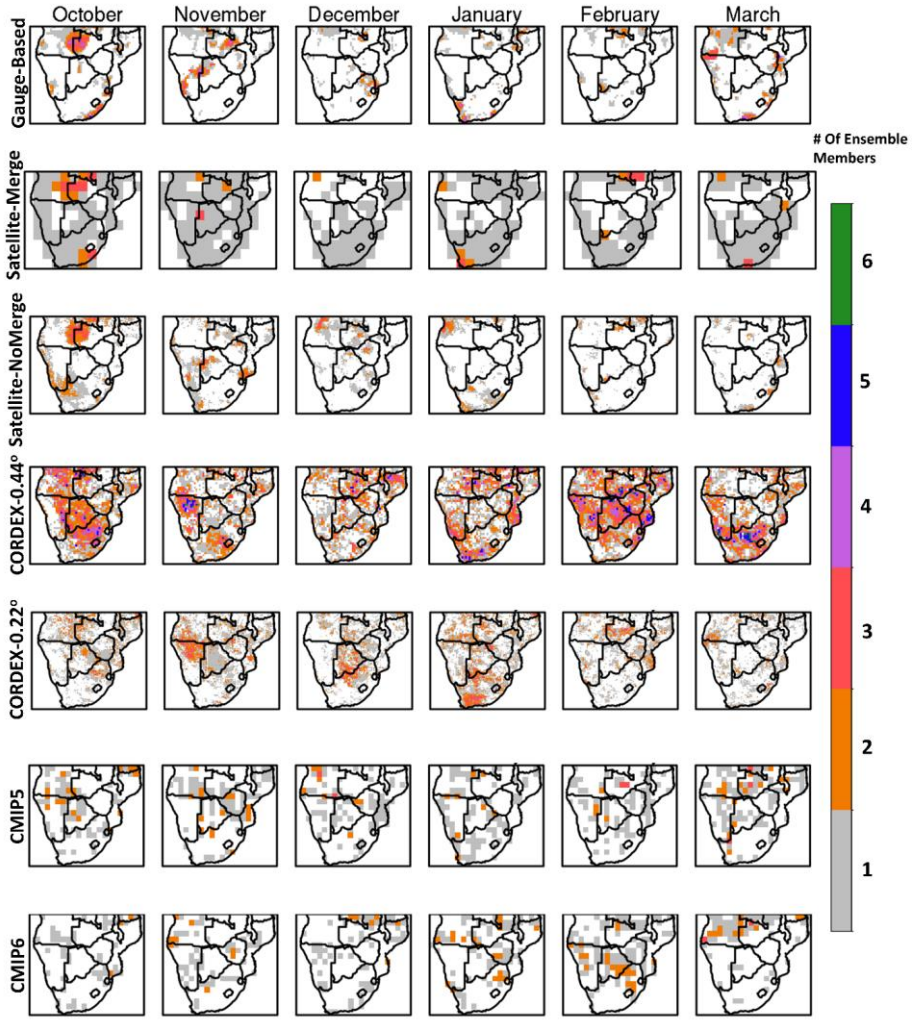

Figure S14. Number of ensemble members yielding statistically significant results for monthly precipitation trends based on the Mann-Kendall test (a=0.05).

Formatted: Line spacing: single

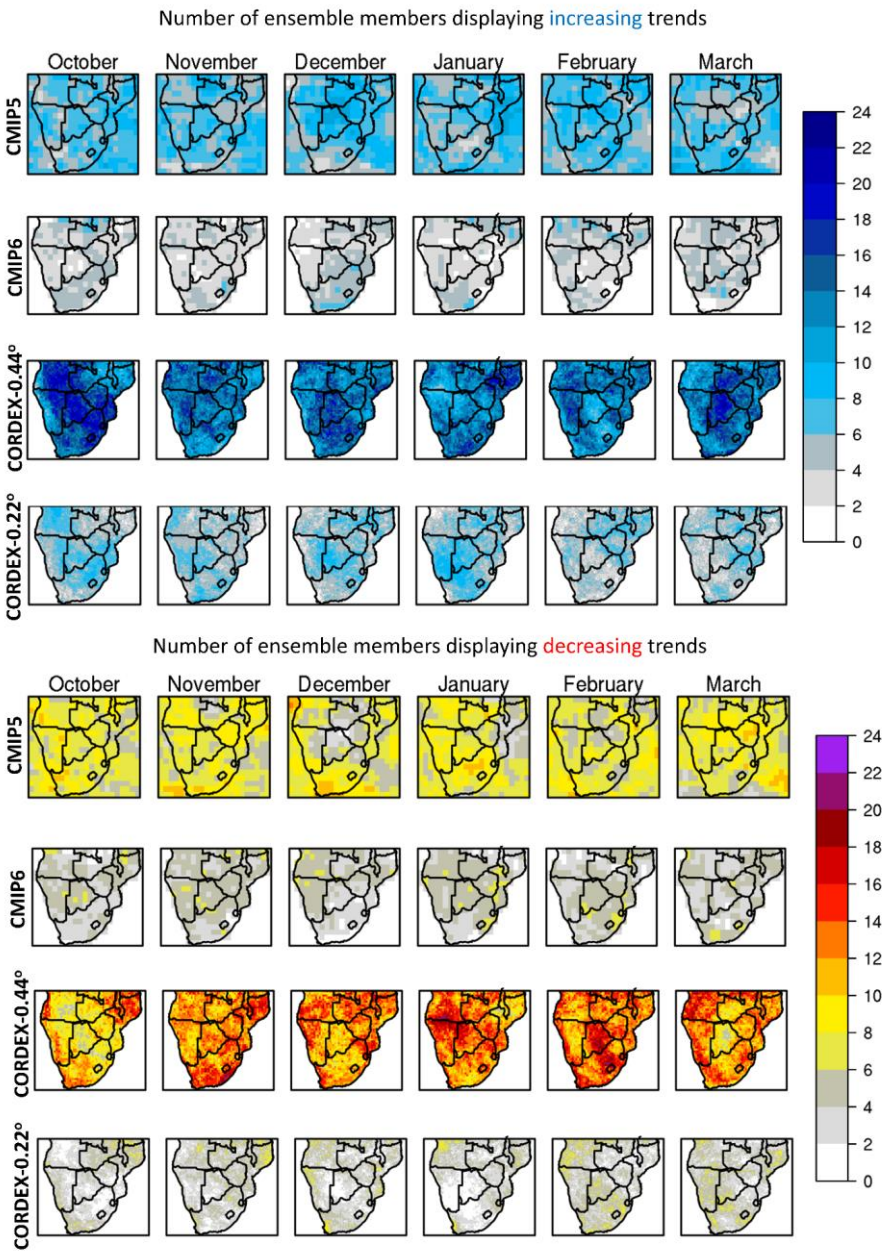
Number of ensemble members displaying increasing trends
October
November
December
January
February
March
CMIP5
CMIP6
CORDEX-0.44°
CORDEX-0.22°
24
22
20
18
16
14
12
10
8
6
4
2
0
Number of ensemble members displaying decreasing trends
October
November
December
January
February
March
CMIP5
CMIP6
CORDEX-0.44°
CORDEX-0.22°
24
22
20
18
16
14
12
10
8
6
4
2
0

Figure S15: Number of ensemble members displaying increasing or decreasing trends for each ensemble.

Formatted: Font: Not Bold, Not Italic

Formatted: Font: Not Bold

References

Adler, R.F., Gu, G., Huffman, G.J., 2012. Estimating Climatological Bias Errors for the Global Precipitation Climatology Project (GPCP). J. Appl. Meteorol. Climatol. 51, 84–99. https://doi.org/10.1175/JAMC-D-11-052.1

Ashouri, H., Hsu, K.-L., Sorooshian, S., Braithwaite, D.K., Knapp, K.R., Cecil, L.D., Nelson, B.R., Prat, O.P., 2015. PERSIANN-CDR: Daily Precipitation Climate Data Record from Multisatellite Observations for Hydrological and Climate Studies. Bull. Am. Meteorol. Soc. 96, 69–83. https://doi.org/10.1175/BAMS-D-13-00068.1

Bentsen, M., Bethke, I., Debernard, J.B., Iversen, T., Kirkevåg, A., Seland, Ø., Drange, H., Roelandt, C., Seierstad, I.A., Hoose, C., Kristjánsson, J.E., 2013. The Norwegian Earth System Model, NorESM1-M – Part 1: Description and basic evaluation of the physical climate. Geosci. Model Dev. 6, 687–720. https://doi.org/10.5194/gmd-6-687-2013

C3S, 2017. ERA5: Fifth generation of ECMWF atmospheric reanalyses of the global climate.

CCCma, 2017. Environment and Climate Change Canada - Climate Change - CanESM2 [WWW Document]. URL http://www.ec.gc.ca/ccmac-cccma/default.asp?lang=En&xml=1A3B7DF1-99BB-4EC8-B129-09F83E72D645 (accessed 6.23.20).

Chen, M., Shi, W., Xie, P., Silva, V.B.S., Kousky, V.E., Higgins, R.W., Janowiak, J.E., 2008. Assessing objective techniques for gauge-based analyses of global daily precipitation. J. Geophys. Res. Atmospheres 113. https://doi.org/10.1029/2007JD009132

Chen, M., Xie, P., Janowiak, J.E., Arkin, P.A., 2002. Global Land Precipitation: A 50-yr Monthly Analysis Based on Gauge Observations. J. Hydrometeorol. 3, 249–266. https://doi.org/10.1175/1525-7541(2002)003<0249:GLPAYM>2.0.CO;2

Collins, W.J., Bellouin, N., Doutriaux-Boucher, M., Gedney, N., Halloran, P., Hinton, T., Hughes, J., Jones, C.D., Joshi, M., Liddicoat, S., Martin, G., O'Connor, F., Rae, J., Senior, C., Sitch, S., Totterdell, I., Wiltshire, A., Woodward, S., 2011. Development and evaluation of an Earth-System model – HadGEM2. Geosci. Model Dev. 4, 1051–1075. https://doi.org/10.5194/gmd-4-1051-2011

COSMO, 2020. COSMO core documentation [WWW Document]. URL http://www.cosmo-model.org/content/model/documentation/core/default.htm#p1 (accessed 6.22.20).

Dufresne, J.-L., Foujols, M.-A., Denvil, S., Caubel, A., Marti, O., Aumont, O., Balkanski, Y., Bekki, S., Bellenger, H., Benshila, R., Bony, S., Bopp, L., Braconnot, P., Brockmann, P., Cadule, P., Cheruy, F., Codron, F., Cozic, A., Cugnet, D., de Noblet, N., Duvel, J.-P., Ethé, C., Fairhead, L., Fichefet, T., Flavoni, S., Friedlingstein, P., Grandpeix, J.-Y., Guez, L., Guilyardi, E., Hauglustaine, D., Hourdin, F., Idelkadi, A., Ghattas, J., Joussaume, S., Kageyama, M., Krinner, G., Labetoulle, S., Lahellec, A., Lefebvre, M.-P., Lefevre, F., Levy, C., Li, Z.X., Lloyd, J., Lott, F., Madec, G., Mancip, M., Marchand, M., Masson, S., Meurdesoif, Y., Mignot, J., Musat, I., Parouty, S., Polcher, J., Rio, C., Schulz, M., Swingedouw, D., Szopa, S., Talandier, C., Terray, P., Viovy, N., Vuichard, N., 2013. Climate change projections using the IPSL-CM5 Earth System Model: from CMIP3 to CMIP5. Clim. Dyn. 40, 2123–2165. https://doi.org/10.1007/s00382-012-1636-1

Dunne, J.P., John, J.G., Adcroft, A.J., Griffies, S.M., Hallberg, R.W., Shevliakova, E., Stouffer, R.J., Cooke, W., Dunne, K.A., Harrison, M.J., Krasting, J.P., Malyshev, S.L., Milly, P.C.D., Phillipps, P.J., Sentman, L.T., Samuels, B.L., Spelman, M.J., Winton, M., Wittenberg, A.T., Zadeh, N., 2012. GFDL's ESM2 Global Coupled Climate–Carbon Earth System Models. Part I: Physical Formulation and Baseline Simulation Characteristics. J. Clim. 25, 6646–6665. https://doi.org/10.1175/JCLI-D-11-00560.1

Funk, C., Peterson, P., Landsfeld, M., Pedreros, D., Verdin, J., Shukla, S., Husak, G., Rowland, J., Harrison, L., Hoell, A., Michaelsen, J., 2015. The climate hazards infrared precipitation with stations—a new environmental record for monitoring extremes. Sci. Data 2, 150066. https://doi.org/10.1038/sdata.2015.66

Giorgetta, M.A., Jungclaus, J., Reick, C.H., Legutke, S., Bader, J., Böttinger, M., Brovkin, V., Crueger, T., Esch, M., Fieg, K., Glushak, K., Gayler, V., Haak, H., Hollweg, H.-D., Ilyina, T., Kinne, S., Kornblueh, L., Matei, D., Mauritsen, T., Mikolajewicz, U., Mueller, W., Notz, D., Pithan, F., Raddatz, T., Rast, S., Redler, R., Roeckner, E., Schmidt, H., Schnur, R., Segschneider, J., Six, K.D., Stockhause, M., Timmreck, C., Wegner, J., Widmann, H., Wieners, K.-H., Claussen, M., Marotzke, J., Stevens, B., 2013. Climate and carbon cycle changes from 1850 to 2100 in MPI-ESM

simulations for the Coupled Model Intercomparison Project phase 5. J. Adv. Model. Earth Syst. 5, 572–597. https://doi.org/10.1002/jame.20038

Harris, I., Jones, P.D., Osborn, T.J., Lister, D.H., 2014. Updated high-resolution grids of monthly climatic observations – the CRU TS3.10 Dataset. Int. J. Climatol. 34, 623–642. https://doi.org/10.1002/joc.3711

Hazeleger, W., Severijns, C., Semmler, T., Ştefănescu, S., Yang, S., Wang, X., Wyser, K., Dutra, E., Baldasano, J.M., Bintanja, R., Bougeault, P., Caballero, R., Ekman, A.M.L., Christensen, J.H., van den Hurk, B., Jimenez, P., Jones, C., Kållberg, P., Koenigk, T., McGrath, R., Miranda, P., van Noije, T., Palmer, T., Parodi, J.A., Schmith, T., Selten, F., Storelvmo, T., Sterl, A., Tapamo, H., Vancoppenolle, M., Viterbo, P., Willén, U., 2010. EC-EarthA Seamless Earth-System Prediction Approach in Action. Bull. Am. Meteorol. Soc. 91, 1357–1364. https://doi.org/10.1175/2010BAMS2877.1

Held, I.M., Guo, H., Adcroft, A., Dunne, J.P., Horowitz, L.W., Krasting, J., Shevliakova, E., Winton, M., Zhao, M., Bushuk, M., Wittenberg, A.T., Wyman, B., Xiang, B., Zhang, R., Anderson, W., Balaji, V., Donner, L., Dunne, K., Durachta, J., Gauthier, P.P.G., Ginoux, P., Golaz, J.-C., Griffies, S.M., Hallberg, R., Harris, L., Harrison, M., Hurlin, W., John, J., Lin, P., Lin, S.-J., Malyshev, S., Menzel, R., Milly, P.C.D., Ming, Y., Naik, V., Paynter, D., Paulot, F., Rammaswamy, V., Reichl, B., Robinson, T., Rosati, A., Seman, C., Silvers, L.G., Underwood, S., Zadeh, N., 2019. Structure and Performance of GFDL's CM4.0 Climate Model. J. Adv. Model. Earth Syst. 11, 3691–3727. https://doi.org/10.1029/2019MS001829

Hersbach, H., Bell, B., Berrisford, P., Hirahara, S., Horányi, A., Muñoz-Sabater, J., Nicolas, J., Peubey, C., Radu, R., Schepers, D., Simmons, A., Soci, C., Abdalla, S., Abellan, X., Balsamo, G., Bechtold, P., Biavati, G., Bidlot, J., Bonavita, M., Chiara, G.D., Dahlgren, P., Dee, D., Diamantakis, M., Dragani, R., Flemming, J., Forbes, R., Fuentes, M., Geer, A., Haimberger, L., Healy, S., Hogan, R.J., Hólm, E., Janisková, M., Keeley, S., Laloyaux, P., Lopez, P., Lupu, C., Radnoti, G., Rosnay, P. de, Rozum, I., Vamborg, F., Villaume, S., Thépaut, J.-N., 2020. The ERA5 global reanalysis. Q. J. R. Meteorol. Soc. 146, 1999–2049. https://doi.org/10.1002/qj.3803

Jacob, D., Elizalde, A., Haensler, A., Hagemann, S., Kumar, P., Podzun, R., Rechid, D., Remedio, A.R., Saeed, F., Sieck, K., Teichmann, C., Wilhelm, C., 2012. Assessing the Transferability of the Regional Climate Model REMO to Different COordinated Regional Climate Downscaling EXperiment (CORDEX) Regions. Atmosphere 3, 181–199. https://doi.org/10.3390/atmos3010181

Jeffrey, S., Rotstayn, L.D., Collier, M., Dravitzki, S.M., Hamalainen, C., Moeseneder, C., Wong, K., Syktus, J., 2013. Australia ' s CMIP 5 submission using the CSIRO-Mk 3 . 6 model.

Maidment, R.I., Grimes, D., Black, E., Tarnavsky, E., Young, M., Greatrex, H., Allan, R.P., Stein, T., Nkonde, E., Senkunda, S., Alcántara, E.M.U., 2017. A new, long-term daily satellite-based rainfall dataset for operational monitoring in Africa. Sci. Data 4, 170063. https://doi.org/10.1038/sdata.2017.63

Massonnet, F., Ménégoz, M., Acosta, M., Yepes-Arbós, X., Exarchou, E., Doblas-Reyes, F.J., 2020. Replicability of the EC-Earth3 Earth system model under a change in computing environment. Geosci. Model Dev. 13, 1165–1178. https://doi.org/10.5194/gmd-13-1165-2020

Mauritsen, T., Bader, J., Becker, T., Behrens, J., Bittner, M., Brokopf, R., Brovkin, V., Claussen, M., Crueger, T., Esch, M., Fast, I., Fiedler, S., Fläschner, D., Gayler, V., Giorgetta, M., Goll, D.S., Haak, H., Hagemann, S., Hedemann, C., Hohenegger, C., Ilyina, T., Jahns, T., Jimenéz-de-la-Cuesta, D., Jungclaus, J., Kleinen, T., Kloster, S., Kracher, D., Kinne, S., Kleberg, D., Lasslop, G., Kornblueh, L., Marotzke, J., Matei, D., Meraner, K., Mikolajewicz, U., Modali, K., Möbis, B., Müller, W.A., Nabel, J.E.M.S., Nam, C.C.W., Notz, D., Nyawira, S.-S., Paulsen, H., Peters, K., Pincus, R., Pohlmann, H., Pongratz, J., Popp, M., Raddatz, T.J., Rast, S., Redler, R., Reick, C.H., Rohrschneider, T., Schemann, V., Schmidt, H., Schnur, R., Schulzweida, U., Six, K.D., Stein, L., Stemmler, I., Stevens, B., Storch, J.-S. von, Tian, F., Voigt, A., Vrese, P., Wieners, K.-H., Wilkenskjeld, S., Winkler, A., Roeckner, E., 2019. Developments in the MPI-M Earth System Model version 1.2 (MPI-ESM1.2) and Its Response to Increasing CO2. J. Adv. Model. Earth Syst. 11, 998–1038. https://doi.org/10.1029/2018MS001400

Novella, N.S., Thiaw, W.M., 2013. African Rainfall Climatology Version 2 for Famine Early Warning Systems. J. Appl. Meteorol. Climatol. 52, 588–606. https://doi.org/10.1175/JAMC-D-11-0238.1

Samuelsson, P., Gollvik, S., Jansson, C., Kupiainen, M., Kourzeneva, E., van de Berg, W.J., 2015. The surface processes of the Rossby Centre regional atmospheric climate model (RCA4). [WWW Document]. https://www.smhi.se/polopoly_fs/1.89803!/Menu/general/extGroup/attachmentColHold/mainCol1/file/meteorologi

_157.pdf. URL https://www.smhi.se/polopoly_fs/1.89803!/Menu/general/extGroup/attachmentColHold/mainCol1/file/meteorologi_157.pdf (accessed 12.9.19).

Schneider, U., Becker, A., Finger, P., Meyer-Christoffer, A., Rudolf, B., Ziese, M., 2015. GPCC Full Data Reanalysis Version 7.0 at 0.5°: Monthly Land-Surface Precipitation from Rain-Gauges built on GTS-based and Historic Data.

Scinocca, J.F., Kharin, V.V., Jiao, Y., Qian, M.W., Lazare, M., Solheim, L., Flato, G.M., Biner, S., Desgagne, M., Dugas, B., 2016. Coordinated Global and Regional Climate Modeling. J. Clim. 29, 17–35. https://doi.org/10.1175/JCLI-D-15-0161.1

Scinocca, J.F., Kharin, V.V., Jiao, Y., Qian, M.W., Lazare, M., Solheim, L., Flato, G.M., Biner, S., Desgagne, M., Dugas, B., 2015. Coordinated Global and Regional Climate Modeling. J. Clim. 29, 17–35. https://doi.org/10.1175/JCLI-D-15-0161.1

Seland, Ø., Bentsen, M., Olivié, D., Toniazzo, T., Gjermundsen, A., Graff, L.S., Debernard, J.B., Gupta, A.K., He, Y.-C., Kirkevåg, A., Schwinger, J., Tjiputra, J., Aas, K.S., Bethke, I., Fan, Y., Griesfeller, J., Grini, A., Guo, C., Ilicak, M., Karset, I.H.H., Landgren, O., Liakka, J., Moseid, K.O., Nummelin, A., Spensberger, C., Tang, H., Zhang, Z., Heinze, C., Iversen, T., Schulz, M., 2020. Overview of the Norwegian Earth System Model (NorESM2) and key climate response of CMIP6 DECK, historical, and scenario simulations. Geosci. Model Dev. 13, 6165–6200. https://doi.org/10.5194/gmd-13-6165-2020

Swart, N.C., Cole, J.N.S., Kharin, V.V., Lazare, M., Scinocca, J.F., Gillett, N.P., Anstey, J., Arora, V., Christian, J.R., Hanna, S., Jiao, Y., Lee, W.G., Majaess, F., Saenko, O.A., Seiler, C., Seinen, C., Shao, A., Sigmond, M., Solheim, L., von Salzen, K., Yang, D., Winter, B., 2019. The Canadian Earth System Model version 5 (CanESM5.0.3). Geosci. Model Dev. 12, 4823–4873. https://doi.org/10.5194/gmd-12-4823-2019

Tarnavsky, E., Grimes, D., Maidment, R., Black, E., Allan, R.P., Stringer, M., Chadwick, R., Kayitakire, F., 2014. Extension of the TAMSAT Satellite-Based Rainfall Monitoring over Africa and from 1983 to Present. J. Appl. Meteorol. Climatol. 53, 2805–2822. https://doi.org/10.1175/JAMC-D-14-0016.1

Tatebe, H., Ogura, T., Nitta, T., Komuro, Y., Ogochi, K., Takemura, T., Sudo, K., Sekiguchi, M., Abe, M., Saito, F., Chikira, M., Watanabe, S., Mori, M., Hirota, N., Kawatani, Y., Mochizuki, T., Yoshimura, K., Takata, K., O'ishi, R., Yamazaki, D., Suzuki, T., Kurogi, M., Kataoka, T., Watanabe, M., Kimoto, M., 2019. Description and basic evaluation of simulated mean state, internal variability, and climate sensitivity in MIROC6. Geosci. Model Dev. 12, 2727–2765. https://doi.org/10.5194/gmd-12-2727-2019

van Meijgaard, E., van Ulft, L.H., van de Berg, W.J., Bosveld, F.C., van den Hurk, B.J.J.M., Lenderink, G., Siebesma, A.P., 2008. The KNMI regional atmospheric climate model RACMO version 2.1 (TR - 302). KNMI, The Netherland.

Voldoire, A., Saint-Martin, D., Sénési, S., Decharme, B., Alias, A., Chevallier, M., Colin, J., Guérémy, J.-F., Michou, M., Moine, M.-P., Nabat, P., Roehrig, R., Mélia, D.S. y, Séférian, R., Valcke, S., Beau, I., Belamari, S., Berthet, S., Cassou, C., Cattiaux, J., Deshayes, J., Douville, H., Ethé, C., Franchistéguy, L., Geoffroy, O., Lévy, C., Madec, G., Meurdesoif, Y., Msadek, R., Ribes, A., Sanchez-Gomez, E., Terray, L., Waldman, R., 2019. Evaluation of CMIP6 DECK Experiments With CNRM-CM6-1. J. Adv. Model. Earth Syst. 11, 2177–2213. https://doi.org/10.1029/2019MS001683

Voldoire, A., Sanchez-Gomez, E., Salas y Mélia, D., Decharme, B., Cassou, C., Sénési, S., Valcke, S., Beau, I., Alias, A., Chevallier, M., Déqué, M., Deshayes, J., Douville, H., Fernandez, E., Madec, G., Maisonnave, E., Moine, M.-P., Planton, S., Saint-Martin, D., Szopa, S., Tyteca, S., Alkama, R., Belamari, S., Braun, A., Coquart, L., Chauvin, F., 2013. The CNRM-CM5.1 global climate model: description and basic evaluation. Clim. Dyn. 40, 2091–2121. https://doi.org/10.1007/s00382-011-1259-y

Watanabe, M., Suzuki, T., O'ishi, R., Komuro, Y., Watanabe, S., Emori, S., Takemura, T., Chikira, M., Ogura, T., Sekiguchi, M., Takata, K., Yamazaki, D., Yokohata, T., Nozawa, T., Hasumi, H., Tatebe, H., Kimoto, M., 2010. Improved Climate Simulation by MIROC5: Mean States, Variability, and Climate Sensitivity. J. Clim. 23, 6312–6335. https://doi.org/10.1175/2010JCLI3679.1

Willmott, C.J., Matsuura, K., 1995. Smart Interpolation of Annually Averaged Air Temperature in the United States. J. Appl. Meteorol. 34, 2577–2586. https://doi.org/10.1175/1520-0450(1995)034<2577:SIOAAA>2.0.CO;2

Xie, P., Arkin, P.A., 1997. Global Precipitation: A 17-Year Monthly Analysis Based on Gauge Observations, Satellite Estimates, and Numerical Model Outputs. Bull. Am. Meteorol. Soc. 78, 2539–2558. https://doi.org/10.1175/1520-0477(1997)078<2539:GPAYMA>2.0.CO;2